CHEMICAL LOOPING GASIFICATION OF BIOMASS FOR HYDROGEN-ENRICHED GAS PRODUCTION

by

Bishnu Acharya

Submitted in partial fulfilment of the requirements
for the degree of Doctor of Philosophy

at

Dalhousie University
Halifax, Nova Scotia
August 2011

DALHOUSIE UNIVERSITY

DEPARTMENT OF MECHANICAL ENGINEERING

The undersigned hereby certify that they have read and recommend to the Faculty of Graduate Studies for acceptance a thesis entitled "CHEMICAL LOOPING GASIFICATION OF BIOMASS FOR HYDROGEN-ENRICHED GAS PRODUCTION" by Bishnu Acharya in partial fulfilment of the requirements for the degree of Doctor of Philosophy.

Dated: August 2, 2011

External Examiner: _____

Research Co-Supervisor: _____

_____

Examining Committee: _____

_____

Departmental Representative: _____

DALHOUSIE UNIVERSITY

DATE: August 2, 2011

AUTHOR: Bishnu Acharya

TITLE: CHEMICAL LOOPING GASIFICATION OF BIOMASS FOR HYDROGEN-ENRICHED GAS PRODUCTION

DEPARTMENT OR SCHOOL: Department of Mechanical Engineering

DEGREE: PhD CONVOCATION: October YEAR: 2011

_____

Signature of Author

To My

Parents: Mahesh Acharya and Sabita Acharya

Sisters and brother: Anita Dahal, Pramod Dahal and Manita Acharya

And

Wife: Sebika Acharya

TABLE OF CONTENTS

LIST OF TABLES

LIST OF FIGURES

LIST OF ABBREVIATIONS AND SYMBOLS USED

ABBREVIATIONS

ASU	Air Separation Unit
Al_2O_3	Aluminum oxide
C	Carbon
CFB	Circulating Fluidized Bed
CLG	Chemical Looping Gasification
CLC	Chemical Looping Combustion
CO_2	Carbon dioxide
CO	Carbon monoxide
CH_4	Methane
CaO	Calcium oxide
$CaCO_3$	Calcium carbonate
CaO/B	Sorbent to biomass ratio
CaS	Calcium sulfide
$CaSO_4$	Calcium sulfate
$Ca(OH)_2$	Calcium hydroxide
Cu	Copper
Cd	Cadmium
Co	Cobalt
CuO	Copper oxide
CLOU	Chemical Looping with Oxygen Uncoupling
CSIC	Consejo Superior de Investigaciones Cientificas
FC	Fixed carbon in biomass
Fe	Iron
Fe_2O_3	Iron oxide
GHG	Greenhouse gas
H, H_2	Hydrogen
H_2O	Water/steam
HHV	Higher heating value of biomass
KIER	Korea Institute of Energy Research
MSW	Municipal solid waste
Mn	Manganese
Mn_2O_3	Manganese oxide
MEA	Monoethanolamine
M	Moisture content in biomass
N_2	Nitrogen
Ni	Nickel
NiO	Nickel oxide
O, O_2	Oxygen
QWM	Quartz wool matrix reactor
RR	Reaction rate

S/B	Steam to biomass ratio
SiO_2	Silicon dioxide
TiO_2	Titanium dioxide
TDH	Transport disengaging height
VM	Volatile mass fraction in biomass
ZrO_2	Zirconium oxide

SYMBOLS

A_{bed}	Cross-sectional area of fluidized bed [m^2]
Ar	Archimedes' number [-]
$d_{reactor}$	Diameter of the reactor [m]
d_{bed}	Bubble diameter [m]
D_{solid}	Diameter of solid particle [m]
D_g	Diffusion coefficient of gas [-]
E_a	Activation energy [kJ/mol]
f_i	Fugacity [-]
f	Bed expansion factor [-]
f_n	Total gas generated by reaction occurring in the emulsion phase [kg/m^3s]
f_i	Flow rate of gas [kg/s]
f_m	Flow rate of solid [kg/s]
$f_{b\text{-}e}$	Mass transfer rate between the bubble and the emulsion phase [kg/m^3s]
g	Acceleration due to gravity [m/s^2]
G	Gibbs free energy [kJ/mol]
h	Enthalpy [kJ/kg]
h_o	Enthalpy at dead state [kJ/kg]
h_{bed}	Bed height [m]
K	Reaction kinetic constant [s^{-1}]
k_o	Reaction rate constant [s^{-1}]
$k_{b\text{-}e}$	Bubble to emulsion mass transfer coefficient [-]
MM	Molecular mass of the substance [gm]
nm^3	Volume occupied by gas at 25°C and 1 atm pressure [m^3]
n	Number of gas components [-]
N	Number of calcination-carbonation cycles [-]
P_{eq}	Equivalent pressure of the calcination reaction [atm]
P_{CO2}	Partial pressure of carbon dioxide [atm]
Q_{med}	Volumetric flow rate of fluidizing medium [m^3/s]
R	Universal gas constant [8.314 J/mol K]
Re	Reynolds number [-]
$RR_{gg}^{\ b}$	Reaction rate of the gas phase reaction in bubble [$kmol/m^3$ s]
$RR_{gg}^{\ e}$	Reaction rate of the gas phase reaction in emulsion [$kmol/m^3$ s]
$RR_{gs}^{\ e}$	Reaction rate of the gas solid reaction in emulsion [$kmol/m^3$ s]
s	Entropy [kJ/Kg K]

s_o	Entropy at dead state [kJ/kg K]
T	Temperature [K]
T_o	Temperature at dead state [K]
U_{mf}	Minimum fluidization velocity [m/s]
U_o	Superficial velocity [m/s]
U_{br}	Bubble rise velocity [m/s]
U_b	Bubble velocity [m/s]
x_i, y_i	Mole fraction of gas components [-]
X	Conversion [-]
Y	Mass fraction of gas and char yield [kg/kg of biomass]
Z	Mass fraction of different components of biomass [-]

GREEK LETTERS

ε^{ph}	Physical exergy [kJ/kg]
ε^{ch}	Chemical exergy [kJ/kg]
ε_{mf}	Voidage at minimum fluidization [-]
ε_b	Bubble voidage [-]
ε_{FB}	Voidage in freeboard [-]
ρ_{med}	Density of fluidizing medium [kg/m^3]
ρ_{solid}	Density of solid particles [kg/m^3]
ρ_{gas}	Density of gas [kg/m^3]
μ_i	Chemical potential of different gas components [kJ/mol]
λ	Lagrangian multiplier
θ	Temperature [^{o}C]
τ	Residence time [min]
μ_{gas}	Viscosity of gas [kg/m s]
φ	Sphericity of particle [-]
α_m	Fraction of solid [-]

SUBSCRIPTS

b	Bubble phase
bed	Gasifier bed
e	Emulsion phase
FB	Freeboard
gg	Gas phase
gs	Gas solid
i	Gas component
m	Hydrogen in biomass
	Solid component
n	Carbon in biomass
o	Dead state
p	Oxygen in biomass

ACKNOWLEDGEMENTS

The author wishes to express eternal gratitude and deep appreciation to his thesis supervisor Dr. Prabir Basu and Dr. Animesh Dutta, who played a key role at every stage of his study with conceptual discussion. Their guidance was crucial and invaluable in bringing this thesis to its fruition.

The author thanks the member of guiding committee Dr. Dominic Groulx and Dr. Su-Ling Brooks for their continuous support. Special thanks are to Dr. Alberto Gomez-Barea of University of Seville, who kindly agreed to serve as the external examiner.

The author acknowledges the support and help of the following individual:

Dr Augustus Leon, Ms. Vichuda Mettanant, Mrs Tanuja Battacharjee, Mr. Alok Dhungana, Mr, Mohit Rizal, Mr. Vijay Jain, Mr. Sagar Pokhrel, Mr. Shailendra Rao, Mr. Manuel Compoy Naranjo, Mr. Ray Dube, Mrs. Sandra Pereira, and Ms. Morgyn MacLeod.

The author is grateful to Mrs. Rama Basu, for her support and parental care during the author's study life at Dalhousie University.

The author acknowledges the financial supports of the National Science and Engineering Research Council (NSERC), Canada; Faculty of Graduate studies, Rosetti Scholarship Fund of Dalhousie; and Greenfield Research Inc. of Halifax. The author also acknowledges the generosity of Nova Scotia Agricultural College for providing the CFB-CLG unit on loan to CFB laboratory of Dalhousie University, and that of Point Aconi Power Plant of Nova Scotia Power for providing limestone used in the experiments.

Finally, the author gratefully acknowledges the continuing patience and encouragement of his beloved parents: Mahesh Acharya and Sabita Acharya, wife: Sebika Acharya, sisters: Anita Dahal and Manita Acharya and the author's brother-in-law: Pramod Dahal, whose love, support and tremendous sacrifices have encouraged the author throughout all his worthwhile life pursuits.

ABSTRACT

Environmental concerns and energy security are two major forces driving the fossil fuel based energy system towards renewable energy. In this context, hydrogen is gaining more and more attention in this 21st century. Presently, hydrogen is produced from reformation of fossil fuels, a process that could not address above two problems. For this it needs to be produced from a renewable carbon neutral energy source. Biomass has been identified as such a renewable energy source. Conversion of biomass through thermo-chemical gasification process in the presence of steam could provide a viable renewable source of hydrogen.

This thesis presents an innovative system based on chemical looping gasification for producing hydrogen-enriched gas from biomass. The other merit of this system is that it produces a pure stream of carbon dioxide by conducting in-process capture and regeneration of sorbent. A laboratory scale chemical looping gasification (CLG) system based on a circulating fluidized bed (CFB) is developed and tested. Experiments conducted to gasify sawdust in CFB-CLG system shows that it could produce a gas with as much as 80% hydrogen and as little as 5% carbon dioxide. A kinetic model is developed to predict the performance of the gasifier of a CFB-CLG system, and is validated against experimental results.

To understand the science of biomass gasification in the presence of steam and CaO, a number of additional studies are conducted. It show that for higher hydrogen and lower carbon dioxide concentration in the product gas, the optimum values of steam to biomass ratio, sorbent to biomass ratio, and operating temperature are 0.83, 2.0 and 670^{o}C respectively.

In CFB-CLG system the sorbent goes through a series of successive calcination-carbonation cycles. Calcination studies in presence of three alternate media, nitrogen, carbon dioxide and steam show, that steam calcination is best among them. An empirical relation for calcination in presence of three media is developed. Owing to the sintering, irrespective of medium used for calcination, the conversion of CaO reduces progressively as it goes through alternate calcination-carbonation cycles. An additional empirical equation is developed to predict the loss in sorbent's ability during carbonation.

CHAPTER 1: INTRODUCTION

This chapter explains the background of this research and defines the objectives, scope and limitation of this thesis.

1.1 BACKGROUND

With today's problem of global warming and urgent need for renewable energies, there is an increasing interest in hydrogen as an energy carrier (Lee et al., 2009). Hydrogen when converted produce water as by product which is benign to the environment. Therefore, introducing hydrogen in energy systems will help to overcome the greenhouse gas emission issues. As it can be produced from different feedstocks - natural gas, oil derived products, coal, biomass and water - it reduces the dependency on particular fuels, therefore enhancing the energy security (Cormos et al., 2008). Although just a concept a few decades ago, its efficient conversion to electricity through fuel cell technology is making hydrogen economy more realistic and practical. Continuous development and improvement in fuel cell technology and optimization of hydrogen production systems push the hydrogen economy forward by rendering it more efficient and cost-effective. However, the large investment needed for the infrastructure development of hydrogen economy is making it less competitive with conventional fossil fuel systems. At present, most of the hydrogen produced comes from the reformation of fossil fuels (Cormos et al., 2008), which does not address the current environmental issues. For hydrogen economy to become sustainable, it needs to be produced from renewable resources. Electrolysis of water could be a renewable option if the electricity for electrolysis comes from a renewable source like wind, geothermal, or solar energy. Typical of current wind and

solar technologies, hydrogen production from electrolysis systems powered by wind or solar energy face the limitation of being seasonal; also, the need for storage of excess energy produced during high winds makes the process difficult and less efficient. On the other hand, geothermal energy is not available everywhere. Thus, biomass could be the renewable energy source for production of hydrogen-rich gas (Hulteberg and Karlsson, 2009), which can be used in fuel cells to produce electricity or in transportation to replace oil. Biomass is more or less evenly distributed around the globe. Biomass not only includes conventional fuels (wood) but also unconventional fuels like municipal solid waste (MSW). With restrictions in the incineration of solid fuel in countries like Canada, gasification has been identified as the optimal technology for the conversion of these wastes into energy (Morris and Waldheim, 1998).

Among different types of gasifiers available, fluidized bed gasifiers offer more flexibility than other types of gasifiers for biomass gasification. Fixed bed gasifiers produce gas diluted with nitrogen and low concentrations of hydrogen. Also, the high methane concentration in the gas requires the reformer upstream to convert methane into hydrogen. Entrained bed gasifiers are best suited for coal as they can gasify almost all types of coal (Higman and Burgt, 2008). However this type of gasifier may not be suited for biomass gasification because of the difficulty in grinding biomass particles to a very small size (Drift et al., 2004). With biomass being highly reactive compared to coal, higher conversion can be achieved even at lower temperature and pressure, which makes the whole system look simple and easy to operate. In this context, fluidized beds offer a unique advantage for the gasification of biomass. Uniform temperatures, fuel flexibility,

and better mixing of solids are the merits of fluidized beds over the other types of gasifiers (Basu, 2006). Also, fluidized beds are more suitable for the allothermal operation of the gasifier: instead of directly combusting some fuel in the gasifier to meet the heat requirement, the same heat can be provided indirectly through the circulation of solids. Depending upon the gasification condition, this helps in many ways to produce a higher heating value gas rich in hydrogen.

Reduction in the release of carbon dioxide to the atmosphere from a thermochemical process has become an important issue. Although biomass is a carbon neutral feedstock, any reduction in carbon dioxide release could earn for the plant operator a direct carbon credit. This is difficult to achieve in conventional gasifiers where the gas is mixed with carbon dioxide and its separation from hydrogen requires separation technique like membranes.

Steam gasification of biomass in the presence of the sorbent calcium oxide (CaO) can produce a gas rich in hydrogen (Acharya et al., 2009; Mahishi and Goswami, 2007; Lin et al., 2002; Moghtaderi, 2007; Guan et al., 2007; Rapanga et al., 2000), which can be directly used as feed gas in fuel cells with minimum treatment of raw product gas. Using sorbent helps to capture carbon dioxide (CO_2) during the process of gasification while moving the reaction in the forward direction, favoring higher hydrogen yield. However, the use of sorbent does not seem viable if it cannot be reused in the system. A circulation system is needed to continuously regenerate and circulate the sorbent back into the gasifier. The concept of chemical looping gasification (Fig. 1.1) is thus born, where the

sorbent enters a loop in between the gasifier and the regenerator. Such type of system can be claimed as a carbon negative emission as it uses carbon neutral biomass as fuel. CO_2 is captured and separated within the process therefore no CO_2 is released directly into the atmosphere. Based on this concept, the carbon dioxide acceptor process was developed in 1970's (Basu, 2006; Fan, 2011). However in 1977, after limited testing, the project was terminated and not much work has been done in this area since then. Now, at the beginning of the 21st century, this technology is again gaining attention as a viable method of using coal as feedstock for energy production coupled with carbon dioxide capture.

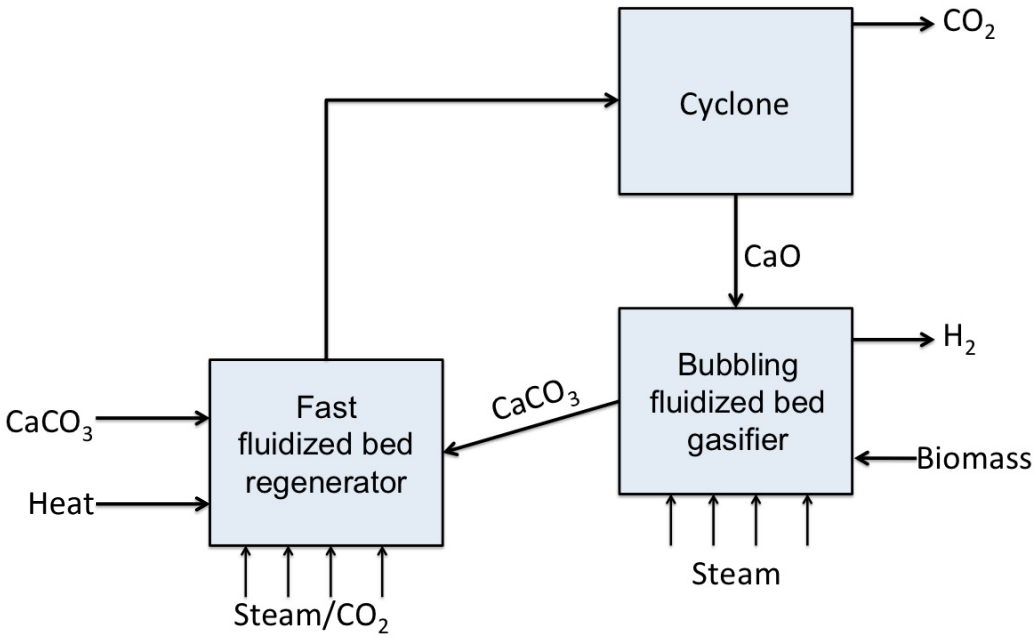

Figure 1.1: Schematic of chemical looping gasification

At present, most of the research in this area involves chemical looping combustion (CLC) and more specifically on the development of oxygen carriers (Fang et al., 2009). Thus not much work has been conducted specifically on the development of chemical looping gasification systems. Though widely recognized by many researchers, the research on

CLG of Dr. Fan and his group at Ohio State University is still a work in progress. Other advanced types of chemical looping system currently under research includes: the HyPr_Ring Process, the ALSTOM process, the fuel flexible advanced combustion-gasification process and the zero emission coal alliance process (Basu, 2006; Lin et al., 2002; Ziock and Lackner, 2000; Fan, 2011; Rizeq et al., 2002).

Almost all types of chemical looping systems face similar challenges, with one of them being the loss in sorbent/catalyst performance with time of operation. Studies are made to determine these losses and identify ways to improve sorbent performance so that the system can run satisfactorily for a longer time. The performance of the sorbent is uncertain and jeopardizes the success of the entire chemical looping system. This effect is most noticeable in the case of chemical looping gasification systems, where the ability of the sorbent to capture CO_2 and regenerate is drastically reduced by the deposition of char and tar and the sintering due to the high temperature operation and cyclic heating and cooling. Loss in sorbent reactivity is not the only challenge; another lies in designing systems to maintain the continuous flow of solid between different reactors operating at high temperatures and pressures.

This thesis proposes an innovative concept of chemical looping for gasification of biomass. Similar to other chemical looping gasification processes, it also aims to produce gas rich in hydrogen and to provide in-process capture of carbon dioxide and regeneration of sorbent to produce a pure stream of carbon dioxide. Innovation lies in its simple design

and capability in generating a pure stream of hydrogen and carbon dioxide using biomass as fuel, something not usually seen in other types of chemical looping systems.

1.2 OBJECTIVES

The broad objective of this study is to design and develop a circulating fluidized bed (CFB) based chemical looping gasification (CLG) system for gasification of woody biomass where CaO is used as a sorbent. Its performance in terms of the concentration of hydrogen and carbon dioxide in the product gas and the regeneration of sorbent is studied both experimentally and theoretically.

The specific objectives are as follows:

1. To investigate biomass gasification in the presence of CaO and steam in a fixed bed reactor and to study the effects of steam-to-biomass ratio (S/B), calcium oxide-to-biomass ratio (CaO/B) and temperature (T) on the hydrogen and carbon dioxide production.
2. To study the performance of the sorbent as it goes through alternative cycles of carbonation and calcination.
3. To study the effects of particle size, temperature and type of fluidization medium on the calcination-carbonation reaction and to develop a kinetic model for calcination carried out in the presence of steam, nitrogen and carbon dioxide.
4. To design and develop a laboratory scale CFB-CLG system.
5. To investigate the calcination-carbonation cycle in a CFB-CLG system.
6. To investigate biomass gasification in a CFB-CLG system.

7. To develop a non-stoichiometric model for biomass gasification in presence of CaO and steam and to compare the results with experimental findings.
8. To develop a kinetic model for gasification of biomass in the gasifier of a CFB-CLG system and to compare the results with experimental findings.

1.3 SCOPE AND LIMITATIONS

The research comprises of eight individual works, the scopes of which are explained below:

Study 1: A fixed bed reactor was used to examine the mechanism of biomass gasification in the presence of CaO and steam. During the experiments, only the gaseous components were measured and analyzed.

Study 2: The study of sorbent performance over a number of calcination-carbonation cycles was conducted in a quartz wool matrix reactor (QWM), with the number of cycles limited to 5. The particle size considered for this study is 45 microns. The calcination was carried out in the presence of three different media: nitrogen (N_2), carbon dioxide (CO_2) and steam (H_2O), while the carbonation in pure carbon dioxide. The temperatures for calcination and carbonation were 950^oC and 650^oC respectively.

Study 3: The effect of particle size on the extent of calcination and carbonation was studied. The sizes were chosen according to size distribution of particle to be used for chemical looping gasification (CLG) system. The effect of temperature on calcination

was studied for temperatures of 700°C, 800°C, 850°C, 900°C, and 1000°C for each type of media studied (N_2, CO_2 and H_2O). A first-order kinetic model was developed to analyze the kinetics of calcination in the presence of these three media.

Study 4: The design of a chemical looping gasifier consists of mainly identifying the dimensions of the reactor (diameter and height) and the operating conditions, which include the flow of gasifying medium. The connections between the reactors are made in such a way that the whole system can be modified to work as a CFB gasifier, or bubbling bed gasifier, which also facilitates easy cleaning. The design was based on empirical relations and years of experience of Prof. Prabir Basu working with circulating fluidized beds.

Study 5: The calcination-carbonation reaction was studied in the designed CFB-CLG system. The regenerator was fluidized with steam while the gasifier was fluidized with a mixture of gas composed of 75% N_2 and 25% CO_2. For comparison, a study was conducted by fluidizing the regenerator with air while maintaining similar operating conditions in the gasifier.

Study 6: Gasification of biomass was investigated in two ways: operating the gasifier as a bubbling bed without running the whole calcium loop cycle and then operating both the BFB and the riser. In the first case biomass was fed to the top of the gasifier bed, which was operated at the following flow conditions: steam flow of 1.5 kg/h and biomass feed rate of 0.5 kg/h. CaO was mixed with biomass in ratio 1:2 and fed along with the

biomass. CaO was used as the bed material in this study and the result was compared with another study done using inert sand as the bed material. The gasifier was operated at a temperature of 550-600^{o}C.

While running the chemical looping gasifier, biomass was fed into the bed through a screw feeder. The biomass feed rate was 0.2 kg/h while maintaining the same flow of steam was kept the same as in the previous experiment. The regenerator and the loopseal were both fluidized with nitrogen. The regenerator was operated at an average temperature of 850-900^{o}C while the gasifier temperature was 550-600^{o}C.

Study 7: A non-stoichiometric equilibrium model was developed based on the concept of the minimization of Gibbs free energy. The result obtained from the study 1 and study 6 was compared with the result obtained from this model. The limitation of this was that it does not consider the kinetics of reaction as it assumes a complete conversion of biomass. Also, the tar formed during the gasification was not accounted for. Therefore, this model gives the maximum amount of hydrogen that can be produced during gasification.

Study 8: A kinetic model was developed to predict the performance of the gasifier of the CFB-CLG system. To model the gasifier, the gasifier was divided into two zones, the lower dense bed zone and the upper free board zone. The dense bed zone is modeled as a two-phase mixture consisting of a bubble and emulsion phase while the freeboard zone is modeled as a single gaseous phase. Furthermore, it was assumed that devolatilization occurs instantaneously as biomass enters the bed and thus the gas produced divides into

the bubble and emulsion phase. The hydrodynamics equation of the bubble and emulsion phase was taken from published literatures. The different reactions considered were: the char gasification reaction, the water gas shift reaction, the Boudouard's reaction, and the carbonation reaction. The results obtained from this model are compared with the results obtained from studies 6 and 7.

1.4 CONTRIBUTION OF THIS DISSERTATION

In addition to the valuable contribution of designing, installing, and operating the circulating fluidized bed (CFB) based chemical looping gasification (CLG) system, this thesis represents an invaluable addition to the efforts for better understanding of gasification of biomass in the presence of the sorbent, calcium oxide. Other valuable scientific contributions are summarized below:

1. The experimental investigation of steam gasification of biomass in the presence of CaO and its validation with a non-stoichiometric model helps in further understanding the process.
2. The investigation of high temperature steam calcination of sorbent and change in its reactivity during carbonation over a number of calcination-carbonation cycle has not been previously carried out in literature. Empirical relations developed for high temperature calcination in the presence steam, nitrogen and carbon dioxide fills this knowledge gap. Also, an empirical relation is developed for loss in sorbent ability to capture carbon dioxide during multiple successive calcination-carbonation. Furthermore, a study done to examine the effects of temperature and

particle size on calcination and carbonation helps in better understanding the process.

3. A kinetic model developed for predicting the performance of the gasifier of CFB-CLG system is new to the modeling of bubbling fluidized bed gasifiers with CaO as bed material. Previously, only simple modeling approaches have been used to simulate the gasification process in a bubbling fluidized bed in presence of CaO.

1.5 CO-AUTHORSHIP

Following is a list of some aspects of this research that underwent peer review and published in archival literatures.

Chapter 2

Production of bio-syngas and biohydrogen via gasification

Dutta A & Acharya B

A book chapter in: Handbook of biofuel production: processes and technologies. Edited by: R Luque, J Campelo and J Clark. Woodhead Publishing, 2011

Chapter 3

Chemical looping gasification of biomass for hydrogen enriched gas production with in-process carbon-dioxide capture

Acharya B, Dutta A and Basu P

Published in *Energy and Fuel*, 2009; 23, 5077–5083

Design methods for fluidized bed gasifiers – a comparison of different approaches

Basu P, **Acharya B** and Kaushal P

Published in the *Journal of Energy Institute*, 2010; 83; eni9454.3d

Chapter 4

An Investigation into Steam Gasification of Biomass for Hydrogen Enriched Gas production in Presence of CaO

Acharya B, Dutta A and Basu P

Published in the *Int. J. of Hydrogen Energy*, 2010; 35; 1582-1589

Chapter 5

Circulating Fluidized Bed Based Chemical Looping Gasifier: Experimental Studies on Calcination-Carbonation Cycle

Acharya B, Dutta A and Basu P

Submitted to the Journal of *Industrial and Engineering Chemistry Research,*

Chemical Looping Gasification - A Study on Calcination/Carbonation Looping Cycle

Acharya B, Dutta A and Basu P

AICHE spring meeting, 13-17 March 2011, Chicago, USA

Study of Calcination-Carbonation of Calcium Carbonate in Different Fluidizing Mediums for Chemical Looping Gasification in Circulating Fluidized Beds

Acharya B, Dutta A and Basu P

International Conference on Circulating Fluidized Beds and Fluidized Bed Technology-CFB 10, 1-5 may 2011, Oregon, USA

Chapter 6

Gasification Of Biomass In A Circulating Fluidized Bed Based Chemical Looping Gasifier For Hydrogen-Enriched Gas Production

Acharya B, Dutta A and Basu P

Submitted to the Journal of *Chemical Engineering Science,*

1.6 ORGANIZATION OF THE THESIS

A schematic of the organization of the contents of this thesis is shown in Fig 1.2. A short outline of main chapters of the thesis is given below:

Chapter 2: This chapter begins with a review of the current status of and different pathways for hydrogen production. It is followed by the literature review on gasification of biomass and the different types of gasifiers. The middle section focuses on the chemical looping system with emphasis given to chemical looping gasification.

Chapter 3: This chapter defines the CFB-based chemical looping system. The energy and exergy balance of the chemical looping gasification system is included along with the design calculation for the CFB-based chemical looping gasifier.

Chapter 4: This chapter presents the gasification study conducted on the fixed bed reactor to understand the effects of steam/biomass ratio, CaO/biomass ratio and temperature on gas composition and yield. The results of the non-stoichiometric equilibrium model and their comparison with experimental results are also included in this chapter.

Chapter 5: Work done to study the calcination-carbonation reaction of sorbent is presented in this chapter. The effect of temperature on calcination was studied and the first order kinetic equation was developed to understand and compare the calcination reaction in the presence of steam, nitrogen and carbon dioxide. Also studied and included in this chapter is the effect of particle size on calcination and carbonation. The

performance of sorbent over a number of calcination-carbonation cycles is investigated and presented here along with the empirical relation developed to predict the loss of sorbent ability to capture carbon dioxide during the carbonation reaction.

Chapter 6: This chapter begins with an experiment carried out to study the calcination-carbonation cycle in CFB-CLG system. This is followed by a gasification experiment performed only in a bubbling bed gasifier. The results of experiment conducted on the complete CFB-CLG system are presented here. Finally the chapter ends with the kinetic modeling of the gasifier and its comparison with the experimental results.

Chapter 7: The conclusions and recommendation for future works are included in this chapter.

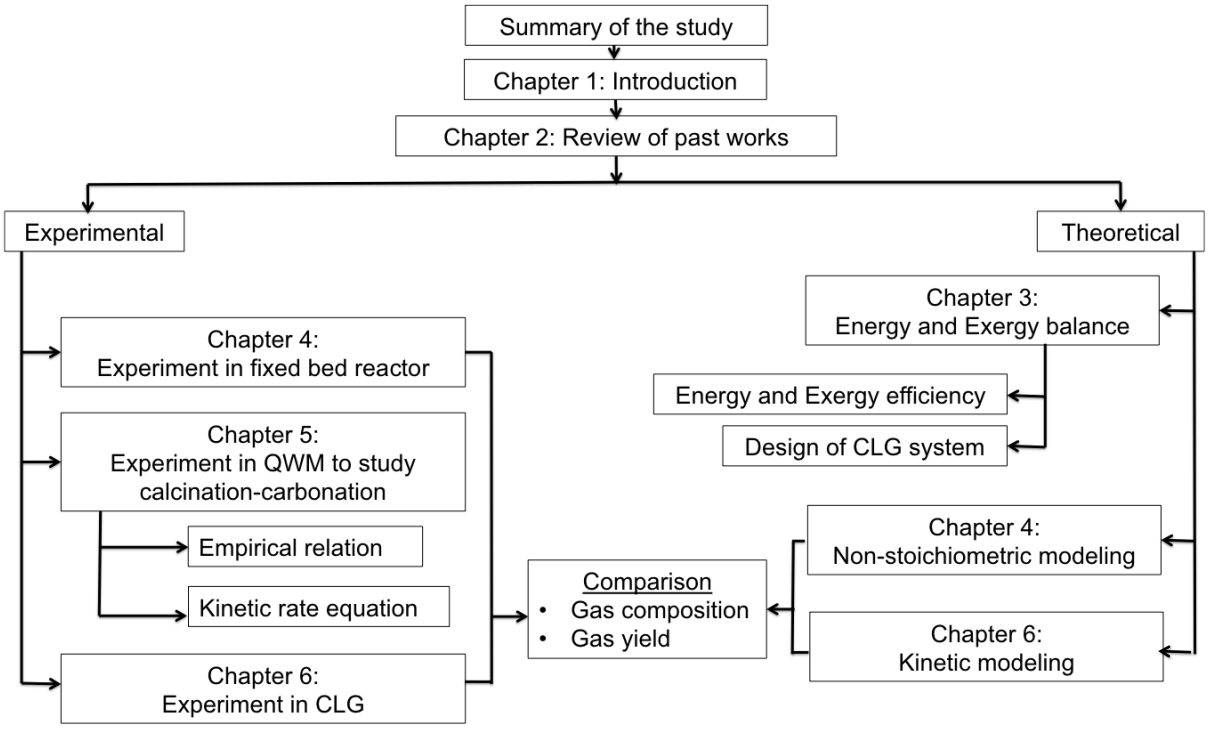

Figure 1.2: Summary of the study

CHAPTER 2: LITERATURE REVIEW

This chapter reviews the state of the art of the existing research on chemical looping system and identifies the knowledge gaps in this field.

2.1 INTRODUCTION

Currently about 87% of the world's energy requirement is met by fossil fuels (BP statistical review). The continuous use of fossil fuels will lead to depletion of these resources, and degrade our environment due to an increased concentration of greenhouse gases (GHG) in the atmosphere. The increasing concentration of GHG is accelerating the global warming and climate change. Thus, to slowdown these environmental problems while considering energy security issues, there is a need to exploit non-polluting and renewable energy sources (Khanal et al., 2004). In this context, as a non-polluting fuel producing only benign water as a by-product, hydrogen energy can be a promising future energy source (Balat, 2008). Furthermore, it has higher conversion efficiency (Das and Veziroglu, 2001) and the highest gravimetric energy density (142 MJ/kg) compatible with the electrochemical and the combustion process for energy conversion (Levin et al., 2004). The major drawbacks of hydrogen are low density and consequently low volumetric heat content. Currently, the main use of hydrogen is as the industrial chemical for the production of ammonia, as well as refinery use for desulfurization and other processes like ethanol production. The annual world production is around 500 billion Nm^3 and 50% of this comes from steam methane reformation (Dutton, 2002).

Hydrogen can be produced from different sources, which are summarized below (Das and Veziroglu, 2001):

A. From fossil fuels
- Steam reforming of natural gas
- Thermal cracking of natural gas
- Partial oxidation of heavier than naphtha hydrocarbons
- Coal gasification

B. From biomass
- Pyrolysis or gasification

C. From water
- Electrolysis
- Photolysis
- Thermochemical process
- Direct thermal decomposition or thermolysis
- Biological production

At present, hydrogen is produced in commercial scale from reformation of natural gas, naphtha, and coal. In doing so it emits equivalent amounts of CO_2 as by combusting these fuels (Sigfusson, 2007). At the laboratory scale, many studies have been carried out on the production of hydrogen from electrolysis, photolysis and thermolysis (Demirbas, 2004). Hydrogen production from the electrolysis process is controversial as the electrolysis of water is energy-intensive. Hydrogen production from this process will be considered renewable only if this energy comes from a renewable source. For example, "wind-to-wheel" efficiency is at least three times greater for electric cars than for hydrogen cars when hydrogen is produced from electrolysis of water. The capital cost of electrolysis is also very high compared to other technologies (Dutton, 2002). The photolysis process has very low conversion efficiency and does not allow for continuous production of hydrogen because it is only feasible in the presence of sunlight.

The future of energy is moving towards hydrogen but it can sustain itself only if it is generated from environmentally friendly, abundant, and renewable biomass (Sigfusson, 2007). The technology for generation of hydrogen from biomass shows great potential (Saxena et al., 2007; Balat, 2008). Biomass is a renewable energy resource, and is also a CO_2 neutral fuel because the CO_2 released during combustion is absorbed back by biomass for growth during photosynthesis (Basu, 2010). Biomass fuel includes wood, short-rotation woody crops, agricultural wastes, wood wastes, sawdust, bagasse, and animal wastes. Municipal solid waste is also included as a source of biomass (Demirbas, 2004; Bhattacharya et al., 2005). Because of its low energy density, biomass is less competitive than other fossil fuels. However, thermochemical processes like gasification is found to be more attractive option for biomass to energy conversion (Rapanga et al., 2000). Along with gasification, fast pyrolysis can also be considered as another thermochemical option for production of hydrogen but the yield depends greatly on temperature, heating rate and residence time, which are difficult to control (Demirbas et al., 2002). However, production of hydrogen from biomass has certain limitations mainly because of its low hydrogen and high oxygen content.

2.1.1 Pathways for Hydrogen Production

Based on the available technology, different pathways for hydrogen production (Fig 2.1) can be categorized into the following (Ni et al., 2006; Sigfusson, 2007):

1. Thermochemical processes: pyrolysis, liquefaction and gasification
2. Electrolysis
3. Photo-electrochemical processes (PEC).

4. Biological processes: bio-photolysis (direct and indirect), photo fermentation, dark fermentation

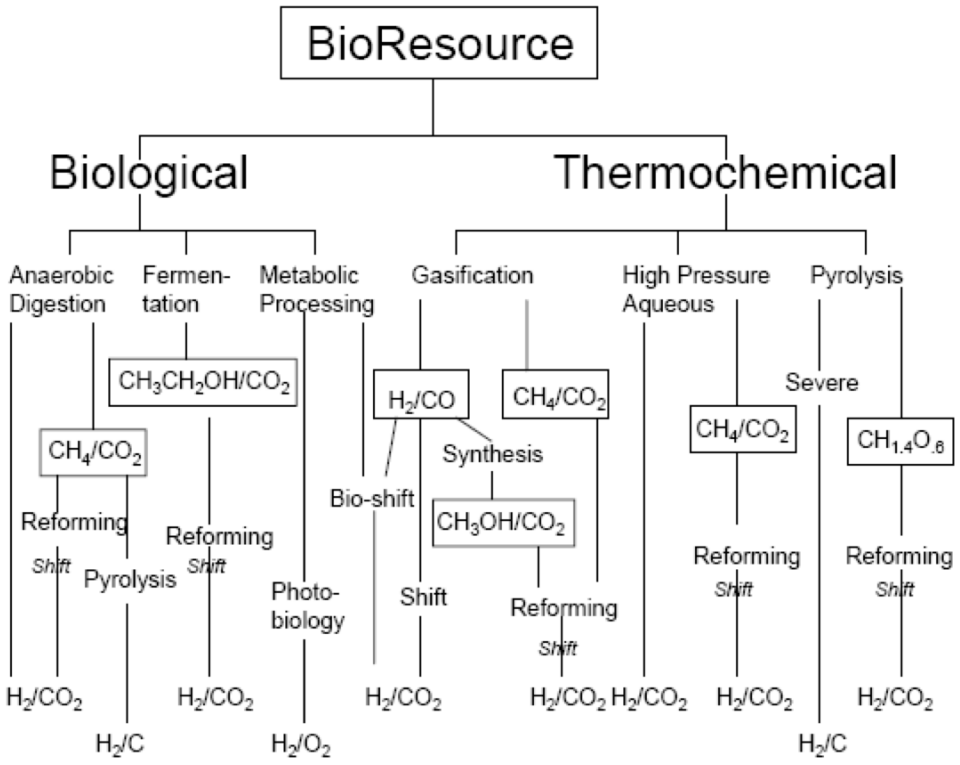

Figure 2.1: Pathways of hydrogen production from biomass

In thermochemical processes, biomass is subjected to an environment of controlled temperature and pressure, with or without the presence of a catalyst. For pyrolysis, the temperature is maintained within 380-530^{o}C in the absence of air. Based on the heating rate, final products vary between solid charcoal, liquid oil and gaseous compounds (Ni et al., 2005). Pyrolysis is a preferred choice only when char or liquid hydrocarbons are primary products of interest. Reformation of these primary products can produce hydrogen rich gas (Demirbas et al., 2002; Evans et al., 2003) but these render the whole system inefficient.

For gas yield, gasification is a better option. The gasification process operates in the presence of gasifying mediums air/oxygen/steam in a temperature range of 700-1500^{o}C and a pressure from 1 bar to over 20 bars. In these conditions, the hydrocarbon undergoes thermal decomposition resulting in higher gas yield. Steam gasification of biomass in the presence of a catalyst can result in a higher hydrogen yield (Acharya et al., 2009; Mahishi and Goswami, 2007; Lin et al., 2006; Moghtaderi, 2007; Guan et al., 2007; Rapanga et al., 2000). Thermochemical cycling (Fig 2.2) is another technology for the production of renewable hydrogen using solar energy or heat from nuclear reactors. However, it is still in the research phase.

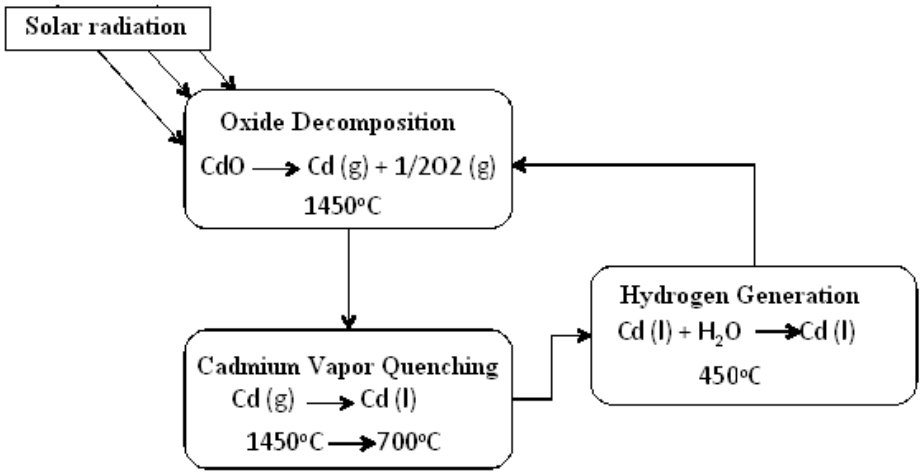

Figure 2.2: Schematic of the cadmium oxide thermochemical cycle

The electrolysis process (breakdown of water molecules into hydrogen and oxygen) is being used commercially in some places even though its share in total hydrogen production is around 4%. This process is a practical renewable option only if the energy required for electrolysis is produced from renewable sources like wind & solar. Iceland is a leading country in renewable hydrogen production with definite plans to shift its energy system to hydrogen economy. The relatively inexpensive electricity produced from

renewable geothermal resources makes hydrogen from electrolysis of water a feasible option for Iceland (Sigfusson, 2007). Photo-electrochemical processes use solar energy to displace electrons from a semiconductor device kept in an electrolyte, producing energy to break water molecules into hydrogen and oxygen. The limitation is the fact that the semiconductor materials are not yet developed to work efficiently in an aqueous environment. Bio-photolysis hydrogen production uses light to split water into hydrogen and oxygen. Depending on the microorganism used, this can be accomplished in two ways. The photosynthetic capabilities of green algae and cyanobacteria can be used to generate oxygen and hydrogen ions, after which a hydrogenase enzyme converts the hydrogen ions to hydrogen gas. The second pathway, present only in cyanobacteria, is similar. It uses direct photolysis to split the water, but employs a nitrogenase (nitrogen fixing) enzyme to produce hydrogen. Dark fermentation uses anaerobic bacteria on carbohydrate-rich substrates grown in the dark. For fermentative processes, the biomass used needs to be biodegradable, available in high quantities, inexpensive, and must possess high carbohydrate content. Table 2.1 summarizes different biological processes.

Considering the maturities of the different technologies mentioned above, gasification has been identified as an attractive option for higher hydrogen yields from biomass and is being discussed in detail here.

Table 2.1: Summary of biological hydrogen production

Methods	Bacteria	Reaction mechanism	Remarks
Direct biophotolysis	Green algae	$2H_2O \xrightarrow{\text{Light energy}} 2H_2+O_2$	Anaerobic condition
Indirect biophotolysis	Cyanobacteria (blue green algae)	$12H_2O + 6CO_2 \xrightarrow{\text{Light energy}} C_6H_{12}O_6+6O_2$ $C_6H_{12}O_6 +12\ H_2O \xrightarrow{\text{Light energy}} 12H_2+ 6CO_2$	
Photo-fermentation	Purple non-sulfur bacteria	$C_6H_{12}O_6 +12\ H_2O \xrightarrow{\text{Light energy}} 12H_2+ 6CO_2$	Catalyzed by nitrogenase under nitrogen deficient conditions
Dark fermentation	Enterobacter Bacillus and Clostridium	$C_6H_{12}O_6 +2\ H_2O \rightarrow 2CH_3COOH+4H_2+ 2CO_2$	Anaerobic bacteria grown in the dark on carbohydrate-rich substrates

2.2 GASIFICATION

Gasification, once extensively used for transportation and lighting during the Second World War, is again gaining momentum and presenting new possibilities. Its growth in the past has been slow but future predictions show a sharp rise (Fig 2.3). At present the energy production from gasification is around 60 GW_{th} with most of it used for chemical production. In coming years, the energy production from gasification is set to grow rapidly, reaching around 150 GW_{th} by 2014 (Higman and Burgt, 2008), which is 1.5 times more than its present-day use. Most of these gasifiers would be used for power generation as shown in Fig 2.4.

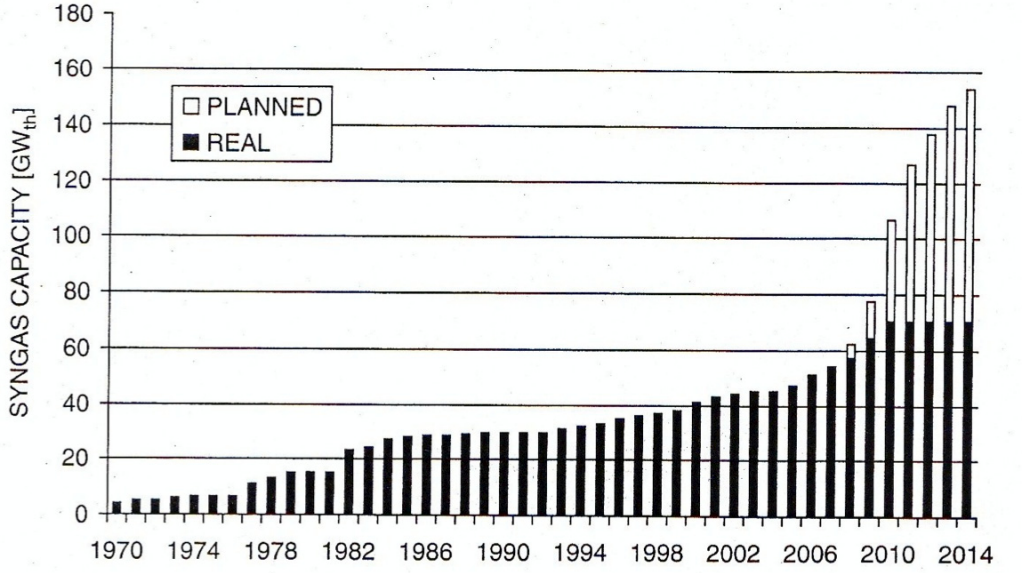

Figure 2.3: Worldwide gasification capacity (Higman and Burgt, 2008)

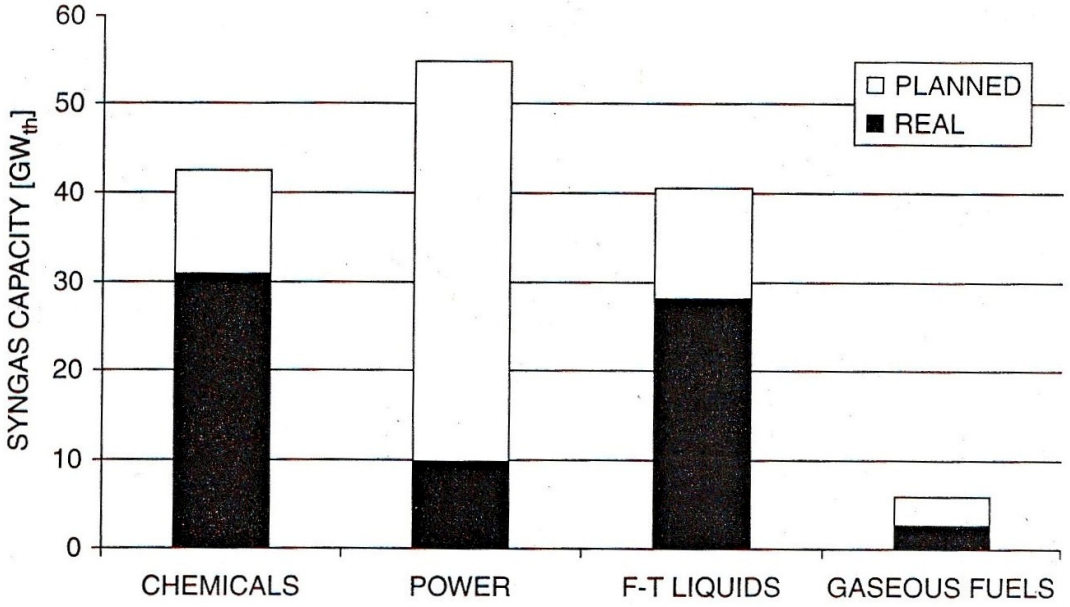

Figure 2.4: Worldwide gasification capacity for different applications (Higman and Burgt, 2008)

Advantages of gasification include production of more valuable, environmentally friendly gaseous products from conventional fuels as well as from non- conventional difficult-to-handle fuels such as biomass. Also, the volume of gas produced is much lower in gasification than in combustion, thus a relatively smaller unit is required for the gas cleaning process. However, lower carbon conversion, production of tar, requirement of complex auxiliary equipment, and lower availability and reliability are some of the barriers in the path of its commercialization (Basu et al., 2009).

2.2.1 Mechanism of Gasification

Solid fuel in the presence of a gasifying agent (air, oxygen, steam) under high heat undergoes chemical decomposition to produce the useful mixture of gas. According to the type of gasifying agent used, the heating value of the product gas obtained will also be different.

The conversion of gasification feedstock can be divided into several gross stages (Dutta and Acharya, 2011, p. 420-459): (1) decomposition of the original feedstock into volatile matter and char; (2) conversion of the volatiles by secondary reactions (combustion and reforming); and (3) conversion of the char by "char gasification" reactions with H_2O and CO_2 to produce fuel gases (CO, H_2, CH_4), in addition to char combustion when oxygen is present. Devolatilization produces a broad spectrum of products ranging from light gases to tars. The products are strongly dependent on the identity of the feedstock and process conditions, such as heating rate. These products may contain valuable species. Partial reforming of these products by contact with components of the char bed may result in improvement of the gas quality. For example, if fuel gas is the desired product, such

conversion would preserve methane while reforming undesirable tars. The progress of such reforming reactions is dependent on the nature of the char, including the inorganic (ash) components, and the type of reactor. The conversion of the entire feedstock to fuel gases by gasification reactions is generally endothermic, and air or oxygen is typically added to heat balance the process. In general, the solid fuel undergoes the following four processes during gasification, which are more distinctive in the case of the moving bed gasifier (such as an up-and-down draft gasifier) than in the case of fluidized bed gasification. The mechanism of gasification is shown in Fig 2.5 and is explained in detail below.

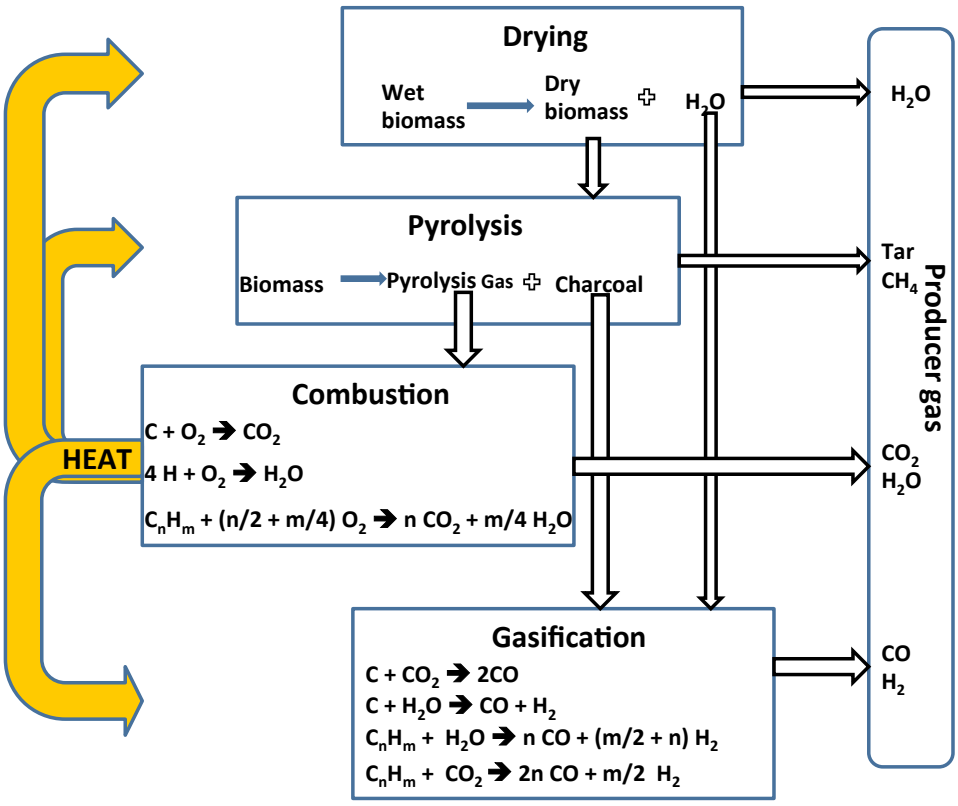

Figure 2.5: Mechanism of gasification

1. Drying: In this zone, the moisture in the feedstock is vaporized. The feedstock is not decomposed because the temperature is not high enough to cause any chemical reactions.

2. Pyrolysis: During pyrolysis or devolatization, the volatile content of the matter is released from the feedstock and char is left over. This reaction occurs in the absence of oxygen and at a temperature around 300-500^{o}C. The reaction occurring in this zone is endothermic in nature, thus the heat required is provided by the combustion of feedstock during the oxidation process.

$$\text{Feedstock} = \text{Char} + \text{Volatiles} + \text{Energy (kJ/kg)} \qquad [2.1]$$

3. Oxidation: In this process, the feedstock is combusted with the air supplied. As gasification is an endothermic process, the overall heat required is produced during this process. To maintain the favorable temperature in the gasifier and also to avoid excess dilution of the product gas, the equivalence ratio (actual air supply/stoichiometric air supply required for complete combustion) is maintained between 0.2-0.4. The reactions taking place in this process are:

$$C + O_2 \rightarrow CO_2 \qquad [2.2]$$

$$2H_2 + O_2 \rightarrow 2H_2O \qquad [2.3]$$

4. Reduction: In the reduction process, several reactions take place. The products from this process are mainly gases consisting of carbon dioxide, hydrogen, methane and carbon monoxide. The following reactions take place:

$$\text{Boudouard Reaction: } C + CO_2 \rightarrow 2CO \qquad [2.4]$$

$$\text{Water-Gas Reaction: } C + H_2O \rightarrow CO + H_2 \quad [2.5]$$

$$\text{Methane Reaction: } C + 2H_2 \rightarrow CH_4 \quad [2.6]$$

$$\text{Water-Gas Shift Reaction: } CO + H_2O \rightarrow CO_2 + H_2 \quad [2.7]$$

2.2.2 Types of Gasifiers

Various gasifier technologies have been developed over many decades, tailored to suit specific needs. These processes operate at pressures from atmospheric to >20 bars and at temperatures between 700-1500°C (Dutta and Acharya, 2010). Depending on the amount of heat provided for gasification, the gasifier can be categorized into two types: autothermal gasification and allothermal gasification. Autothermal gasification means the heat required to sustain the gasification reaction is generated within the process. Generally air/O_2 gasification falls into this category, where a part of the fuel is combusted to generate the heat required for the gasification reaction to occur. Autothermal gasification results in low/medium heating value product gas. On the other hand, allothermal gasification is one in which the heat required is generated separately and is transferred to the gasifier. An example of such system is the dual fluidized bed gasifier where the solids in the gasifier carry the heat. This type of gasification results in a product gas with medium or high heating value. Also, allothermal gasification can produce a gas rich in hydrogen (Dutta and Acharya, 2010).

According to the way the feedstock is brought in contact with the gasifying agent, the gasifier is classified into the following types:

2.2.2.1 Fixed Bed Gasifier

Fixed bed gasifiers, which consist of a fixed bed of biomass through which the oxidation medium flows in updraft or downdraft configuration, are simple and reliable designs and can be used to gasify wet biomass economically on a small scale for CHP applications (Wang et al., 2008). However, they produce syngas with large quantities of either tar and/or char due to the low and non-uniform heat and mass transfer between solid biomass and gasifying agent (Wang et al., 2008). Product gas must thus be extensively cleaned before use. Moreover, the throughput for this type of gasifier is relatively low and therefore for large-scale applications with very strict requirements concerning the purity of the syngas, as in the case of Biomass to Liquid (BTL), fixed bed gasifiers are considered unsuitable.

There are three types of fixed bed gasifiers, as shown in Fig. 2.6: updraft (counter-current), downdraft (co-current), and cross draft gasifiers. In the case of the updraft gasifier, the fuel is supplied at the top and the air at the bottom such that the fuel moves against the airflow. Whereas in the case of the downdraft, air is introduced above the oxidation zone and product gas is removed from the bottom. In cross draft gasifiers, feedstock moves downward while the product gas leaves in a cross direction. Fig. 2.7 shows the temperature distribution along the height of the fixed bed gasifier.

In an updraft gasifier, the tar formed does not pass through the combustion zone since it lies below the pyrolysis zone. This results in higher tar content in the product gas, which ultimately means that updraft gasifiers are not suitable for engine applications. This is

opposite to the case of downdraft gasifiers where the entire pyrolyzed product passes through the oxidation zone and the product gas has lower tar content. As in the case of updraft gasifiers, the hot gases move upward so that their energy is available to vaporize the moisture. Due to this property, updraft gasifiers can gasify relatively higher moisture content fuel than downdraft gasifiers. Furthermore, constriction in the oxidation zone of the downdraft gasifier makes its designing more complicated and difficult to upscale. Cross draft gasifiers are used mainly for charcoal gasification. However, during the process the temperature can reach 1500^{o}C, which could lead to material problems (Stassen and Knoef, 2001).

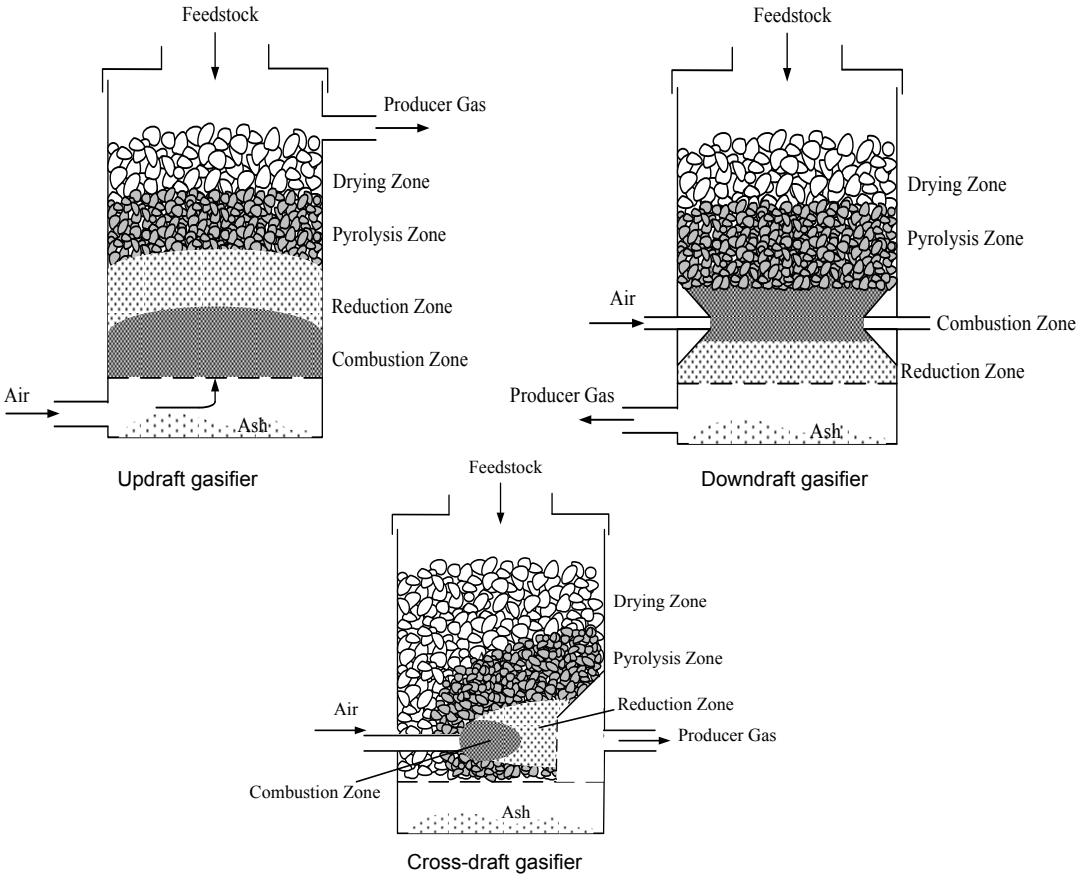

Figure 2.6: Different types of fixed bed gasifiers

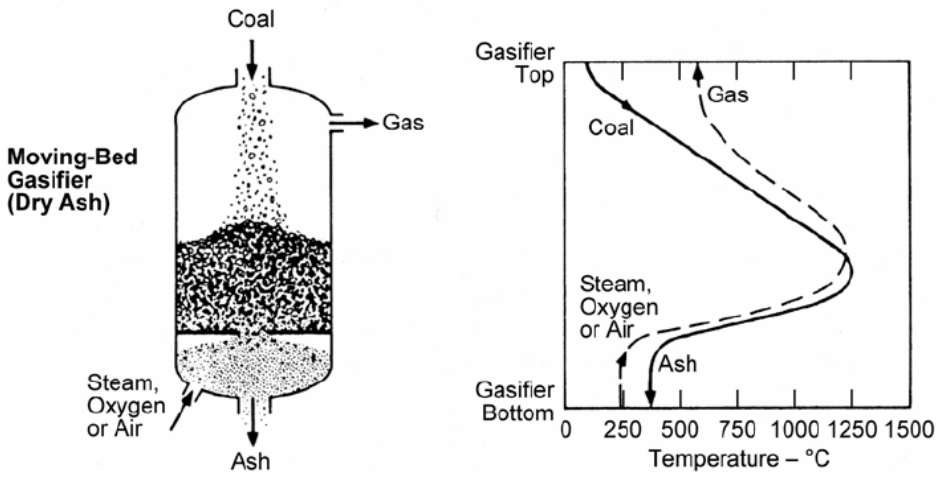

Figure 2.7: Temperature distribution in an updraft gasifier (Higman and Burgt, 2003)

2.2.3.2 Fluidized Bed Gasifier

The first fluidized bed gasifier was developed by Fritz Winkler of Germany in 1921. It was later used for powering gas engines. Since 1921, several companies have been involved in making fluidized bed gasifiers more efficient and competitive with other technologies.

Fluidized bed gasifiers provide excellent gas/solid mixing. They can be operated at lower temperatures (around 800-900^{o}C) than fixed bed gasifiers. This reduces NO_X emission. Also, better fuel flexibility and efficiency in capturing carbon dioxide are some of the advantages of this type of gasifier. Moreover, fluidized bed gasifiers offer short residence time, high productivity, low char/tar contents, high cold-gas energy efficiency and reduced ash-related problems (Wang et al., 2008).

A fluidized bed gasifier mainly consists of the bed of hot solid that is fluidized by the gasifying agent (air, oxygen, or steam). When the feedstock is fed into the hot bed it undergoes gasification in the presence of the gasifying agent and the product gas leaves

from the top of the gasifier. If the bed solid leaving the furnace is captured and again re-circulated into the gasifier, it is called a circulating fluidized bed (CFB) and if not, it is a bubbling fluidized bed (BFB). The bubbling bed gasifier is generally operated at a lower velocity (2~2.5 m/s) to ensure particles do not leave the reactor. The circulating fluidized bed is operated at a higher velocity (3~5 m/s) and particles leaving the reactor are separated in a cyclone and fed back to the reactor. CFB gasifiers are very suitable for large-scale syngas production (Hamelinck et al., 2004; Wang et al., 2008; Tijmensen et al., 2002; Zhang, 2010). Besides H_2 and CO, the gas produced by CFB gasifiers (operated at ~900°C) contains considerable amounts of CO_2, H_2O and hydrocarbons like CH_4, C_2H_4, benzene and tars. Thus, the product needs further treatment to convert the hydrocarbons to H_2 and CO. The temperature distribution along the height of the fluidized bed gasifier is shown in Fig. 2.8. In the case of fluidized bed gasifiers, the temperature is more uniformly distributed.

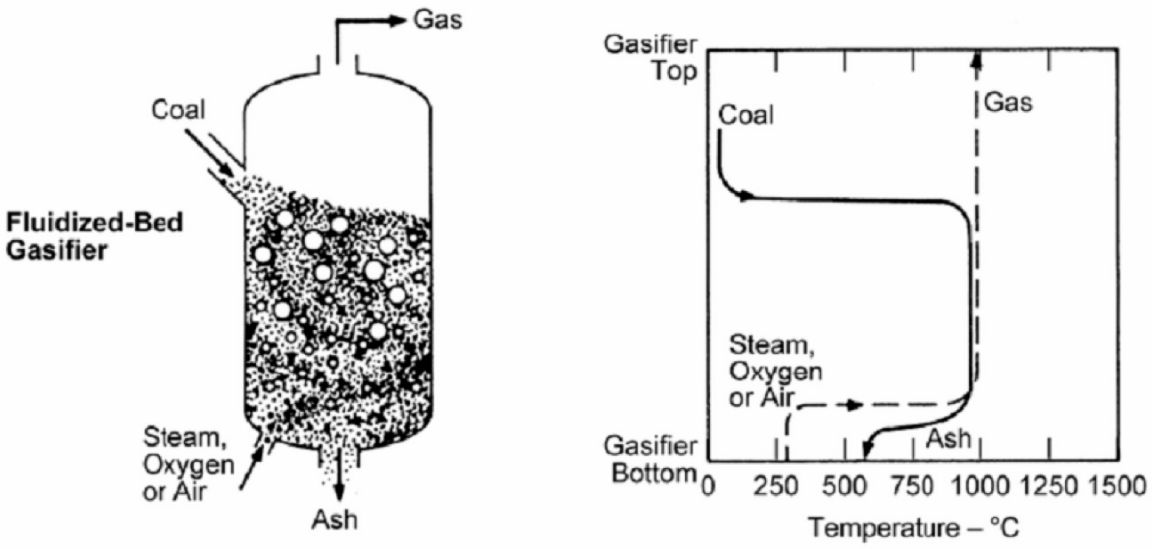

Figure 2.8: Temperature distribution in a fluidized bed (Higman and Burgt, 2003)

Fig. 2.9 shows the different types of fluidized bed gasifiers that are commercially developed. The Winkler gasifier invented in 1920 was probably the first type of gasifier to use fluidization on an industrial scale to gasify pulverized coal.

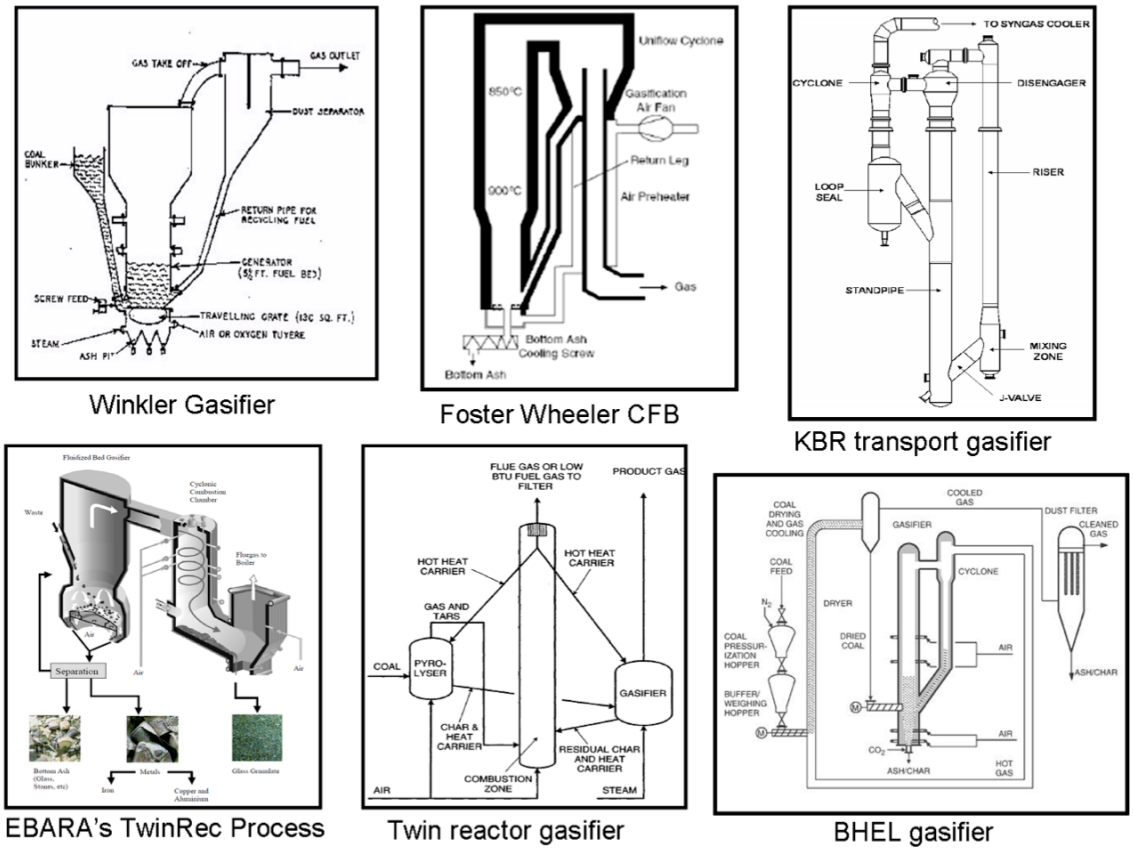

Figure 2.9: Different types of fluidized bed gasifiers (Dutta and Acharya, 2011)

The foster wheeler CFB is an air-blown gasifier operating at atmospheric pressure. Depending on the fuel and the application, it operates at a temperature within the range of 800-1000^{o}C. The hot gas from the gasifier passes through a cyclone, which separates most of the solid particles associated with the gas and returns them to the bottom of the gasifier. In the twin reactor gasifier, pyrolysis, gasification and combustion take place in different reactors. In the combustion zone, the tar and gas produced during pyrolysis are combusted to heat the inert bed material, which is then circulated into the gasifier and the pyrolysis reactor to supply the heat. The char and the heat carrier from the pyrolyzer are

taken into the gasifier. The gasification of char in the presence of steam produces the product gas. The residual char and the heat carriers from the gasifier are taken back into the combustor. This system was developed to overcome the problem of tar. The KBR transport gasifier is a hybrid gasifier having characteristics of both entrained bed gasifiers and fluidized bed reactors. The KBR gasifier operates at considerably higher circulation rates, velocities (11-18 m/s), and riser densities than a conventional circulating fluidized bed. This results in higher throughput, better mixing, and higher mass and heat transfer rates. The transported solids are separated from the product gas in two stages and returned to the base of the riser. The gasifier operates at 900-1000^{0}C and 11-18MPa (Higman and Burgt, 2008). EBARA's TwinRec Process gasifier is used primarily to recover recyclable materials by removing their organic components through gasification and combustion (Steiner et al., 2002). Bharat Heavy Electrical Limited (BHEL) developed a pressurized fluid bed gasifier to take into account the higher ash-containing coal. Raw product gas from the cyclone is cycled and mixed with the feed in the drier zone. Again the feed is separated and cooled gas is taken for cleaning while the feed is supplied to the gasifier. BHEL is developing a 125 MW_e IGCC demonstration plant at Auraiya in Uttar Pradesh, India (Higman and Burgt, 2008).

2.2.3.3 Entrained Bed Gasifier

Most of the gasifiers developed since 1950 are of the entrained flow type. The advantages of using entrained flow gasifiers lie in their flexibility in handling any type of coal as feedstock and ability to produce clean, tar-free product gas. With the development of the Integrated Gasification Combined Cycle (IGCC) as a prospective technology for overcoming the greenhouse gas emission issues and for increasing efficiency, use of

entrained bed gasifiers in power generation will further increase in the future. Entrained bed gasifier can supply product gas at high pressure to the IGCC system without the need for additional compression.

In entrained flow gasifiers, a dry pulverized solid is gasified with oxygen (much less frequently air) in co-current flow. The gasification reactions take place in a dense cloud of very fine particles (typically < 100μm). The much smaller biomass particles mean that the fuel must be pulverized, which requires somewhat more energy than the other types of gasifiers. Entrained flow gasifiers operate at high temperatures (1300-1500°C) and high pressures (20-50bar), and thus high throughputs can be achieved (Drift et al., 2004). The high temperatures also mean that tar and methane are not present in the product gas. Thermal efficiency is however lower to some extent as the gas must be cooled before it can be cleaned with existing technology. By far the most energy-intensive process related to entrained bed gasifiers is the production of oxygen used in gasification.

There are two types of entrained bed gasifiers: slagging and non-slagging. One differs from the other by the state of the ash when it is removed from the system. If the ash is removed in molten form then it is of the slagging type. If the ash is removed in solid form then it is of the non-slagging type. To ensure proper operation of the slagging type, the flow of molten ash should be 6% of the fuel flow. The non-slagging type is mostly favored if the ash content of the fuel is below 1% (Drift et al., 2004).

To feed the fuel at higher pressures, particle size needs to be very small. This limits the use of biomass as fuel as it is fibrous in nature and very difficult to cut into smaller sizes. Also, lower bulk density and low heating value reduce its suitability as fuel for entrained bed gasification. To use biomass as fuel a larger amount of carrier gas is required. This translates into higher energy for compression of gas and also product gas with poor heating value due to dilution with the carrier gas. In the case of pneumatic feeding the power penalty is high. For instance, pressurizing biomass up to 40 bars using pneumatic feeding consume 0.025 $kW_e/kW_{th\ wood}$ reducing efficiency by $0.04kW_{syngas}/\ kW_{th\ wood}$ (Drift et al., 2004).

Because of the tendency of biomass to be more irregular in shape, non-uniform; fluidized bed gasifiers have been considered as superior type to other types for hydrogen-rich gas production using biomass as fuel.

2.3 THE CHEMICAL LOOPING SYSTEM

Excessive combustion of fossil fuels in the past century has resulted in increased concentrations of carbon dioxide in the atmosphere. As the present economy is still mostly carbon based, a major issue is presented in how we can effectively shift from this fossil fuel based economy to renewable energies without compromising on energy consumption.

There is an increasing agreement that capture and storage will be required if atmospheric concentrations of CO_2 are to be stabilized. The cost of sequestration is small (for example

$4–8/t C) compared to the costs of separating CO_2 from typical flue gases ($100–200/t C) (Scott et al., 2006). Thus capturing CO_2 is only a viable option if a pure stream of carbon dioxide can be produced. Technologies used at present are post capture technologies, which decreases plant efficiency by 16% to 28% and increase the cost of electricity by 24% to 73% (Harrison, 2004). Investment on such technology will not be justified unless economical subsidies are provided. There is therefore a dire need to develop technologies for the efficient use of renewable biomass fuel, while at same time capturing carbon dioxide without much affecting the efficiency of the system and the energy cost. Chemical looping systems have emerged as such a technological solution as needed (Fan, 2011). They produce clean energy while separating carbon dioxide during the process and capturing it.

A chemical looping system comprises a solid carrier in a loop between reactors. The reactors can be a combination of fluidized bed and fixed beds. The chemical looping process can be divided into two types:

1. Chemical looping combustion
2. Chemical looping gasification

Chemical looping combustion (Fig 2.10) is an advanced concept of burning fuels without using nitrogen during combustion, therefore avoiding dilution of the flue gas with nitrogen (Mattisson and Lyngfelt, 2001). Instead, a metal oxide carries a pure stream of oxygen into the fuel reactor (combustor), avoiding the additional expense of oxygen preparation.

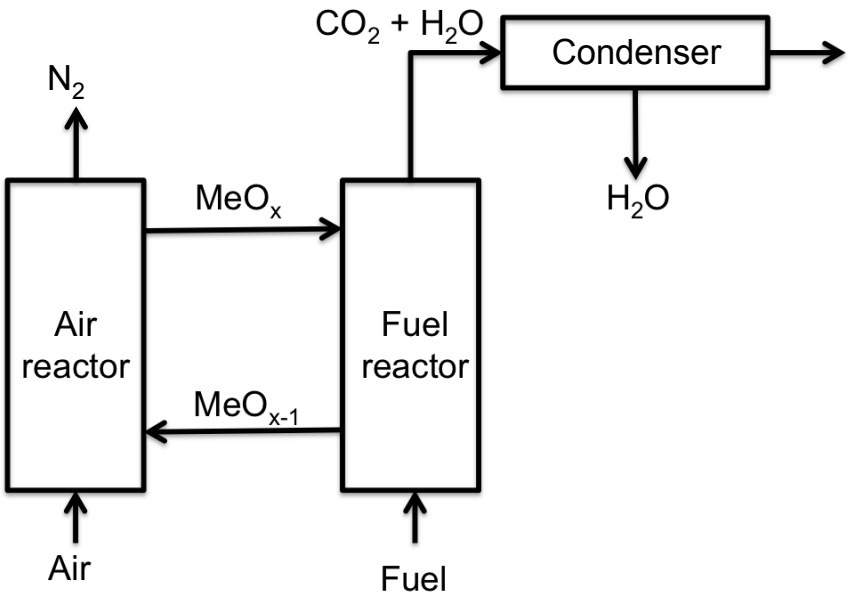

Figure 2.10: Schematic of chemical looping combustion

A chemical looping combustion (CLC) system consists of an air reactor and fuel reactor. The metal gets oxidized in air reactor and is then taken into the fuel reactor where it releases the oxygen to facilitate combustion of the fuel fed into it. The reduced metal is then circulated back into the air reactor, acting as the oxygen carrier separating the two reactors and avoiding dilution of flue gas with the nitrogen in the air.

Air Reactor:

$$M_yO_{X-1} + ½\ O_2 = M_yO_X \qquad [2.8]$$

Fuel Reactor (Combustor):

$$(2n + m)\ M_yO_X + C_nH_{2m} = (2n + m)\ M_yO_{X-1} + mH_2O + nCO_2 \qquad [2.9]$$

Until now the research in this area has mostly focused on developing an oxygen carriers with the following features: high reactivity with fuel and air, low fragmentation and attrition as well as low tendency for agglomeration, low production cost, environmentally friendly, easy to fluidize and stable under repeated reduction and oxidation cycles at high

temperatures (Fang et al., 2009). Different metal oxides that have been studied for use in CLC include; copper (Cu), cadmium (Cd), nickel (Ni), manganese (Mn), iron (Fe) and cobalt (Co) (Fang et al., 2009). Generally these metal oxides are combined with inert materials: Al_2O_3, SiO_2, TiO_2, ZrO_2, $NiAl_2O_4$, and $MgAl_2O_4$, which not only act as binders to increase the mechanical strength but also to increase reactivity, and durability and to improve fluidization characteristics. Among these, Al_2O_3 is gaining popularity because it has superior fluidization properties, higher thermal stability and is relatively cheap (Fang et al., 2009). Among the different metal oxides, nickel oxide is found most promising. NiO/Al_2O_3 has good reactivity and high mechanical strength, however it is expensive and poses health hazard.

Based on reactivity, the oxygen carriers studied can be ranked as $NiO > CuO > Mn_2O_3 > Fe_2O_3$. Of these four metal oxides, CuO has the highest oxygen carrying capacity and therefore it reduces the amount of solid circulation required in the CLC system. Also reaction involving CuO in both the fuel reactor and air reactor is exothermic, which reduces the heat requirement in the fuel reactor. However without a binder, the reactivity of pure CuO decreases drastically over a few cycles (10% in 20 minutes of operation) (Diego et al., 2004).

Iron oxides, on the other hand, are cheap, easily available and environmentally friendly and are gaining more attention as viable oxygen carriers for CLC. Pure Fe_2O_3 showed better chemical stability and reactivity when operated at a temperature of 720-800^oC when compared to other oxide. But above 900^oC it showed the sign of agglomeration.

Cho et al., (2004) compared nickel, copper, iron and manganese based oxygen carriers and found that with the exception of manganese, all other oxygen carriers had good reactivity, with iron based oxygen carriers showing the most agglomeration. Manganese oxide based oxygen carriers are less extensively studied than other oxides (Fang et al., 2009). The same study by Cho et al., (2004) showed poor reactivity of Mn_3O_4/Al_2O_3.

In most of the CLC studies carried out so far, methane has been the primary fuel used. But limited studies have been done to directly combust a solid fuel. Chemical looping with oxygen uncoupling (CLOU) as proposed by Mattisson et al., (2009), uses the chemical looping concept to directly combust the solid fuel, by burning it with the oxygen given off by the oxygen carrier. It was found that burning rate of petroleum coke was 50 times higher when combusted in a CLOU system.

Major contributors to the study of chemical looping combustion are the Tokyo Institute of Technology, Chalmers University of Technology in Sweden, CSIC-ECB in Spain and the Korea Institute of Energy Research (Johansson and Mattission, 2008; Fang et al., 2009). Table 2.2 lists the location and the type of the different chemical looping combustion system under research.

Table 2.2: The chemical looping combustion system (Lyngfelt, 2010)

Location	Capacity	Oxides
Chalmers University	10 kW	NiO, Fe_2O_3
	10 kW	ilmenite
	0.3 kW	NiO, Fe_2O_3, Mn_3O_4, ilmenite
KIER, S. Korea	50 kW	NiO, CoO
Daejong, S. Korea	1 kW	NiO, Fe_2O_3
CSIC, Spain	0.5 kW	CuO, NiO
Vienna Tech. University	140 kW	Ilmenite, NiO
ALSTOM	15 kW	NiO
Nanjing	10 kW	NiO, Fe_2O_3

2.3.1 Chemical Looping Gasification

Chemical looping gasification is an advanced concept of gasifying fuel with two attractive features: It captures carbon dioxide during process and produces a gas rich in hydrogen that can have a wide range of applications besides combustion. However, research on the chemical looping gasification has been limited to gaseous fuel. Limited studies have been done on gasifying solid fuel in chemical looping system (Scott et al., 2006).

Based on the type of carrier solid, the chemical looping gasification can be categorized as:

1. Chemical looping system with an oxygen carrier
2. Chemical looping system with a carbon dioxide carrier

2.3.1.1 Chemical Looping System with an Oxygen Carrier

In this type of chemical looping system, an oxygen carrier circulates between the fuel reactor and the air reactor. The metal oxide picks up oxygen in the air reactor then gives it up in the fuel reactor for combustion with the fuel to produce the product gas. After reduction, the metal oxide circulates back into the air reactor and the process is repeated. This way, nitrogen in the air is not allowed to come into contact with the fuel, thus avoiding the dilution of product gas with nitrogen. The reactions taking place in the air and fuel reactor are:

$$\text{Air Reactor: } M_yO_{x-1} + \tfrac{1}{2}O_2 \rightarrow M_yO_x \qquad [2.10]$$

$$\text{Fuel Reactor: } M_yO_x + C_nH_{2m} \rightarrow M_yO_{x-1} + mH_2 + (n - a)CO_2 + aCO \qquad [2.11]$$

This type of chemical looping system can be further subdivided into two types:

I. In the first type of chemical looping gasification system, the fuel is directly gasified in a fuel reactor. The oxygen concentration is maintained below the stoichiometric level so that the fuel gets gasified instead of combusted. Presently, research work is being done to gasify the gaseous fuel. Chemical looping reforming of methane is an example. The reaction between gaseous fuels and oxygen carriers is much faster than that with solid fuel. This may be the motivation for using CLG for reforming gases. When using solid fuel, the solid-to-solid contact between the metal oxide and the fuel is small resulting in low conversion (Leion, 2008). Deposition of char, tar and ash particles on the oxygen carrier also reduces its performance. Scott et al. (2006) studied the feasibility of using Fe_2O_3 as a carrier for solid fuel. They found gasification to be a limiting step and concluded that further research is needed to confirm that the oxygen carrier can retain its properties over a number of oxidation-reduction cycles. On the contrary, a study conducted by Fan (2011) showed iron oxide to be a suitable oxygen carrier for such a system. A system called coal direct chemical looping process (Fig 2.11) was also developed. In this process, the coal is fed into the reducer, where it gets oxidized to carbon dioxide and steam by iron oxide (Fe_2O_3) acting as an oxygen carrier. The reduced oxygen carrier then moves into the oxidizer, where it reacts with steam producing a pure stream of hydrogen. Iron oxide is further oxidized in the combustor and recycled back to the reducer for another cycle. The reaction taking place in the different reactors can be summarized as:

Reducer

$$C_{11}H_{10}O \text{ (coal)} + 8.67Fe_2O_3 \rightarrow 11CO_2 + 5H2O + 17.34Fe \quad [2.12]$$

Oxidizer

$$3Fe + 4H_2O \rightarrow Fe_3O_4 + 4H_2 - 44.68 \text{ kJ/mol} \quad [2.13]$$

Combustor

$$4Fe_3O_4 + O_2 \rightarrow 6Fe_2O_3 - 219.33 \text{ kJ/mol} \quad [2.14]$$

Although this type of system shows great promise, more studies are needed to understand the effect of fuel contaminants on oxygen carrier performance, in order to determine the viability of oxygen carrier particles to be used for this type of system.

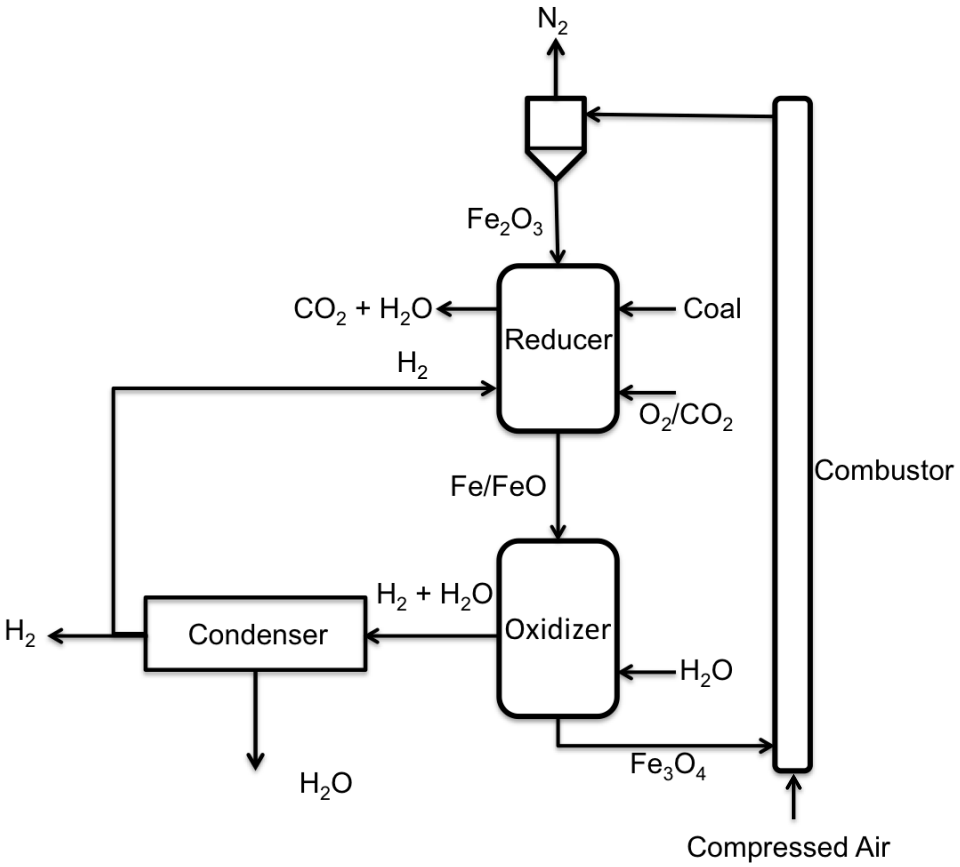

Figure 2.11: The coal direct chemical looping system (Fan, 2011, P. 332)

II. To overcome the difficulty of directly gasifying solid fuels in the fuel reactor, a second type of chemical looping system is developed in which the solid fuel is gasified in a separate gasifier and then the product gas is fed into the looping system. Syngas chemical looping system (Fig 2.12) developed by Liang-Shih Fan of Ohio State University is of this type (Fan, 2011, p. 241). Coal is gasified in an entrained bed gasifier. Product gas is then fed into the reducer where the carbon monoxide and hydrogen oxidizes to carbon dioxide and steam. After condensing the steam, pure stream of carbon dioxide is produced. The rest of the looping process is similar to the coal direct chemical looping system described previously.

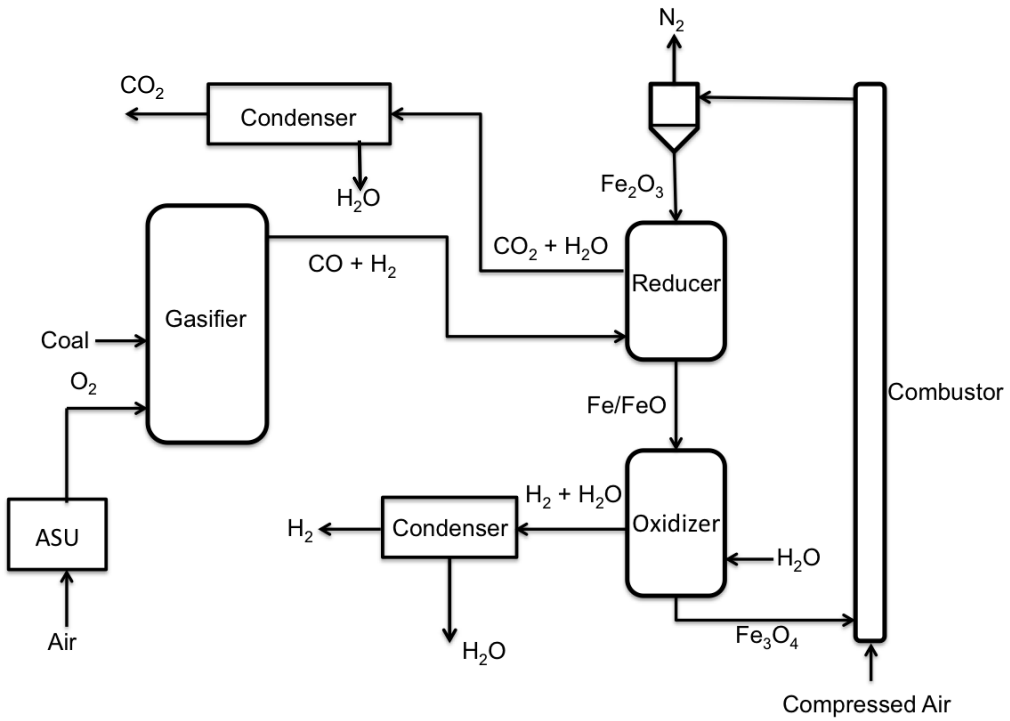

Figure 2.12: Schematic of Syngas chemical looping system (Fan, 2011, P. 270)

The reactions taking place in the different reactors of the syngas chemical looping system are:

Reducer

$$3CO + Fe_2O_3 \rightarrow 3CO_2 + 2Fe - 18.36 \text{ kJ/mol} \quad [2.15]$$

$$3H_2 + Fe_2O_3 \rightarrow 3H_2O + 2Fe + 28.791 \text{ kJ/mol} \quad [2.16]$$

Oxidizer

$$3Fe + 4H_2O \rightarrow Fe_3O_4 + 4H_2 - 44.68 \text{ kJ/mol} \quad [2.17]$$

Combustor

$$4Fe_3O_4 + O_2 \rightarrow 6Fe_2O_3 - 219.33 \text{ kJ/mol} \quad [2.18]$$

2.3.1.2 Chemical Looping System with a Carbon Dioxide Carrier

This system uses a sorbent that carries CO_2 instead of oxygen between the two reactors. Here, the sorbent goes through a series of calcination/carbonation cycle. The system comprises of two reactors: a gasifier and a regenerator. Solid fuel is gasified in the gasifier in the presence of CaO and steam, producing gas rich in hydrogen. The sorbent CaO captures carbon dioxide produced during gasification.

Gasification reaction: $CH_hO_o + (2\text{-}o)\ H_2O \rightarrow CO_2 + (h/2+2\text{-}o)\ H_2$ [2.19]

Carbonation reaction: $CaO + CO_2 \rightarrow CaCO_3$ [2.20]

Calcination reaction: $CaCO_3 \rightarrow CaO + CO_2$ [2.21]

Afterwards, the calcium carbonate formed during the carbonation reaction moves to another reactor, the regenerator. Here the sorbent is calcined to CO_2. The calcined limestone (CaO) is then fed back to the gasifier for another cycle. The use of CaO as sorbent has the additional benefits of accelerating the gasification reaction and the water gas shift reaction moving in the forward direction. It results in higher gas yields with high percentage of hydrogen. CaO also acts as a catalyst breaking down more tar and char into gases. Thus unlike the Syngas chemical looping gasification as proposed by Fan (2011) where the gasification occurs in separate gasifier, the looping system using CaO can produce a gas rich in hydrogen with minimal CO_2 within the same gasifier reactor, and as such the gas can be directly used for fuel cell application.

There are several types of chemical looping systems that uses the calcium oxide loop to capture carbon dioxide such as the carbon dioxide acceptor process, the HyPr-ring process, the zero emission coal alliance process, the ALSTOM process and the advanced gasification-combustion process. The difference lies in the methods of providing the energy required for calcination.

a) The Carbon Dioxide Acceptor Process (Fan, 2011 and Basu, 2006)

This process was developed by the Consolidation Coal Company and latter by the Conoco Coal Development Company for the production of synthetic natural gas from coal. The gasifier in this process is a pressurized fluidized bed gasifier operated at temperatures of 800-850^{o}C and a pressure of 10 atm. The sorbent, calcined limestone or dolomite is fed from the top of the gasifier to absorb the carbon dioxide produced during the gasification reaction. The product gas thus becomes rich in hydrogen, and is then cleaned and methanated to produce synthetic natural gas. The calcium carbonate formed in the gasifier is then fed into a regenerator. The char from the gasifier is combusted in the regenerator to provide the heat required for calcination reactions. The regenerator is also a fluidized bed reactor with air as the fluidizing medium. The high pressure required for this operation makes the system expensive and complex.

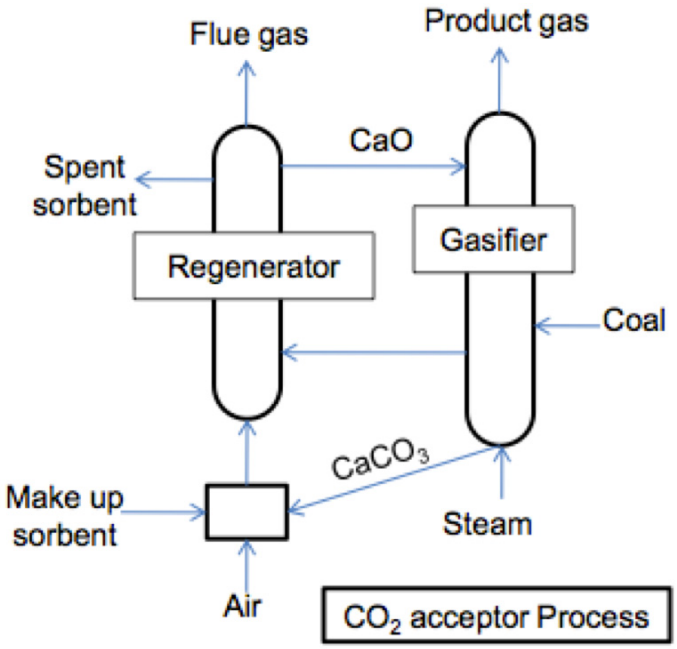

Figure 2.13: The carbon dioxide acceptor process

b) The HyPr-Ring Process (Lin et al., 2002; Lin et al., 2011; Fan 2011)

This process is similar to the CO_2 acceptor process with the main difference lying in the operating condition of the gasifier. The gasifier is operated at the lower temperature of about 650^{o}C but at a much higher pressure, 30 atm. Unlike in the CO_2 acceptor process, the calcium oxide here is first converted into calcium hydroxide in steam which then captures carbon dioxide. Thus the system is operated at a lower temperature and higher pressure to favor these reactions. The advantage of doing so is the ability to maintain the reactivity of the sorbent used. In fact this method is proposed to enhance the performance of the sorbent in other CLG processes. This process is intended to produce gas rich in hydrogen while the CO_2 acceptor process produces methane rich gas as the final product. By using pure oxygen in the regenerator to combust the char, this process also produces a pure stream of carbon dioxide and steam. However, high operating pressures and the need for an oxygen separation plant makes this process expensive and complex.

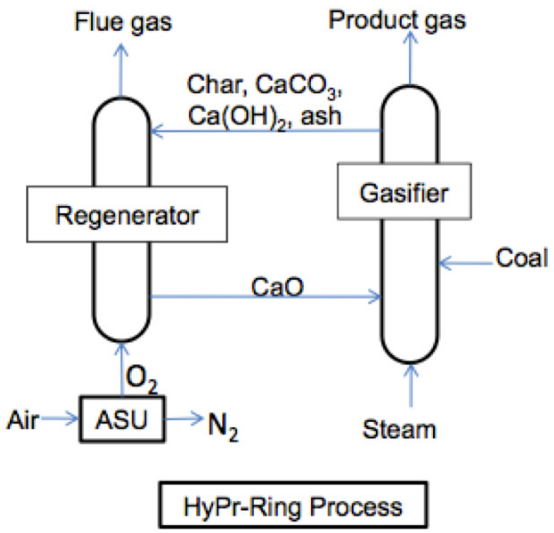

Figure 2.14: The HyPr-Ring Process

c) The Zero Emission Coal Alliance Process (Ziock and Lackner, 2000; Fan, 2011)

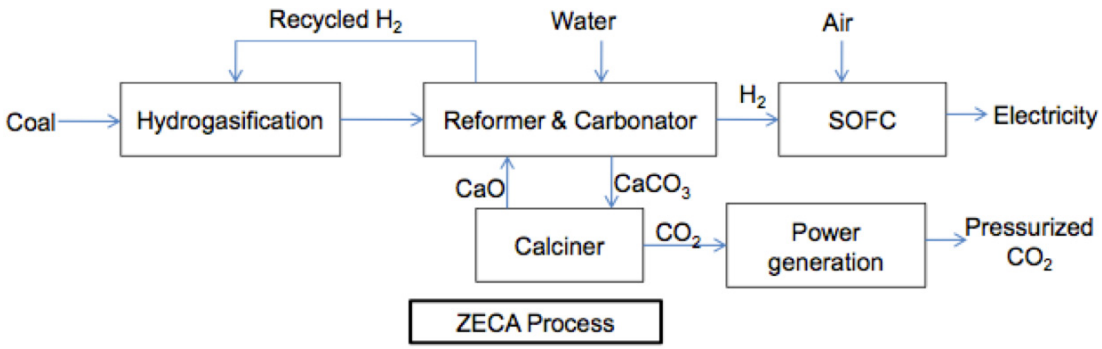

Figure 2.15: The zero Emission Coal Alliance Process

In this process coal is first converted into methane by hydrogasification ($C + 2H_2 \rightarrow CH_4$). The methane produced is taken into a reformer where it is reformed to produce hydrogen. The hydrogen is then divided into two streams- one is recycled back for hydrogasification and the other is taken into the solid oxide fuel cell (SOFC) for power generation. The CaO from the calciner is fed into the reformer where it absorbs the carbon dioxide produce during reformation. Unlike the other two processes mentioned above which directly combust char to provide heat needed for calcination, the residual

heat produce in the SOFC is used as a source of heat for calcination. However, for this to be possible, the SOFC needs to be operated at a temperature above 1000^{o}C, which may be difficult to achieve because of the material constraint (Fan, 2011, p. 314). This process is still in the conceptual phase and has not yet been tested experimentally.

d) The ALSTOM Hybrid Combustion-Gasification Process (Fan, 2011)

The air separation unit (ASU) that produces the pure oxygen required for the combustion of char in the calciner is expensive in terms of both capital and operating cost. To avoid the use of ASU, the ALSTOM hybrid combustion gasification process adds one more reactor- an oxidizer where the oxygen carrier ($CaS/CaSO_4$) is oxidized. This avoids the mixing of air/N_2 with the product gas obtained from the reducer. A part of hot solid from the oxidizer is recycled into the calciner to provide the heat required for the calcination. Also the solid particles from the oxidizer provide the heat for the endothermic gasification reaction in the reducer. The coal gets gasified in the reducer in the presence of steam and CaO to produce gas rich in hydrogen. The reducer operates at a temperature of 880-980^{o}C at 6 atm pressures while the oxidizer operates at 1100^{o}C and one atmospheric pressure.

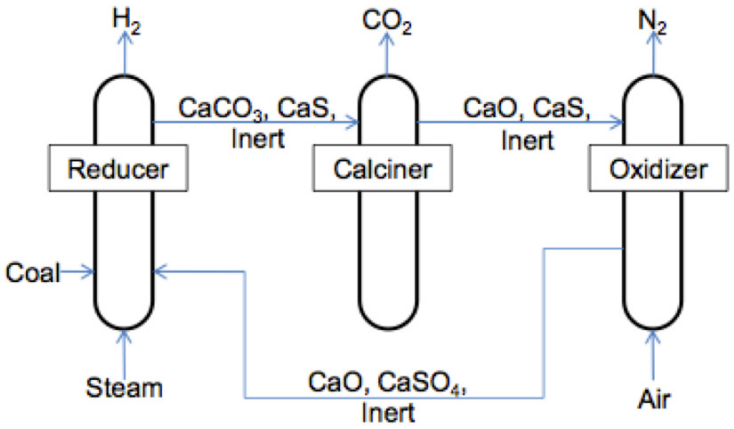

Figure 2.16: The ALSTOM hybrid combustion-gasification process

e) The Fuel Flexible Advanced Gasification-Combustion Process (AGC) (Fan, 2011; Rizeq et al., 2002)

This process consists of three reactors, a gasifier (750-850^{o}C, 17-20 atm), a reducer (900-1000^{o}C, 17-20 atm) and an oxidizer (1000-1200^{o}C). Coal is gasified in the presence of steam and CaO in the gasifier, producing gas rich in hydrogen. The char and calcium carbonate from the gasifier are taken into the reducer, which receives the oxygen carrier Fe_2O_3 from the oxidizer. Thus, char in the reducer is gasified with steam in the presence of the oxygen carrier. The oxygen carrier oxidizes the carbon monoxide and hydrogen to carbon dioxide and steam. The reduced oxygen carrier is then recycled into the oxidizer where it is oxidized with air. The heat required for the gasification process is carried by the calcium oxides from the reducer. The AGC process has neither been tested nor verified for its fuel flexibility (Fan, 2011).

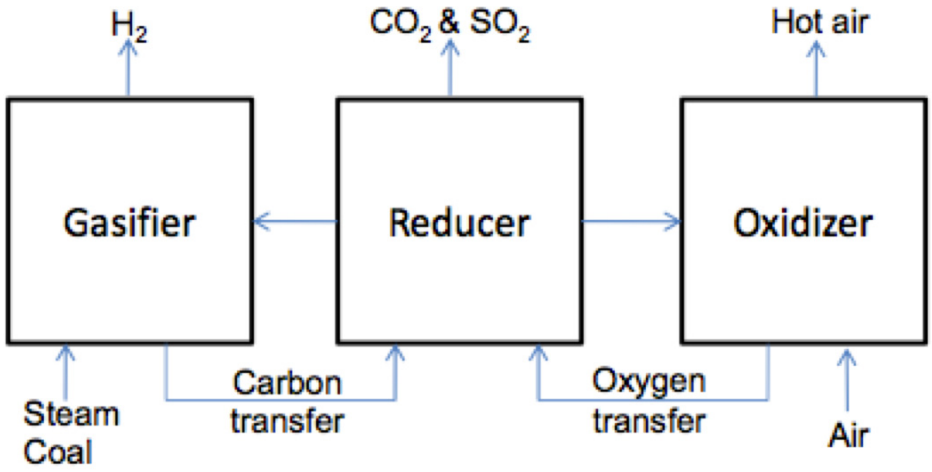

Figure 2.17: The fuel flexible advanced gasification-combustion process

Table 2.3: Comparison of different chemical looping process using calcium oxide (Fan, 2011, p. 302-328)

Parameters	CO_2 acceptor Process	HyPr-Ring process	ZECA process	ALSTOM process	AGC process
Product	CH_4 and flue gas	H_2 and CO_2	H_2 and CO_2	H_2, N_2 and CO_2	H_2, hot air and CO_2
CO_2 capture	No	Yes	Yes	Yes	Yes
ASU requirement	No	Yes	No	No	No
Heat for calcination	Direct*	Direct	Direct	Indirect**	Indirect
Gasifier operating condition	800-850^oC, 10 atm	650^oC, 30 atm	-	880-980^oC, 6 atm	750-850^oC, 17-20 atm
H_2 %	65.6	76%	-	-	80%
Fuel	Coal	Coal	Coal	Coal	Coal
Reactor type	Fluidized bed	Pressurized reactors	Pressurized reactors	Fast fluidized bed	Fluidized bed
Status	40 t/d pilot plant. Test ended in 1977	3.5 kg/h pilot plant	Conceptual	Two loops tested separately	Each reactor tested in bench scale

(*Heat for calcination is provided by direct combustion of fuel, ** Heat for calcination is provided indirectly by recycling hot solids carriers)

Table 2.3 summarizes the characteristics of CaO based chemical looping gasification plants. With the exception of the CO2 acceptor process, which was successfully operated but has not been in use since 1977, one can see that the concept of chemical looping gasification including is still in the laboratory testing phase. All of the above mentioned systems developed thus far are aimed at using coal as fuel and most of them are of recent origin. Owing to the complexity in developing such systems, their development is still in the laboratory stage. As most of them operate at high temperature and pressure, designing such reactors is challenging. Even more challenging would be to maintain the continuous flow of solids through different pressurized reactors. Furthermore, more research is needed in developing an oxygen carrier/sorbent that can be used directly for solid fuel. Chemical looping gasification must become less expensive and complex for it to have an

easier time finding commercial use in the biomass and bio-waste industries. To this end, it is necessary to develop a system that operates at atmospheric pressure and relatively low temperatures. The subject area being new and unexplored, detail research can bridge the knowledge gaps.

2.4 CaO AS SORBENT FOR GASIFICATION

Solid sorbents have several operational advantages in absorbing carbon dioxide. They have higher capture efficiency at high temperature where other liquid based sorbents cannot perform (Alvarez et al., 2007). Several sorbents that have been studied include rhodium (Asadullah et al., 2001), aluminum oxide and nickel-based solid absorbent (Asadullah et al., 2001; Moghtaderi, 2007), dolomites (Javier et al., 1999; Rapanga et al., 2000) and CaO (Dalai et al., 2003; Guan et al., 2007; Lin et al., 2006; Mahishia and Goswami, 2008). Metal-based sorbents are expensive and are not economically feasible, where as calcium oxide are cheap and abundant and can be effective at capturing carbon dioxide at very high temperatures (Grasa and Abanades, 2006). Among the four different naturally occurring minerals, namely calcined dolomites, magnesium-based mineral, olivine and calcined limestone, calcined limestone shows the most promise for carbon dioxide capture and is the best choice as an additive in fluidized bed steam gasification (Alvarez et al., 2007). CaO based capture systems also have higher equilibrium capacities when compared to other sorbents currently being used. The absorption capacities of the different sorbents are: MEA = 60 g of CO_2/kg, silica gel = 13.2 g of CO_2/kg, activated carbon = 88 g CO_2/kg and CaO-based process = 393 g of CO_2/kg. Assuming a 50% conversion of CaO over repeated cycles, the CaO based process requires lower amount of

sorbent, small size reactors, and lower pressure drops in the reactors to capture the same amount of CO_2 as the other sorbents (Gupta and Fan, 2002).

Carbon dioxide capture or scrubbing of flue gas in a power plant is a critical issue in the utility industries. Several researchers (Gupta and Fan, 2002; Abanades et al., 2004; Sun et al., 2007) proposed the use of limestone for capturing CO_2 from the flue gas. A CaO based sorbent can capture CO_2 at a relatively high temperature, while other convectional techniques requires the flue gas to be cooled to low temperature for effective capture. As CO_2 represents a small fraction in the flue gas, once separated only a small amount of auxiliary power is required for compression of the CO_2 for sequestration.

Several researchers (Acharya et al., 2009; Mahishi and Goswami, 2007; Lin et al., 2002; Moghtaderi, 2007; Guan et al., 2007; Rapanga et al., 2000) have recognized the potential of the gasification of biomass in the presence of CaO in a fluidized bed reactor and have studied some aspects of this concept. Acharya et al. (2010), Hanaoka et al. (2005), Guoxin et al. (2009) and Luo et al. (2009) conducted similar studies, but in fixed bed reactors. The perceived catalytic effect of CaO was examined by Dalai et al. (2003). Their work on steam gasification of cedar wood and aspen using CaO as a catalyst shows that the hydrogen and the total gas yields increase with increase in CaO loading up to a point and then eventually reach a constant value. The use of dolomites (15-30% by wt) in beds has been found to reduce the tar content to 1 gm/m^3 and to increase the yield of gas (Javier et al., 1999). Mahishi and Goswami (2007) examined the effect of addition of sorbent CaO in a bubbling bed at different gasification temperatures. The sorbent to

biomass molar ratio was maintained at unity and it was observed that the hydrogen yield at 500°C and 600°C was higher than the conventional hydrogen yield at 700°C. At 600°C, the hydrogen yield and carbon conversion efficiency with the addition of sorbent increased by 48.6% (573–852.3 ml/g) and 83.5% (30.3–56%), respectively. Lin et al. (2002) studied the steam gasification of woody biomass in the presence of CaO. The effect of pressure and temperature and [Ca]/[C] ratio, on the yield of hydrogen were studied by Lin et al. (2002), who noted that the concentration of CO_2 in the producer gas is nearly zero for a [Ca]/[C] ratio of 1, and the yield of hydrogen is maximum for a [Ca]/[C] ratio of 2 due to the catalytic action of the sorbent. On the contrary, Guan et al. (2007) observed that the yield of hydrogen was maximum for a [Ca]/[C] ratio of 1 at 800°C and 2 MPa and with the mole ratio of water to carbon being 2. The CO and CH_4 concentrations in the product gas were lower when using the sorbent CaO (Mahishi and Goswami, 2007). Guoxin and Hao (2009) used the fixed bed reactor to study the kinetics of hydrogen enriched gas production from biomass in the presence of CaO. They found the optimum operating conditions to be steam to biomass ratio (S/B) = 0.9, calcium to carbon molar ratio (Ca/C) = 0.5, and reaction temperature (T) = 923 K. The maximum yield of hydrogen was 219 ml/g of biomass for pine sawdust, while similar experiment done in an autoclave by Hanaoka et al. (2005) observed a maximum hydrogen yield of 800 ml/g of biomass at Ca/C = 2 using Japanese oak as the biomass feed. The observed difference in optimum operating conditions can be due to different biomass properties (such as type of biomass, moisture content, ash content) as well as the different methodologies adopted.

In any case all studies done using calcined limestone confirm its usefulness as a sorbent to capture carbon dioxide. However its use in a chemical looping system is still questionable, as its ability to capture carbon dioxide reduces within a few numbers of cycles. This will require frequent addition of fresh sorbent making the system less attractive from an economical point of view (Manovic and Anthony, 2010).

During the process of capturing CO_2, a sorbent CaO can undergo degradation through several ways as explained below and shown in Fig 2.18.

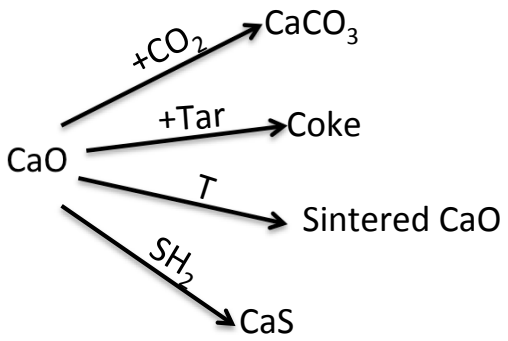

Figure 2.18: Overall reaction that CaO undergoes when introduced in gasifier (Corella et al., 2006)

a) Besides taking part in the carbonation reaction, CaO may react with tar formed during gasification to form a layer of coke on the surface.

b) The inorganic components in the feedstock can also react with calcined limestone to form inert inorganic complex compound.

c) Sintering or ageing after many cycles of carbonation and calcinations also reduces the reactivity of CaO.

d) If the feedstock contains high sulphur content then calcium sulphide may form.

Beside these factors, another major issue is the operating temperature. For best gasification results, the gasification temperature should be in the range of 850-900^{o}C; however, because of the equilibrium limitations (Grasa & Abanades, 2006), the temperature for carbonations should be 600-720^{o}C. At lower temperatures tar formation will be higher and to overcome this loss of CaO, the amount of CaO to be supplied to the gasifier should be in the range of 2 to 80 kg of CaO/kg of carbon (Corella et al., 2006).

The carbonation reaction is initially governed by a surface reaction. The calcium carbonate formed being higher in molar volume than CaO (molar volume of CaO is 17 cm^3/mol; molar volume of $CaCO_3$ is 37 cm^3/mol), leads to the plugging of the pores of CaO. Also, after number of cycles, calcium carbonate sinters to a sufficiently high extent (Sun et al., 2007), rendering the interior of CaO particles partially unavailable for carbonation. Sintering of CaO over multiple calcination cycles reduces the micro porosity of CaO (sites for the carbonation reaction to occur) while increasing the number of meso and macro pores, resulting in reduced conversion during the fast carbonation reaction phase, and therefore reduced CO_2 capture capacity over successive cycles (Sun et al., 2007; Abanades and Alvarez, 2003). As reported by Fan (2011, p. 307), the calcium atom is highly reactive during the gasification/regeneration operating condition leading to fast CaO crystalline growth through formation of bridges between neighboring CaO particles during the carbonation phase. Such crystals are highly stable during calcination and grow continuously in size. This reduces the gas diffusion rate and lowers conversion during carbonation.

According to Abanades and Alvarez (2003), the reduction in conversion depends only on the number of cycles and is independent of the reaction time and conditions. Sun et al. (2007) also showed that the carbonation time does not have any effect on sintering as the structural changes in CaO during carbonation can be eliminated during calcination, but it is the increase in calcination time that results in sintering as they found the increase in calcination time resulted in decrease in pore volume.

Some methods suggested to recover the reactivity of sorbent over successive calcination-carbonation cycles includes: water hydration, high temperature and pressure steam hydration, thermal self-activation and vacuum calcination. In 2 cycles, the extent of carbonation was for vacuum calcined precipitated calcium carbonate-calcium oxide (PCC-CaO) sorbent studied was found to be over 90%. No drastic decline in pore volume and pore surface area was observed (Fan, 2011). In steam or water hydration (Fan, 2011, p. 131; Manovic and Anthony, 2010; Laursen et al., 2004), smaller water molecules can easily penetrate into the sintered CaO forming calcium hydroxide. The higher molar volume of calcium hydroxide compared to CaO results in the expansion of the crystals, leading to cracks and sites for further carbonation to occur, and ultimately increased conversion. Laursen et al., (2004) found that to maximize reactivation it is more beneficial to subject a spent sorbent to a smaller number of long-term hydration periods than too many short term hydration periods. Fan (2011, p. 133) noted that the capture of carbon dioxide with CaO obtained by water hydration is higher than that from steam hydration at 600^{o}C and 8 atm pressures. Fan (2011, p. 133) also suggested using steam directly for calcination. Ayer et al. (2005) studied steam calcination and its effects on the

reactivity of CaO produced. They found that CaO obtained from calcination performed at a temperature of 700^{o}C with an 80% H_2O-20% N_2 environment has a higher surface area and pore volume than that done with 100% N_2 at same operating condition. Manovic & Anthony (2010) found that conversion during carbonation reaches 70% in 10 cycles once reactivated with saturated steam. However, according to Sun et al. (2007) and Alvarez et al. (2007), the presence of steam may lead to higher sintering. However, using steam, allows calcination to be performed at lower temperature, which helps to reduce the sintering effect (Fan, 2011, p. 133). Manovic & Anthony (2010) reported that the thermal treatment of the sorbent also known as self-reactivation, could also help in recovering sorbent activity. Initially the conversion obtained from thermally treated sorbent may be lower however it has been found to increase in latter cycles. For fine particles (<50 microns), the self-reactivation occurred for 30 cycles with 49% conversion at the last cycle. Nevertheless, water/steam hydration renders the particles more fragile, making it unsuitable for fluidized bed applications. Manovic & Anthony (2010) thus suggested the use of pellets (calcium aluminate pellets) for CO_2 capture. which increase conversion more than neutral limestone. Although they also lose reactivity after a number of cycles, it can be easily recovered with water hydration.

2.5 CONCLUDING REMARKS

Chemical looping system are gaining a lot of attention due to their unique ability to produce hydrogen rich gas along with pure streams of carbon dioxide for sequestration, with minimum loss in efficiency. Several types of chemical looping systems have been developed since the beginning of this century; however, they are still in the laboratory

testing phase due to the complexity in developing such systems for commercial use. Thus, chemical looping gasification systems offer room for new research and innovation in developing much simpler systems (operating at atmospheric pressure and relatively low temperatures) that can utilize both biomass and bio-waste.

Calcium oxide based chemical looping systems could be a more favorable choice because they use limestone sorbent, which is easily available and cheap. Limestone has already been used in circulating fluidized bed boilers so its compatibility with dual fluidized bed systems would not be an issue. Its only limitation for use in looping systems is its quick loss in reactivity due to sintering. Research at the moment is focused on developing methods for predicting this loss in reactivity of sorbent and recovering it. However, many other factors are responsible for the decay in sorbent reactivity during gasification. These problems must be dealt with by rigorously testing the systems in real time examine their viability.

CHAPTER 3: CIRCULATING FLUIDIZED BED BASED CHEMICAL LOOPING GASIFICATION

This chapter introduces the concept of circulating fluidized bed (CFB) based chemical looping gasification (CLG) system. The efficiency of CLG systems based on the first law of thermodynamics is calculated and is presented in this chapter. Furthermore, a sensitivity analysis is conducted to examine how a loss in the ability of the sorbent to capture carbon dioxide (in the gasifier) and to regenerate (in the regenerator) might influence the overall system efficiency. An exergy analysis of the system is performed as well to assess the viability of the process. Based on the mass and energy balance and empirical relation for fluidization, a laboratory scale CFB based CLG system is designed.

3.1 CFB-CLG SYSTEM

A CFB-CLG system (Fig 3.1) consists of two reactors: one is a bubbling fluidized bed gasifier and the other is a circulating fluidized bed regenerator. The fuel is fed into the gasifier, which receives calcium oxide from the regenerator and steam as a fluidizing medium from an external source.

The gasification of biomass in the presence of steam will produce a mixture of gases containing H_2, CO, CO_2, CH_4, tars and unconverted steam. Along with this mixture, solid char is also produced. This is shown in Eqn. 3.1.

$$\text{Biomass}+H_2O \rightarrow H_2 +CO+CO_2+CH_4+H_2O+ \text{tar}+\text{char} \qquad [3.1]$$

CO further reacts with steam to produce more hydrogen and carbon dioxide (water gas shift reaction).

$$CO+H_2O \rightarrow H_2 + CO_2 - 42.2 \text{ kJ/mol} \quad [3.2]$$

In the case of biomass gasification in the presence of CaO, the carbon dioxide produced during the biomass gasification reaction and the water gas shift reaction reacts with CaO to produce calcium carbonate.

$$CaO + CO_2 \rightarrow CaCO_3 - 178.8 \text{ kJ/mol} \quad [3.3]$$

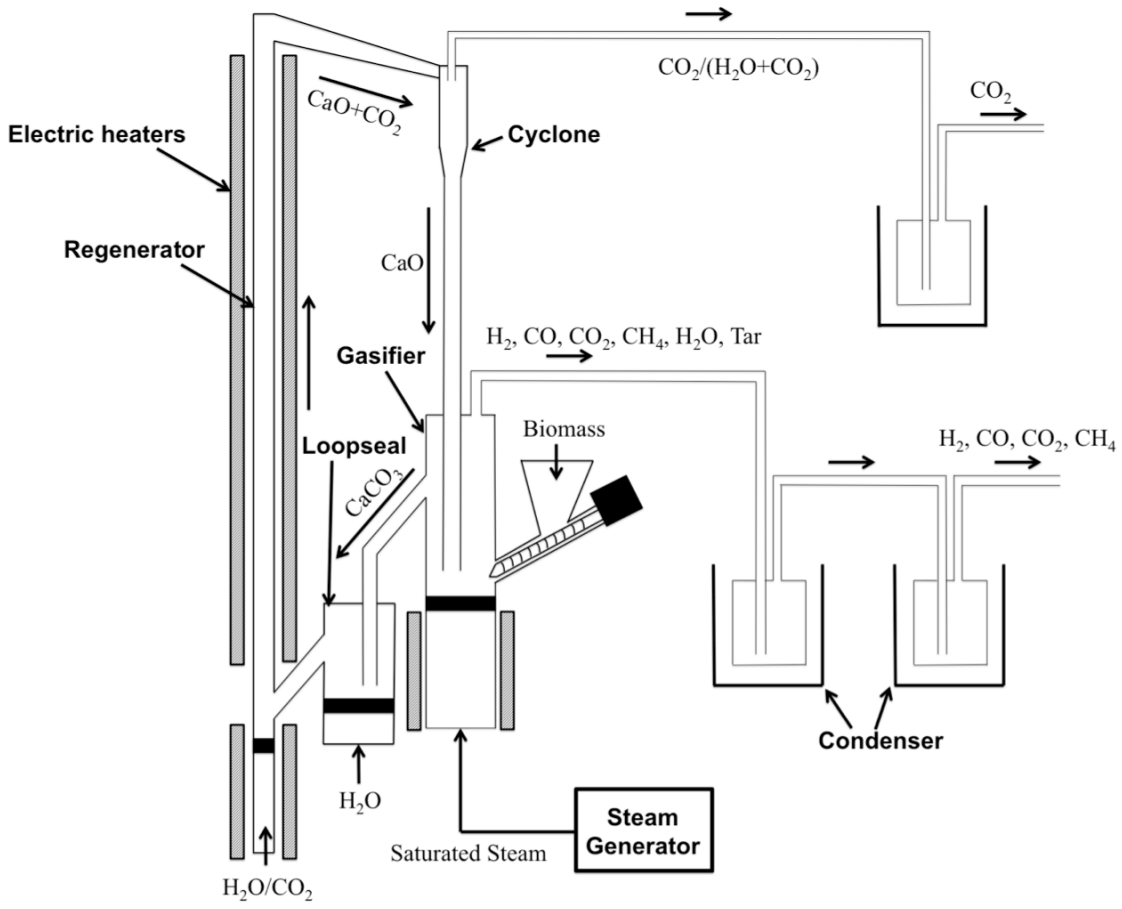

Figure 3.1: Schematic of CFB-CLG

Immediate removal of the reaction products CO_2 from the system favors the conversion of carbon monoxide into hydrogen and carbon dioxide, increasing the hydrogen yields. The exothermic nature of the carbonation reaction will help to meet the heat required by the endothermic gasification reaction. Also, the heat carried by the solids coming from

the regenerator maintains the temperature of the gasifier to its optimum operating condition.

The solid product consisting of calcium carbonate ($CaOCO_3$), calcium oxide (CaO) and char then moves into the loop seal, which is fluidized with steam. Loopseal acts as a seal that prevents gas from the regenerator to escape into the gasifier and vice versa. It also helps to regulate the solid circulation between the two reactors. Lastly, the solid enters into the regenerator. Ideally all the biomass should be converted in the gasifier so that no char enters the regenerator, however complete char conversion is not possible because of the relatively short residence time in the gasifier. In order to avoid unconverted char going into the regenerator, another reactor can be placed in between the gasifier and the regenerator. This can be a bubbling fluidized bed acting as a classifier, which by maintaining a certain operating velocity, entrains the char particles and recycles them back into the gasifier while solid calcium moves into the regenerator.

The calcium carbonate in the regenerator gets calcined to produce calcium oxide and carbon dioxide. The calcination reaction is highly endothermic. The heat required for calcination can be provided either directly by supplying air into the regenerator and combusting the char coming from the gasifier or indirectly by combusting some of the product gas. However, the former method will dilute carbon dioxide with nitrogen, which will require an additional downstream separation system.

$$CaCO_3 \rightarrow CaO + CO_2 + 178.3 \text{ kJ/mol} \qquad [3.4]$$

Calcium oxide particles are carried out of the regenerator by the fluidizing medium, which maintains a superficial velocity such that the regenerator operates at a fast bed fluidization regime. The mixture of gas and solid particles are separated in a cyclone and the solid calcium oxide is recycled back into the gasifier. For experimental purpose, the gas stream obtained was cooled before being released to the atmosphere, however the gas coming out from the cyclone is pure carbon dioxide that in commercial systems can be directly taken back for sequestration. Also, there is a possibility that part of the pure stream of carbon dioxide can be recycled back into the regenerator as the fluidizing medium. This will however increase the partial pressure of the carbon dioxide in the regenerator, which then needs to be operated at temperature above 950^{o}C to achieve higher calcination. This will inevitably increase the energy requirement for calcination and will reduce the overall efficiency of the system. Using steam as an alternative-fluidizing medium is instead proposed here because it can be easily condensed to obtain a pure stream of carbon dioxide. Steam calcination is discussed in more detail in chapter 5.

3.2 ENERGY EFFICIENCY OF CFB-CLG SYSTEMS

Figure 3.2 shows the overall mass and energy balance of the CFB-CLG system. To obtain this balance, the CFB-CLG system is divided into two sub-systems, the gasifier and the regenerator. The energy moving in and out and the energy required for each of the sub-systems are accounted for in the calculation of the system efficiency.

The main assumptions made were:

1. The gasifier is operated at an ideal condition with complete conversion of biomass.
2. Gasification of biomass produces only carbon monoxide and hydrogen

3. All the carbon monoxide is converted back into carbon dioxide and hydrogen
4. Capture of carbon dioxide is complete
5. Complete regeneration of sorbent takes place in the regenerator

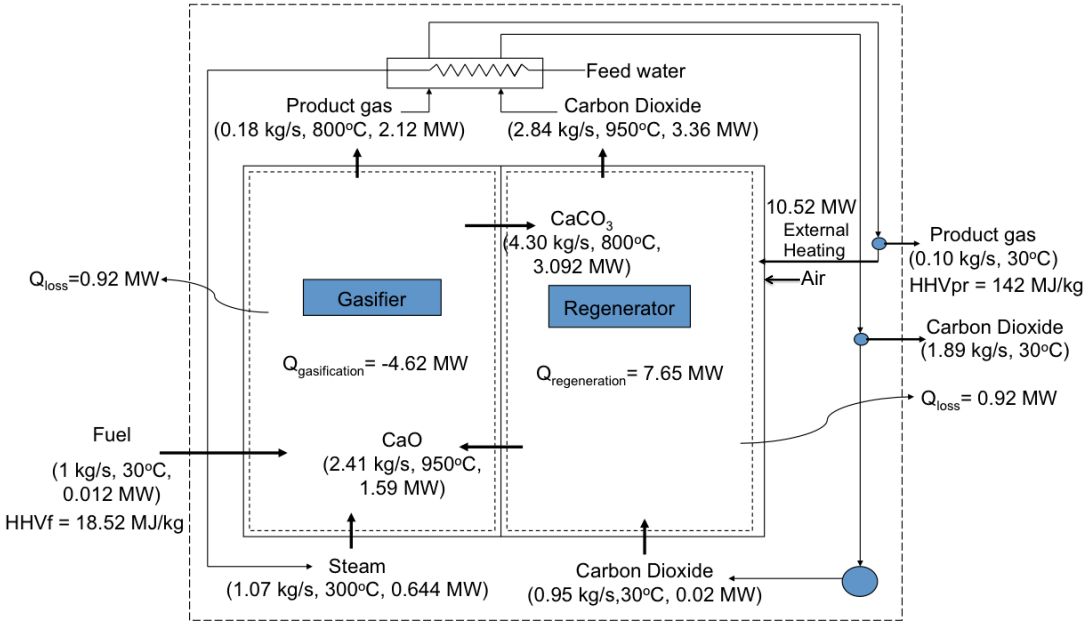

Figure 3.2: Mass and Energy balance for chemical looping gasification

The following reactions take place in the gasifier:

$$C_nH_mO_p + (n - p)\ H_2O \rightarrow nCO + (m/2 + n - p)\ H_2 + 112\ kJ/mol \quad [3.5]$$

$$CO + H_2O \rightarrow CO_2 + H_2 - 41.2\ kJ/mol \quad [3.6]$$

$$CaO + CO_2 \rightarrow CaCO_3\ -178.3\ kJ/mol \quad [3.7]$$

Thus the overall reaction in the gasifier could be written as:

$$C_nH_mO_p + (2n - p)\ H_2O + nCaO \rightarrow nCaCO_3 + (m/2 + 2n - p)\ H_2 - 107.5\ kJ/mol \quad [3.8]$$

The reaction-taking place in the regenerator is:

$$CaCO_3 \rightarrow CaO + CO_2 + 178.3\ kJ/mol \quad [3.9]$$

The calculations are based on a biomass with composition of C = 51.13%, H = 6.10% and O = 41.96%. This composition was taken from the experimental work of Mahishi and Goswami, 2007). The flow rates of the different streams as shown in Fig 3.2 are calculated based on a biomass flow of 1 kg/s. In an ideal scenario, the heat produced during the carbonation reaction provides all the energy necessary for the gasification reaction. Thus, no external heating is needed by the gasifier under steady state. The energy required for heating the regenerator is estimated as 10.52 MW, while the heat required for steam generation is 3.08 MW. The product gas leaving the gasifier and the carbon dioxide leaving the regenerator are above 800^{o}C, so their sensible energies are used for steam production. Based on all these energy flows, the theoretical thermal efficiency of the system is found to be 87.49 %. The sample calculation for the energy efficiency is shown in Appendix A.

For better understanding of the effect of carbon dioxide capture efficiency and regeneration efficiency on the overall system efficiency, a sensitivity study is carried out. This study has been conducted for the following two scenarios:

Scenario 1: The carbon dioxide capture efficiency in the gasifier varies, but the regenerator efficiency remains constant at 100%

The following assumptions are made for this scenario:

1. The energy balance in the regenerator remains the same, as with the ideal scenario.

2. The energy generated during the carbonation reaction in the gasifier changes with CO_2 capture efficiency.
3. The product gas contains mainly hydrogen and a small fraction of carbon dioxide that was not captured by CaO in the gasifier.
4. The sensible heat of carbon dioxide is added with that of hydrogen to calculate the total sensible energy of the product gas.

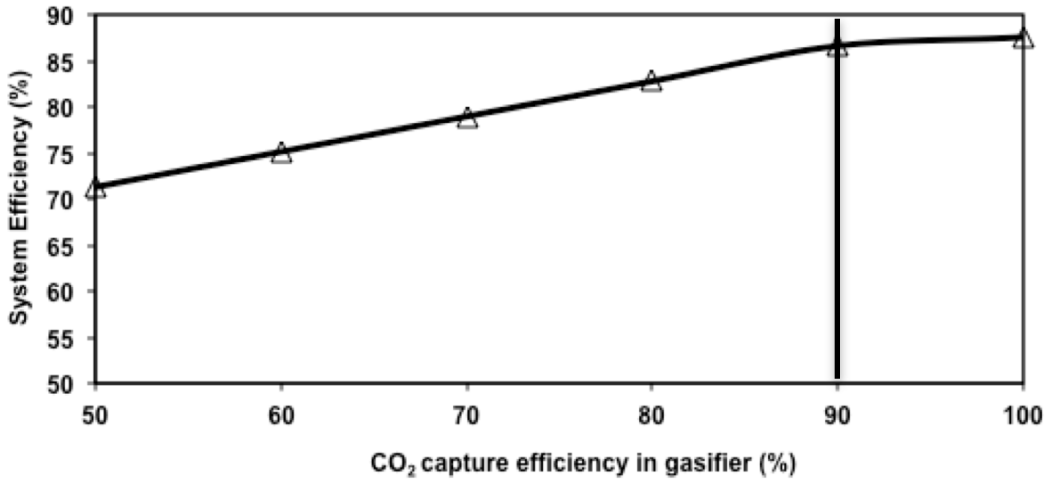

Figure 3.3: Effect of efficiency of carbon dioxide capture by CaO in the gasifier on the overall system efficiency

With reduction in capture of carbon dioxide by calcium oxide, the energy released during the carbonation reaction is lower, making the overall energy balance for the gasifier endothermic. An external heating source is therefore required. If that energy comes from the combustion of part of the product gas, then the efficiency of the system will drop. It is apparent from Fig 3.3 that, when CO_2 capture is 100%, the overall system efficiency is 87.49%, which reduces to 71% for a 50% CO_2 capture. Calculation further shows that approximately 90% capture efficiency should be maintained if the gasifier were to operate under auto-thermal conditions.

The reduction in CO_2 capture (or the effectiveness of CaO to capture CO_2) can occur because of several reasons:

1. Tar, which is formed during gasification, may deposit on the CaO particles, thus reducing its surface availability for CO_2 capture.
2. With repeated number of carbonation and calcination cycles, the properties of the sorbent may change, resulting in a lower CO_2 capture.
3. The sintering and agglomeration problem involving CaO, $Ca(OH)_2$ and $CaCO_3$.

Given that the CO_2 produced during the gasification process is not entirely captured, the composition of gases will also change.

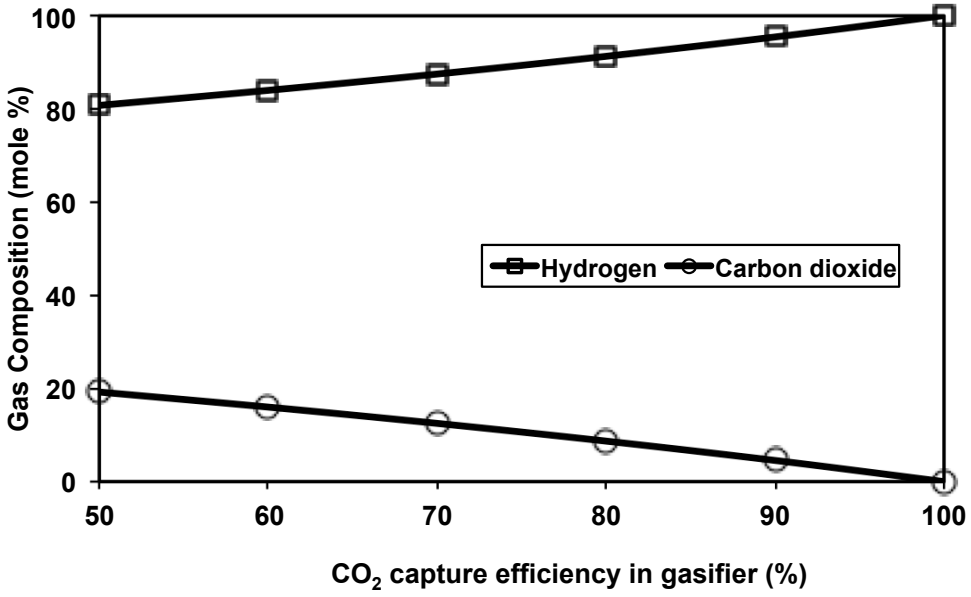

Figure 3.4: Effect of CO_2 capture efficiency on composition of product gas

Fig 3.4 shows the composition of gases at different CO_2 capture efficiencies. At 50% CO_2 capture, the hydrogen fraction is estimated to be up to 80% in the product gas while 20% will be carbon dioxide. This analysis indicates that a higher capture of carbon dioxide

during the gasification process is necessary for high hydrogen in the product gas. One way to achieve this is to have a higher 'CaO to biomass ratio' in the gasifier, which helps to increase the carbon dioxide capture on one hand but also increases the heat requirement of the regenerator on the other.

Scenario 2: Regeneration efficiency in the regenerator changes while the carbon dioxide capture efficiency in the gasifier remains steady at 60% and 80%

To study the combined effect of change in regeneration efficiency as well as carbon dioxide capture efficiency on the overall system efficiency, the following assumptions are made:

1. The solid leaving the regenerator for the gasifier consists only calcium oxide
2. The total amount of fresh calcium carbonate to be fed into the regenerator is:

   = [100/56* (CaO for 100% CO_2 capture in gasifier + CaO re-circulating inside regenerator – un-reacted CaO coming from gasifier + CaO leaving from regenerator with bed drain)]/regeneration efficiency – [$CaCO_3$ coming from gasifier – non-calcined $CaCO_3$ leaving regenerator as bed drain]
3. A fraction (5%) of the solids is drained from the regenerator.
4. The product gas contains mainly hydrogen and a fraction of the carbon dioxide not captured by CaO in the gasifier.
5. The sensible energy of the carbon dioxide is added with the hydrogen sensible energy to calculate the total product gas sensible energy.

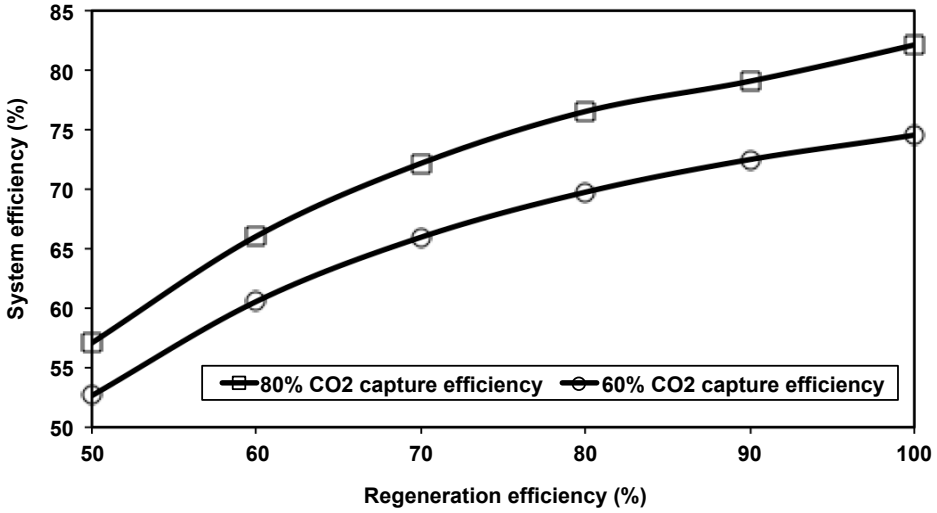

Figure 3.5: Effect of regeneration efficiency on the overall system efficiency for 80% and 60% carbon dioxide capture in the gasifier

Fig 3.5 shows the effect of regeneration efficiency on the overall system efficiency for 80% and 60% carbon dioxide capture in the gasifier. For an 80% CO_2 capture efficiency in the gasifier, the system efficiency varied from 57% to 82% by changing the regeneration efficiency in the regenerator from 50% to 100%. Similarly, for a 60% CO_2 capture efficiency, the system efficiency varied from 53% to 74.5% for the previously mentioned regeneration efficiency.

3.3 EXERGY ANALYSIS OF CFB-CLG SYSTEM

The limitation of the energy analysis based on the first law of thermodynamics is that it does not consider irreversibility between different processes. Thus, one needs to carry out an exergy analysis to find out the maximum obtainable work, which involves defining the local environment or dead state. The local environment or dead state signifies that

anything close to it will produce lower work. The dead state conditions considered here are, a temperature 25^{o}C and pressure of 1 atm.

Exergy consists of two parts: physical exergy and chemical exergy. Physical exergy is a result of the state of the substance being at a temperature and pressure not equal to that of the dead state. Chemical exergy is due to the different chemical composition of the substance from the dead state.

Physical exergy, ε^{ph} is calculated by using the following relation:

$$\varepsilon^{ph} = (h - h_o) - T_o\,(s - s_o) \qquad [3.10]$$

Where, h_o, T_o and s_o represent the enthalpy (kJ/kg), temperature (K) and entropy (kJ/kg K) respectively, at dead state. h and s represent enthalpy and entropy at any temperature and pressure.

The chemical exergy, ε^{ch} for a mixture of gases is calculated using the relation (Ivar, 2006):

$$\varepsilon^{ch} = \sum_i x_i \varepsilon_i^{ch} + RT_o \sum_i x_i\, ln(x_i) \qquad [3.11]$$

Where, x_i is the mole fraction of gases in the mixture and ε_i^{ch} is the standard chemical exergy of the i^{th} component in the mixture of gases.

The chemical exergy of solid biomass is calculated using the relation (Ptasinski et al., 2007):

$$\varepsilon_{ch,biomass} = Z_{org}\left(\beta \times LHV_{org}\right) + Z_s\left(\varepsilon_{ch,S} - C_S\right) + Z_W \times \varepsilon_{ch,water} + Z_A \times \varepsilon_{ch,ash} \qquad [3.12]$$

Where, Z= mass fraction organic component, sulphur, moisture and ash in the biomass and β represents the ratio of chemical exergy to the LHV of the organic fraction of biomass, calculated as:

$$\beta = \frac{1.044+0.016\frac{H}{C}-0.3493\frac{O}{C}\left(1+0.0531\frac{H}{C}\right)+0.0493\frac{N}{C}}{1-0.4124\frac{O}{C}} \quad [3.13]$$

Here, H/C, O/C and N/C represent atomic ratios in the fuel.

The same system as shown in Fig 3.1 is considered here for the exergy analysis. The energy required for regeneration is obtained from the combustion of part of the hydrogen from the gasifier. To carry out the exergy analysis, it is therefore assumed that the regenerator and the combustor are enclosed and isolated from the outside. The exergetic efficiency of the overall system was found to be 83.14%. The calculation for the exergy efficiency is shown in Appendix A. The exergy efficiency is close to the energy efficiency. This may be due to the fact that during gasification only the chemical energy in solid form (in biomass) is converted into the gaseous form. As the calculation of exergy efficiency assumes complete conversion without any loss, therefore exergy loss during this conversion process is very minimal resulting in efficiency close to theoretical energy efficiency.

3.4 DESIGN OF THE CFB-CLG SYSTEM

Biomass properties like high volatile and moisture contents and complex reaction kinetics influence the design of the gasifier to obtain a desired output. To design the CFB-CLG system, the methodology suggested by Basu (2006) was followed. Detail calculations are shown in Appendix A.

3.4.1 Reactor Dimensions

The volume flow rate of the gasifying medium (steam/air or oxygen) is divided by the chosen fluidizing velocity to give the reactor cross-sectional area of a fluidized bed gasifier.

$$A_{bed} = \frac{Q_{med}}{\rho_{med} U} \quad [3.14]$$

Where, ρ_{med} and U are the density and the fluidization velocity of the medium (air, oxygen, steam or their mixture) at the operating bed temperature respectively. The fluidizing velocity is chosen based on the bed particle characteristics, the bed hydrodynamics and the process occurring in the gasifier and the regenerator.

3.4.2 Bed Height

The bed height of a bubbling fluidized bed gasifier should be chosen such that it provides the required residence time for better carbon conversion, and at the same time avoids slugging. Its selection is also governed by operating costs, as a higher bed height means a higher-pressure drop, a taller reactor, and greater auxiliary power consumption. However, due to lack of information on choosing the optimum height for the gasifier, avoid slugging was given priority here. To avoid slugging for group B particle (sand like particles with size within the range of 40-500 microns), the expanded bed height should be less than 2 times the diameter of the reactor i.e $h_{bed} \leq 2\ D_{reactor}$ (Basu, 2006).

3.4.3 Freeboard Height and its Diameter

Ideally, the freeboard height should exceed the transport disengaging height (TDH), so that particle entrainment with upward flowing gases will be as low as possible. This is usually too expensive and a compromise between cost and performance is made.

The calculations for the design of the different components are shown in Appendix A. Table 3.1 shows a summary of the dimensions of the major CFB-CLG systems components.

Table 3.1: Dimensions of the major components of the chemical looping gasifier

	Diameter (mm)	Height (mm)
Gasifier	101.6	450
Regenerator	25.4	1500
Loopseal	101.6	135
Cyclone	38.1	200

3.5 CONCLUDING REMARK

The higher energy and exergy efficiencies of CFB-CLG systems make them attractive technologies for biomass gasification. In practice however, the efficiency reduces with loss in sorbent performance and low conversion of biomass. Therefore a sensitivity analysis is conducted to account for these losses. The analysis shows that a minimum efficiency of 53%, if 60% carbon dioxide produced in the gasifier is captured. The exothermic carbonation reaction provides the heat required for gasification; so a higher carbon dioxide capture will lower the energy requirement and therefore increase the overall efficiency of the system. Based on the empirical relations of fluidization and some other practical considerations for the design of the fluidized bed boilers, a laboratory scale CFB- based chemical looping gasification system is designed.

CHAPTER 4: STEAM GASIFICATION OF BIOMASS WITH IN-SITU CARBON DIOXIDE CAPTURE

This chapter presents the experimental results of the gasification of biomass in the presence of steam and CaO. The effects of several operating parameters on the product gas composition, such as temperature, steam to biomass ratio (S/B) and calcium oxide to biomass ratio (CaO/B) were studied and are presented in this chapter. A non-stoichiometric mathematical model based on gibbs free energy minimization is also developed and its results are validated with the experiment findings.

4.1 BACKGROUND

Hydrogen is an important energy carrier that can be very environmentally friendly if derived from renewable resources such as biomass (Shen et al., 2008; Yildiz et al., 2009). Biomass to energy conversion can be achieved through several thermo-chemical processes namely 1) combustion, 2) pyrolysis and 3) gasification. Among these three processes, gasification has become an attractive method (Saxena et al., 2009). Gasification with steam as the gasifying agent favors production of hydrogen enriched gas. The steam reformation and water gas shift reaction that occur in the presence of steam result in higher yields of hydrogen. Carbon dioxide produced during gasification if captured during the process then conversion system using biomass can be considered as the carbon negative emitter. Thus, steam gasification of biomass with in-process carbon dioxide capture is a promising option for sustainable hydrogen production (Florin and Harris, 2007).

Guoxin and Hao (2009) and Hanaoka et al. (2005) examine the effect of operating condition on hydrogen yield in the fixed reactor. Even though the composition of the product gas obtained in both studies was similar, the yield of gases was much different. As suggested by Florin and Harris (2008), this difference may be attributed to the type of biomass used or the difference in methods applied for carrying out the experiment. Until a universal relationship between the optimum operating conditions and the feedstock characteristics is developed, a rational approach towards a scientific investigation would be to conduct experiments with the different types of feedstock. Such experiments will expand the limited knowledge we have on this process.

4.2 EXPERIMENTAL METHODOLOGY

The biomass sample used was sawdust (particle size 0.425-0.5 mm) and its proximate analysis results are shown in Table 4.1. The CaO used in the experiment was produced by the calcination of limestone at 950^{o}C for two hours.

Table 4.1: Ultimate and proximate analysis of biomass

Biomass type	C (%)	H (%)	O (%)	N (%)	S (%)	HHV (MJ/kg)	M (%)	VM (%)	Ash (%)	FC (%)
Saw dust	49	5.98	44.75	0.01	0.01	19.95	8.88	76.53	0.25	14.33

A schematic diagram of the experimental set up used is shown in Fig 4.1. The reactor comprises a stainless steel cylinder tube with a 6.35 mm internal diameter. An electrically heated bubbling fluidized bed was used to heat the reactor rapidly to the operating temperature. The temperature of the reaction was directly measured by a thermocouple inserted in the biomass. The weight of the reactor tube was measured first in a quad beam balance (sensitivity of 0.01g). After that known volume of water and weighted amount of

biomass (0.2 gm) and CaO were added to the reactor. The reactor was then closed and checked for any air leakage. To ensure the absence of any air or oxygen inside the reactor, the gas inside the reactor, a gasbag and syringe were used for evacuation. The pressure relief valve was set to 20 psi and was connected to the reactor. A gasbag was connected to the other end of the pressure relief valve. To ensure maximum conversion of biomass for proper comparison with the model results, the reactor was kept at the desired temperature for 30 minutes. During this period, the water gets evaporated into steam and reacts with biomass in presence of CaO. The reactor was then removed and allowed to cool to room temperature. When the temperature of the reactor reached room temperature, the gas from the gasbag was transferred into another bag. In doing so, the total amount of gas yield was calculated and the gas was then analyzed in a gas chromatograph. The weight of the reactor was again measured on the quad beam balance to calculate the amount of solid (char calcium oxide and calcium carbonate) left in the reactor. However, further analysis of the leftover solid particles was not carried out.

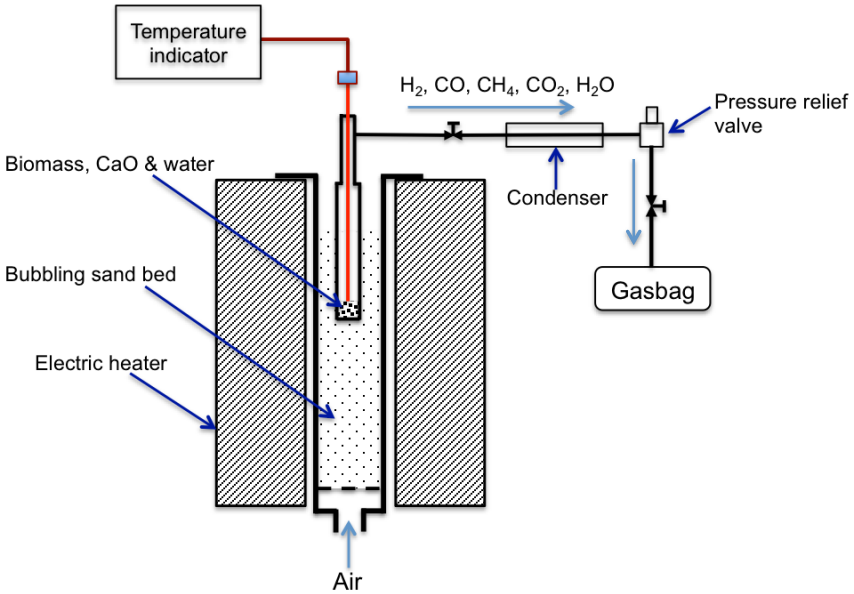

Figure 4.1: Experimental set up for gasification in a fixed bed reactor

4.3 EXPERIMENTAL RESULTS

4.3.1 Effect of S/B Ratio

The effect of steam to biomass (S/B) ratio on the composition of product gas and on the gas yield is shown in Fig 4.2. An increase in S/B ratio from 0.58 to 1.08 increased the hydrogen volume concentration by 7%, but with further increase in S/B ratio only a marginal increase (0.6%) in the hydrogen volume concentration was noted. A consistent decline in the total gas yield with increase in S/B ratio was observed. This suggests that excess steam does not help to increase the gas yield. The decrease in gas yield with increase in steam to biomass ratio may be attributed to decrease in heating rate because of relatively longer time taken by the excess moisture to heat up to the desired temperature. The heating rate for a low S/B ratio is expected to be higher than that for a higher S/B ratio. A higher heating rate favors more gas yield, therefore gas yield decreases with an increasing S/B ratios. Recent experiments were conducted in an ideal situation of batch reactor with maximum contact between the biomass, CaO and steam in a fixed bed with a residence time of 30 minutes. In commercial units, the contact between the biomass and steam will be less than perfect and the residence time will be. This may allow the bypassing of steam fed into gasification. To account for this excess steam, S/B>1.0 might be necessary.

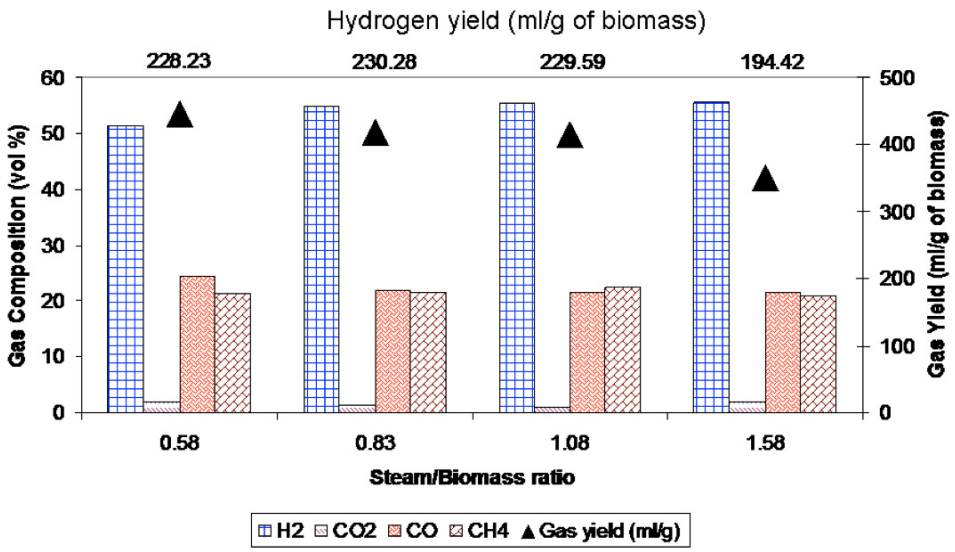

Figure 4.2: Effect of Steam to biomass ratio (CaO/B = 1.5, T = 670^{o}C)

4.3.2 Effect of Temperature

The product gas composition and gas yield were studied at three different temperatures; 600^{o}C, 670^{o}C and 710^{o}C and the results are shown in Fig 4.3. The hydrogen concentration in the product gas first increasesd as the temperature increased from 600^{o}C to 670^{o}C; however, a further increase in temperature caused the hydrogen concentration to start decreasing. The decrease in reactivity of the water gas shift reaction with increase in temperature could be the reason behind the drop in hydrogen fraction. However, the lack of change in carbon monoxide concentration suggests that there could be some conversion of carbon monoxide to carbon dioxide as there is an increase in the carbon dioxide concentration in the gas. Higher temperature favors higher conversion of char and tar into gases, so the gas yield increases with the increase in temperature. According to Florin and Harris (2008), the higher gas yield may be due to the increase in the initial rate of pyrolysis and steam cracking and the reformation of char, tar and other higher hydrocarbons into gases. They also reported that, even though an increase in temperature

favors higher gas yield, the hydrogen concentration decreases. Hence, there exists an optimum temperature (700^{o}C) for steam gasification in the presence of CaO. However the optimum temperature obtained here i.e. 670^{o}C is slightly lower, which may be because of the different experimental methodology. Even though in Fig 4.3, there is noticeable peak for hydrogen concentration at 670^{o}C, but still this concentration is close to the concentration obtained at 600^{o}C and 710^{o}C. So to conclude the effect of temperature based on the experiment and as mentioned in literature, it can be said that there exists an optimum temperature in between 650^{o}C to 700^{o}C for higher concentration of hydrogen in product gas from biomass gasification in presence of CaO.

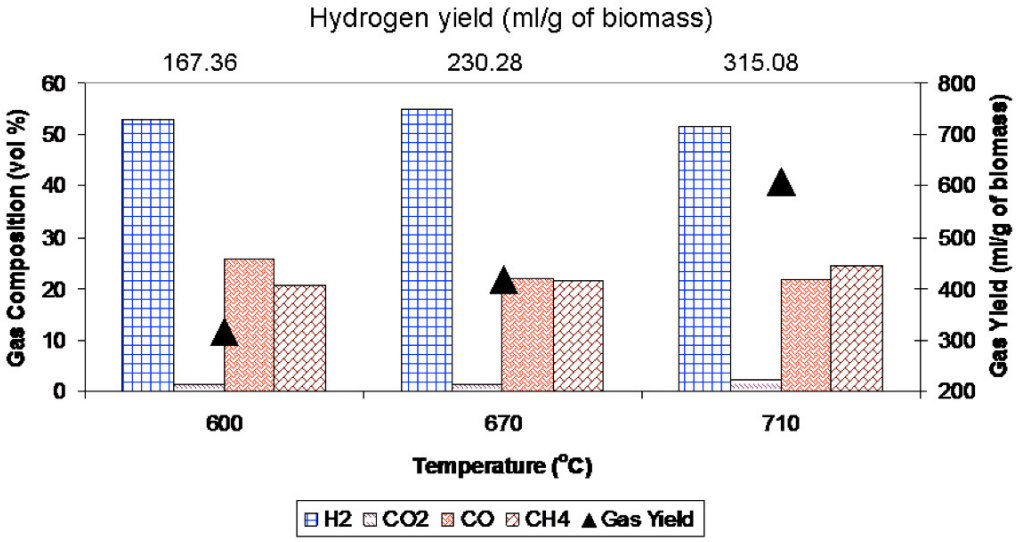

Figure 4.3: Effect of temperature on the gas composition and yield (S/B = 0.83, CaO/B = 1.5)

4.3.3 Effect of Cao/Biomass Ratio

To study the effect of calcium oxide on gas composition and gas yield, experiments were conducted for CaO to biomass feed ratios of 0, 1, 1.5 and 2 and the results obtained are shown in Fig 4.4. By increasing this ratio from 0 to 1.0, the volumetric composition of hydrogen increased from 22.29% to 53%, but increasing the ratio further to 1.5 resulted in only a marginal increase (to 55%). The yield of hydrogen more than doubled (from

101.33 to 230.28 ml/g of biomass), when CaO/biomass ratio was increased from zero to 1.0. According to Le Chatelier's principle, a reaction moves in the forward direction if the partial pressure of the product is less than the partial pressure of the reactant. The instantaneous removal of carbon dioxide by CaO lowers the partial pressure of carbon dioxide, moving the water gas shift reaction in forward direction and thus resulting in a higher yield of hydrogen.

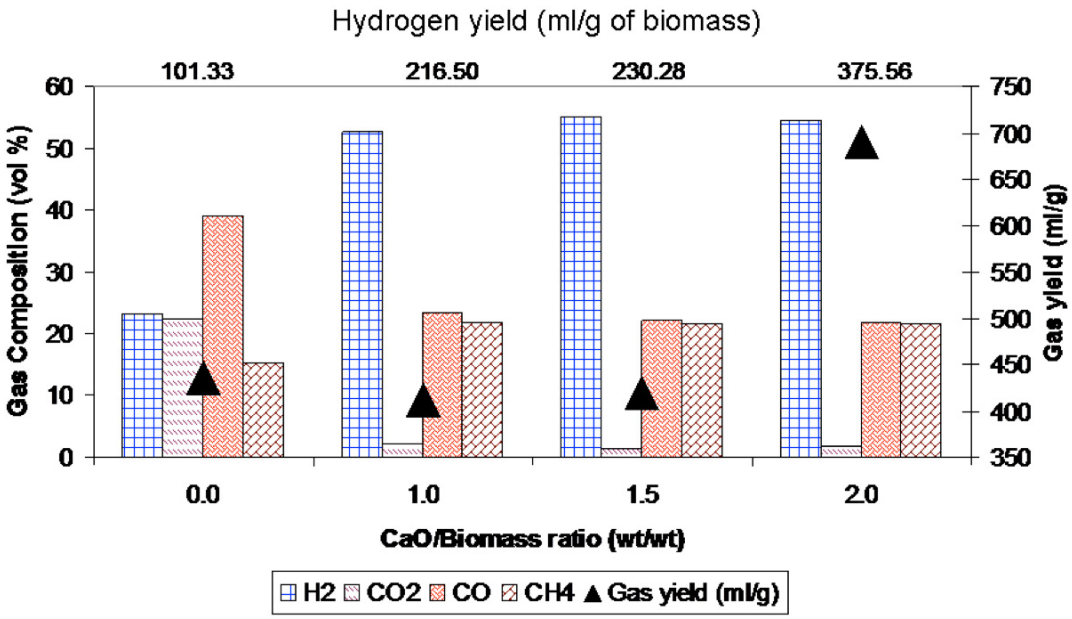

Figure 4.4: Effect of CaO/B ratio (S/B = 0.83, T = 670^{o}C)

Even though the increase in percentage of hydrogen in the product gas was marginal above CaO/biomass ratio 1, its yield as well as the total gas yield continued to increase up to CaO/biomass ratio 2. This phenomenon was also reported by Hanaoka et al. (2005). They found that at Ca/C = 1, the carbon dioxide concentration in the product gas was zero but gas yields were highest at Ca/C = 2. Carbonation is an exothermic reaction releases heat when capturing carbon dioxide, increasing the temperature of the surrounding. This higher temperature results in increased cracking of tar and conversion of char present in its neighbor. Therefore, the use of CaO not only helps to capture carbon

dioxide but also to break the tar and char into gas. Increasing the CaO/biomass ratio from 1 to 1.5 resulted in a 2% increase. However, a drastic increases of 63% in gas yields was observed when the CaO/biomass ratio was raised from 1.5 to 2. CaO appears to have catalytic behavior to break the tar and could result in higher gas yield (Siyi et al., 2009). Therefore, even though the amount of CaO required for capturing CO2 has been satisfied, the excess CaO displays a catalytic behavior that breaks tar and ultimately increases gas yield.

The tests were conducted in a fixed bed reactor where the mixing of CaO with the reactants is not as through as that in a fluidized bed reactor. Therefore, one may find that it would take a little more CaO to capture CO_2 compared to what is theoretically required. This explains why the increase in gas yield for a CaO/biomass ratio of 1.5 was not as significant as that corresponding to the CaO/biomass ratio of 2.

The concentration of carbon dioxide in the product gas without using CaO was 22.50% which then dropped to 1.56% for CaO/biomass = 2. For the rest of the CaO/biomass ratios studied, the carbon dioxide concentration maintained a steady value of approximately 1.5%.

4.4 EQUILIBRIUM MODELING OF BIOMASS GASIFICATION

Equilibrium models, also referred to as zero dimensional (i.e. space independent models), are helpful in predicting the maximum possible conversion of biomass (Huang and Ramaswamy, 2009). Equilibrium model can be developed using two approaches:

stoichiometric and non-stoichiometric. The stoichiometric model is based on equilibrium constants and requires knowledge of the specific chemical reactions and the reaction path taking place.. It, therefore, requires a selection of appropriate chemical reactions, and information concerning the value of their equilibrium constants. This makes this method unsuitable for complex problems where the chemical formulas of the feed or the reaction equations are not known. The second model under this category involves minimization of gibbs free energy (non-stoichiometric model), which is an effective tool for finding the composition of gases when the reaction paths are unknown (Florin and Harris, 2008). Ramaya et al. (2006) used the stoichiometric equilibrium model to carry out a feasibility study of gasification of coffee husk in a fluidized bed gasifier. Huang and Ramaswamy (2009) have also developed a stoichiometric equilibrium model, which can be used for different types of the gasifiers. Jarungthammachote and Dutta (2007) used the stoichiometric model to study a downdraft waste gasifier.

The equilibrium model applying the concept of gibbs free energy minimization has being used considerably for the gasification of coal, and to a limited extent for the gasification of biomass (Florin and Harris, 2008). Adhikari et al. (2007) used the non-stoichiometric equilibrium model to study hydrogen production from the steam reformation of glycerin. Jarungthammachote and Dutta (2008) used non-stoichiometric model for both spout bed and spout fluid bed gasifiers. Non- stoichiometric equilibrium modeling can be very helpful for the prediction of gas composition in complex biomass gasification whose reaction kinetics cannot be easily identified.

The reactions taking place during steam gasification in the presence of CaO can be written in the form:

$$CH_hO_o + aH_2O \rightarrow \eta_{CO2}CO_2 + \eta_{CH4}CH_4 + \eta_{CO}CO + \eta_{H2}H_2 + \eta_{H2O}H_2O \quad [4.1]$$

$$CO + H_2O \rightarrow H_2 + CO_2 - 41.2 \text{ kJ/mol} \quad [4.2]$$

$$CaO + CO_2 \rightarrow CaCO_3 - 178 \text{ kJ/mol} \quad [4.3]$$

The overall reaction of steam gasification in the presence of CaO is:

$$CH_hO_o + aH_2O + bCaO \rightarrow \eta_{CO2}CO_2 + \eta_{CH4}CH_4 + \eta_{CO}CO + \eta_{H2}H_2 + \eta_{H2O}H_2O + \eta_{CaCO3}CaCO_3 \quad [4.4]$$

To calculate the coefficients $\eta_{CO_2}, \eta_{CH4}, \eta_{CO}, \eta_{H_2}, \eta_{H_2O}$ & η_{CaCO_3} for different values of '*a*', '*b*' and temperature, the non-stoichiometric equilibrium model is used.

At equilibrium, the total gibbs free energy is at its minimum. The total Gibbs free energy is given by:

$$G^t = \sum_{i=1}^{N} n_i \mu_i \quad [4.5]$$

Where, n_i = number of moles of species *i*

μ_i = Chemical potential of species *i* given by,

$$\mu_i = G^o{}_i + RT \ln\left(\frac{f_i}{f^o{}_i}\right) \quad [4.6]$$

f_i = fugacity of species *i*

$G^o{}_i$ & $f^o{}_i$ = standard gibbs free energy and standard fugacity of species *i*, respectively

Equation [4.6] can be written in terms of pressure as

$$\mu_i = G^o{}_i + RT \ln\left(\frac{\phi P_i}{P^o}\right) \quad [4.7]$$

Where ϕ = Fugacity coefficient

For the ideal gas case at atmospheric conditions

$$\mu_i = \Delta G^o{}_{f,i} + RT \ln(y_i) \quad [4.8]$$

Where, y_i = mole fraction of gas species *i*

$$y_i = \frac{n_i}{\text{Total moles in the mixture}, n_{total}}$$

$\Delta G^o{}_{f,i}$ is the standard Gibbs free energy of formation of species *i*, and is set equal to zero for all chemical elements.

Now, substituting equation [4.8] into equation [4.5], we get

$$G^t = \sum_{i=1}^{N} n_i \Delta G^o{}_{f,i} + \sum_{i=1}^{N} n_i RT \ln\left(\frac{n_i}{n_{Total}}\right) \quad [4.9]$$

The value of n_i should be found such that the G^t will be minimum. The Lagrange multiplier method can be used for this purpose. To use this method, the constraints are defined in terms of the elemental balance on both reactant and product sides:

$$\sum_{i=1}^{N} a_{ij} n_i = A_J \text{ , J = 1, 2, 3… K} \quad [4.10]$$

a_{ij} = Number of atom of j^{th} element in a mole of i^{th} species.

A_J = Total number of atom of j^{th} element in the reaction mixtures

Thus, the Lagrange function (L) is defined as:

$$L = G^t - \sum_{J=1}^{K} \lambda_J \left(\sum_{i=1}^{N} a_{ij} n_i - A_J \right) \quad [4.11]$$

Where λ = the Lagrangian multiplier.

So, to find the extreme point,

$$\left(\frac{\partial L}{\partial n_i} \right) = 0 \quad [4.12]$$

Substituting the value of G^t from equation [4.9] into equation [4.11] and taking its partial derivative as defined by equation [4.12], the final equation is of the form given by equation [4.13]:

$$\left(\frac{\partial L}{\partial n_i} \right) = \frac{(\Delta G^o{}_{f,i})}{RT} + \ln\left(\frac{n_i}{n_{total}} \right) + \frac{1}{RT} \sum_{J=1}^{K} \lambda_J a_{ij} \quad [4.13]$$

Using equation [4.13] for the different product species and conducting carbon, hydrogen oxygen and calcium balances, one can get a set of equation which can be solved to obtain the composition of the product gas. Newton Raphson's method was used to solve the simultaneous non-linear equations.

4.4.1 Mathematical Model Results

Figure 4.5 shows the gas composition obtained from the equilibrium model. The peak hydrogen concentration is found to be 65.85% at the S/B ratio of 0.68. At S/B ratio lower than this CO increases but above 0.68 it start decreasing. The decrease in CO is due to the participation of CO in the water gas shift reaction while the slight increase at the beginning may be a result of the steam reformation of methane. As the methane

concentration drops sharply with the increase in S/B ratio, it causes the overall CO concentration to increase.

$$CH_4 + H_2O = CO + 3\ H_2 \qquad [4.14]$$

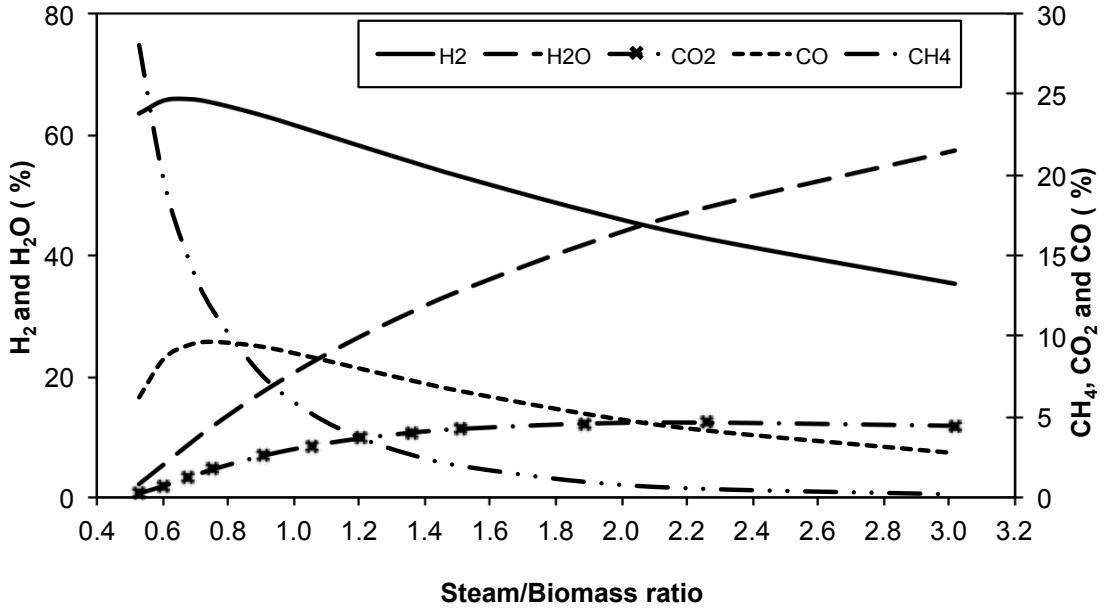

Figure 4.5: Gas composition obtained from the mathematical model
(T = 670^{o}C, CaO/Biomass = 1.5)

Figure 4.6 shows the fraction of hydrogen and carbon dioxide in the product gas at CaO/biomass ratios of 0, 0.5, 1 and 1.5. Increasing the amount of CaO increases the hydrogen fraction in the product gas. The peak hydrogen concentration of 65.85% is found at CaO/biomass = 1.5. Increasing the CaO/biomass ratio not only increases the hydrogen concentration but also shifts the equilibrium point such that the maximum hydrogen concentration can be obtained at lower steam to biomass ratios. For steam gasification without CaO, the maximum hydrogen concentration is obtained around the S/B ratio of 0.93 while for the CaO/Biomass ratio of 1.5, the maximum hydrogen is obtained at the S/B ratio of 0.68. Using CaO reduces the carbon dioxide in the product gas. The concentration of carbon dioxide drops to nearly zero at S/B = 0.53 and

CaO/Biomass = 1.5. The drop in percentage of hydrogen with increased steam to biomass ratio is due to the dilution of the product gas with steam.

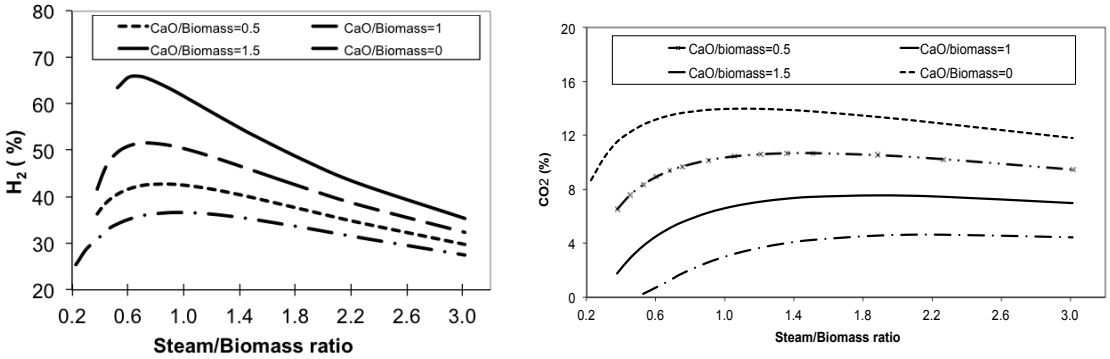

Figure 4.6: Effect of Steam to biomass ratio on hydrogen and carbon dioxide production at different CaO/Biomass ratios

4.4.2 Validation of Experimental Results with the Mathematical Model

The gas composition obtained experimentally and from the mathematical model are compared in Fig 4.7. Although the hydrogen fraction increased with increasing steam to biomass ratio in both cases, the equilibrium model predicts maximum conversion and thus gave greater values than the experimental ones. On the other hand, the fraction of carbon dioxide obtained in the batch experiment matched quantitatively with the mathematical results and the CO decreased at higher S/B ratios in both cases. However, the model under predicted the methane fraction. Its percentage remained more or less constant (21%-22%) in the experiment, but constantly decreased (from 28% to 2.94%) with increasing steam to biomass ratio (from 0.53 to 1.51) in the model. Methane reformation occurs at a higher temperature (above 750^{o}C-800^{o}C). At our experimental temperature of 670^{o}C, methane is formed due to the devolatilization of biomass. As the volatile content of the sample biomass is same, the percentage of methane produced during devolatilization also remains constant and does not undergo any further conversion because of the lower temperature. Thus the percentage of methane obtained

experimentally remains more or less constant, while the model does not consider the kinetics of reaction and the methane continuously gets reformed as the steam to biomass ratio increases.

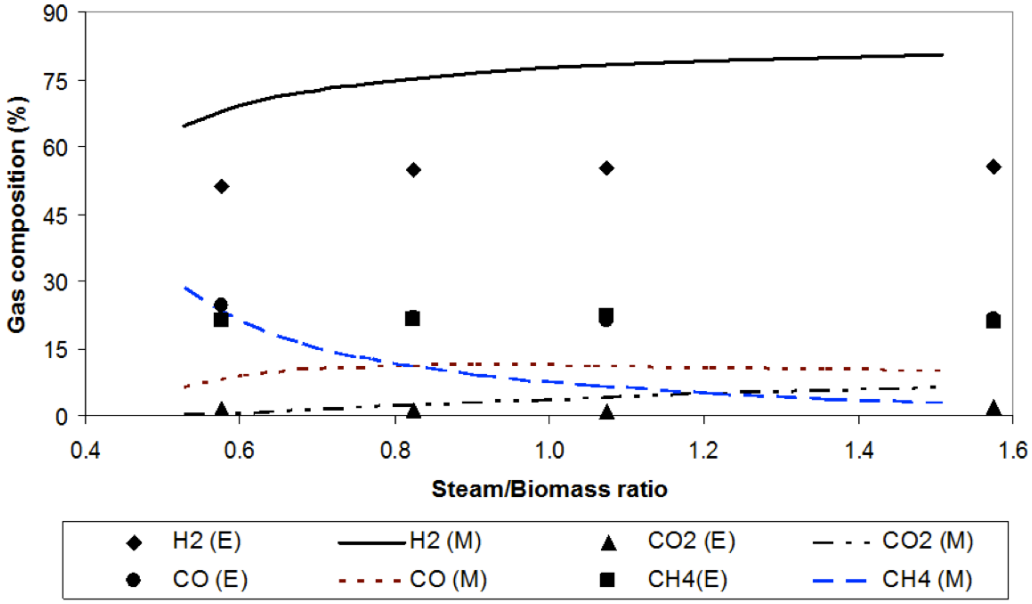

Figure 4.7: Effect of Steam to biomass ratio: comparison between experimental (E) and mathematical model (M) results

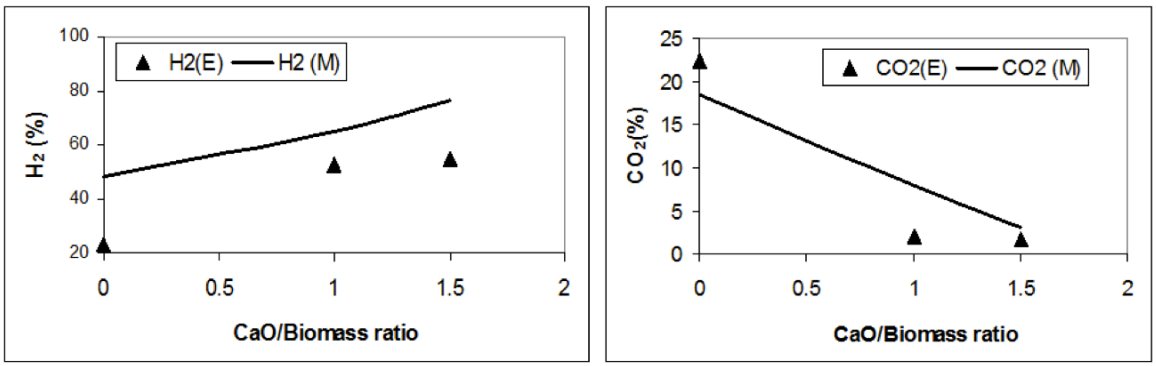

Figure 4.8: Effect of CaO/biomass ratio: comparison between experimental (E) and mathematical model (M) results

Figure 4.8 shows the effect of CaO/Biomass ratio on the hydrogen and carbon dioxide fractions, comparing the results obtained experimentally with those from the model. During the experiment, only 2/3 of the reactor is inside the heater while the upper 1/3 is exposed to the atmosphere. Once the gas is formed, it moves to the relatively cooler

upper section, and get quenched quickly. This limits the gas phase reaction to occur any further. The water gas shift reaction, which converts carbon monoxide and produces hydrogen, is the major gas phase reaction that is supposed to take place. As this reaction is limited, carbon monoxide is not completely converted, resulting in a lower hydrogen concentration in the product gas. It is observed from the experimental results as well that the carbon monoxide concentration is reasonably higher. The short residence time of the product gas in the reactor could be another reason for the differences in gas composition obtained experimentally with that obtained from the non-stoichiometric equilibrium model. As the set pressure can only hold the gas for a few seconds, all the gases may escape into the gasbag without leaving much gasifying agent in the reactor for further reaction to occur. Thus, this might be the reason for the lower prediction of hydrogen concentration by the equilibrium model.

4.5 CONCLUDING REMARKS

The following conclusions can be drawn from the results obtained from studying the effect of steam to biomass ratio, temperature and the CaO to biomass ratio on hydrogen production from steam gasification of biomass:

- A maximum hydrogen yield of 230 ml/g of biomass was obtained at S/B = 0.83 when increasing the S/B ratio from 0.58 to 1.58. The hydrogen concentration at S/B = 0.83 was 54.96%. The carbon dioxide concentration was around 1% for different ratios of S/B studied at CaO/Biomass = 1.5.

- Increasing temperature increases the hydrogen yield but temperature above 670^{o}C lower the concentration of hydrogen in the product gas.
- Increasing CaO/Biomass ratio greatly increases the yield and concentration of hydrogen in the product gas. The hydrogen concentration increased from 23.29% (CaO/biomass = 0) to 54.54% (CaO/Biomass = 2) while the hydrogen yield increased by 2.7 times. The maximum hydrogen yield of 376 ml/g of biomass was obtained at CaO/Biomass = 2.
- Although the equilibrium model developed with the concept of gibbs free energy minimization overestimates the hydrogen concentration, its trends on hydrogen and carbon dioxide fractions agree well with the experimental results.

CHAPTER 5: STUDY ON THE CALCINATION/CARBONATION CYCLE

This chapter presents a study on the calcination/carbonation cycles of limestone as it goes through the CFB-CLG system. The effects of different gasifying media on calcination, such as particle size and temperature are presented. Kinetic rate equations are developed for calcination in the presence of different media in order to determine the viability of its use as a fluidizing medium in the regenerator of a circulating fluidized bed (CFB) based chemical looping gasification (CLG) system. Experiments on alternate calcination/carbonation cycle are conducted to measure the loss in the absorbing capacity of sorbent. An empirical relation is developed to estimate this loss for a given number of cycles following the loop.

5.1 BACKGROUND

Chapter 3 defined the chemical looping gasification system where the sorbent calcium oxides, enters into a loop of carbonation ($CaO + CO_2 = CaCO_3$) and calcination ($CaCO_3 = CaO + CO_2$); capturing carbon dioxide in one case and releasing it in the other. The significance of using CaO as the sorbent for in-process carbon dioxide capture during the gasification of biomass was then illustrated in chapter 4. It was shown that in-process capture of carbon dioxide moves the composition of product gas towards higher hydrogen content and results in higher gas yield. However, the loss in sorbent ability to capture carbon dioxide from the product gas has not yet been discussed. Ideally, the sorbent of a looping process should retain its capture properties irrespective of the number of calcination/carbonation loops it goes through. In practice however, this is not the case.

This loss in capture ability may be due to the deposition of char and tar during gasification, sintering or agglomeration. This phenomenon can be a serious issue while running a chemical looping system as it increases the fresh sorbent requirement, and therefore the overall cost. Thus this aspect of sorbent needs a close attention. Also in chapter 3 it is suggested that there might be a possibility of recycling a part of the carbon dioxide as a fluidizing medium for the regenerator (calcination). This however will increase the equilibrium temperature of calcination. Also conversion of limestone in presence of CO_2 is not predictable. Therefore, steam is proposed as an alternative fluidizing medium for the regenerator of CFB-CLG. Studies done by Ayer et al. (2005) showed that use of steam resulted in higher conversion obtained at a lower calcination temperature, an effect that helps to reduce sintering of sorbent. The temperature suggested by Ayer et al. (2005) and Florin and Harris (2008) was 700^{o}C. In a CFB-CLG system, the temperature in the regenerator cannot be reduced to as low as 700^{o}C because the heat required to maintain the gasifier temperature is carried by the solid from the regenerator and any drop in temperature of the regenerator will also lower the gasifier temperature. Therefore it becomes necessary to examine the effect of higher temperature steam calcination on the conversion during carbonation as the sorbent goes through number of calcination-carbonation cycles. Hence, the study is conducted on the calcination reaction with steam as a medium and the loss in sorbent ability to capture carbon dioxide over the number of alternate calcination-carbonation cycles is examined. A comparison is also made between carbon dioxide and steam as fluidizing media in the regenerator. The results are compared with those of inert nitrogen, which is a commonly used medium for calcination studies. For further comparison, a kinetic rate equation is

developed for calcination in the presence of H_2O, N_2 and CO_2. In CFB-CLG systems, the particle size will vary and the conversion obtained will also vary accordingly. Thus, experiments are conducted to examine the effect of particle size on the conversion obtained during the calcination and carbonation reactions. All experiments are conducted in a quartz wool matrix (QWM) reactor developed by Wu and Basu (1993) to simulate the highly expanded bed of a CFB riser. In the QWM reactor, the gas velocity is adjusted to a value similar to the typical gas-solid slip velocity typically attained in a fast bed. This way, the results obtained in the QWM reactor can closely simulate the calcination reaction taking place in the regenerator of a CFB-CLG system.

5.2 METHODOLOGY

Figure 5.1 shows a schematic of the QWM reactor , which consists of a 50 mm diameter stainless steel reactor encased in an electric heater. A temperature controller controls the temperature inside the reactor, which is continuously monitored with a K type thermocouple. A precision balance sits on top of the reactor that facilitates the continuous measurement of the mass of the substance being examined. A wire basket, which hangs from the balance, holds the sample being studied inside the reactor. The flow rate of the gases is continuously controlled and measured with an electronic flow meter. For steam, it is first calibrated to measure the flow with valve opening and then fed into the reactor.

A weighted sample of calcium carbonate of size 45 micron is sprinkled over the quartz wool that is placed inside a wire basket. In order to minimize the interparticle heat and mass transfer effect in gas-solid reaction, small size particle is chosen for the study. The

reactor is heated to the desired temperature and then the gas is supplied to the bottom of the reactor. Once the system is stabilized and a constant temperature is noted in the reactor, the basket with quartz wool and calcium carbonate is lowered into the reactor. The basket is suspended from the balance at the top. The sample is kept this way for 30 minutes and afterwards it is taken out, cooled and weighed.

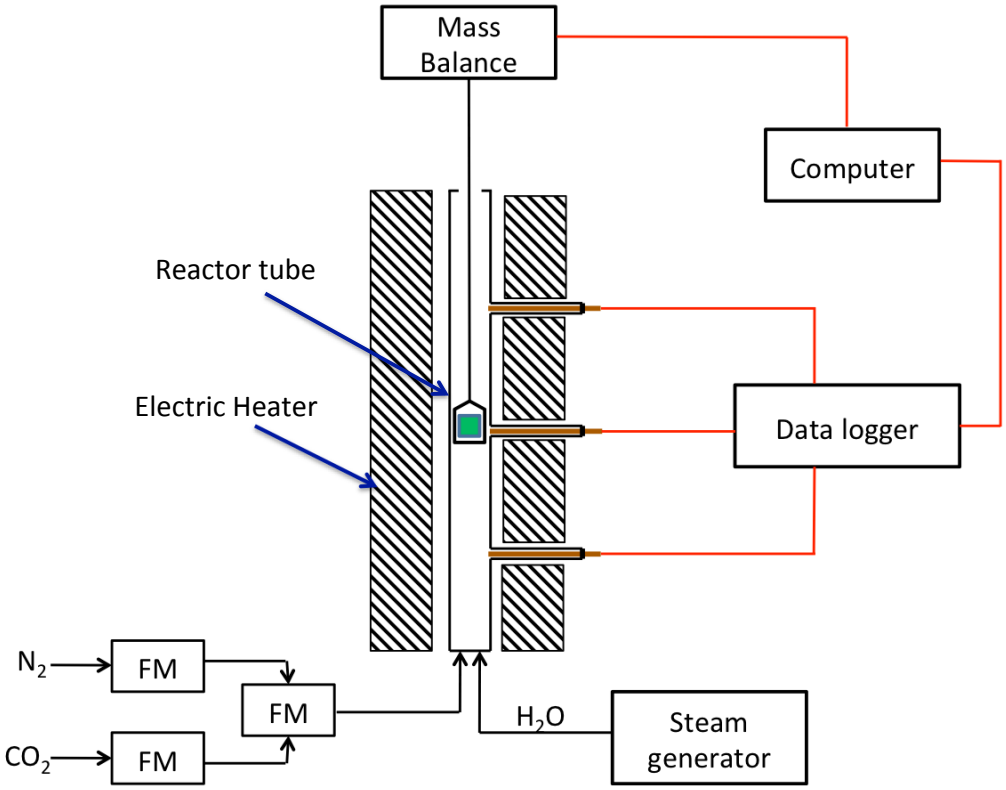

Figure 5.1: Schematic of the QWM experimental setup

The calcination reaction ($CaCO_3 = CaO + CO_2$) was studied at four temperatures: 800°C, 900°C, 950°C and 1000°C for each of the three media, CO_2, H_2O and N_2. The carbonation reaction ($CaO + CO_2 = CaCO_3$) was studied at 650°C with CO_2. Experiments at 100% CO_2 were done to ensure that the fast stage of carbonation went to completion, so that any loss in conversion through the cycle will only be due to the sintering of the particle.

To study the effect of particle size on calcination and carbonation reactions, limestone particle of sizes 325, 275, 230 and 135 micron were subjected to calcination at 950^{o}C with N_2 as the medium. The calcined particles were later carbonized at 650^{o}C with a gas mixture containing 25% CO_2 and 75% N_2.

The calcination test was carried out for 30 min, and then the sample was moved out into a cooler environment to quench the calcination reaction. Meanwhile, the medium in the QWM was changed to carbon dioxide and the temperature controller of the reactor was set to 650^{o}C. Once the temperature dropped to 650^{o}C, the previously calcined sample was lowered into the reactor, and was left there for another 30 min for the carbonation reaction to occur. And thus the sample underwent alternate calcination and carbonation. The study was conducted for five alternating cycles of calcination and carbonation.

A first order reaction kinetic model has been used to examine the kinetics of calcination as well as to compare the rate of calcination in presence of three media.

$$\frac{dX}{dt} = K\frac{(1-X)(P_{eq}-P_{CO2})}{P_{eq}} \qquad [5.1]$$

Where,

$$K = k_o e^{\frac{E_a}{RT}}$$

$$X = \left(\frac{W_0 - W_t}{W_o}\right) \times \left(\frac{100}{44}\right)$$

The equilibrium decomposition partial pressure, P_{eq} (atm) is given as (Stanmore and Gilot, 2005):

$$P_{eq} = 4.137\times10^{7}\, e^{-\frac{20474}{T}}$$

Where, K = intrinsic rate constant (s^{-1}), X = Conversion (-), P_{CO2} = partial pressure of CO_2 (atm), k_o = reaction rate constant (s^{-1}), E_a = activation energy (kJ/mol), R = universal gas constant (kJ/mol K), T = temperature (K), W_o = initial weight of calcium carbonate (gram), W_t = weight of calcium carbonate after time t (gram).

5.3 RESULTS AND DISCUSSION

5.3.1 Effect of Temperature and Residence Time on Calcination

Table 5.1 shows the conversion obtained during calcination at different temperatures in the presence of three different media.

Table 5.1: Calcination of $CaCO_3$ into CaO under three different media

Medium	N_2		CO_2		H_2O	
Temperature (^oC)	Conversion (%)	Time (mins)	Conversion (%)	Time (mins)	Conversion (%)	Time (mins)
600					8.78	30
700	52.29	30			73.22	30
800	96.32	25.50	7.58	30	96.94	30
900	99.39	12.5	20	30	100	25
950	99.31	10	72.89	30	100	19.16
1000	100	10	92.95	30	100	10

[Conversion %= (initial weight – final weight)/initial weight*100 %]

In the N_2 environment at 900^{o}C, 99% conversion was obtained in 12.5 minutes. The same level of conversion was obtained but in a shorter time (10 minutes) when the temperature was increased to 950^{o}C. Meanwhile in the CO_2 environment, the conversion at 900^{o}C after 30 minutes was 72.89% and increased to only 92.95% when the temperature was raised to its maximum value of 1000^{o}C. Conversion in a CO_2 environment is much lower even at very high temperatures because the partial pressure of CO_2, which is very close to

the equilibrium decomposition pressure, inhibits the calcination reaction. With steam as a medium, the maximum possible conversion of 100% is obtained in a short residence time of 10 min at a temperature of 1000^{o}C. Here we note that steam offers a conversion higher than both CO_2 and N_2. Even at only 700^{o}C, 73.22% conversion can be obtained which is 28% more than the conversion obtained with N_2 at the same temperature. Steam seems to have a catalytic effect that lowers the equilibrium decomposition temperature for the calcination reaction to occur, thus allowing conversion to be complete even at very low temperatures. Other researchers have observed the same phenomenon. Ayer et al. (2005) and Florin and Harris (2008) also mentioned 700^{o}C as the minimum temperature for calcination in the presence of steam to occur. Wang and Thompson (1995) found that the surface adsorption of H_2O molecules weakens the CaO-CO_2 bond resulting in enhanced calcination rates even at relatively low temperatures. On the other hand, the calcination conversion obtained with N_2 is higher than that with CO_2 because supply of N_2 quickly removes carbon dioxide and thus lowers its partial pressure.

The calcination with steam can occur at a lower temperature, but it needs longer residence time. As shown in Fig 5.2, it takes a very long time to achieve full conversion with CO_2 as the medium, whereas it only takes 10 min with N_2 and 19 min with steam at 950^{o}C. Both Fig 5.2 and Table 5.1 show that conversion is influenced by temperature as well as residence time. Thus, a linear regression model has been developed for each of the three media to assess the combined effect of temperature and residence time.

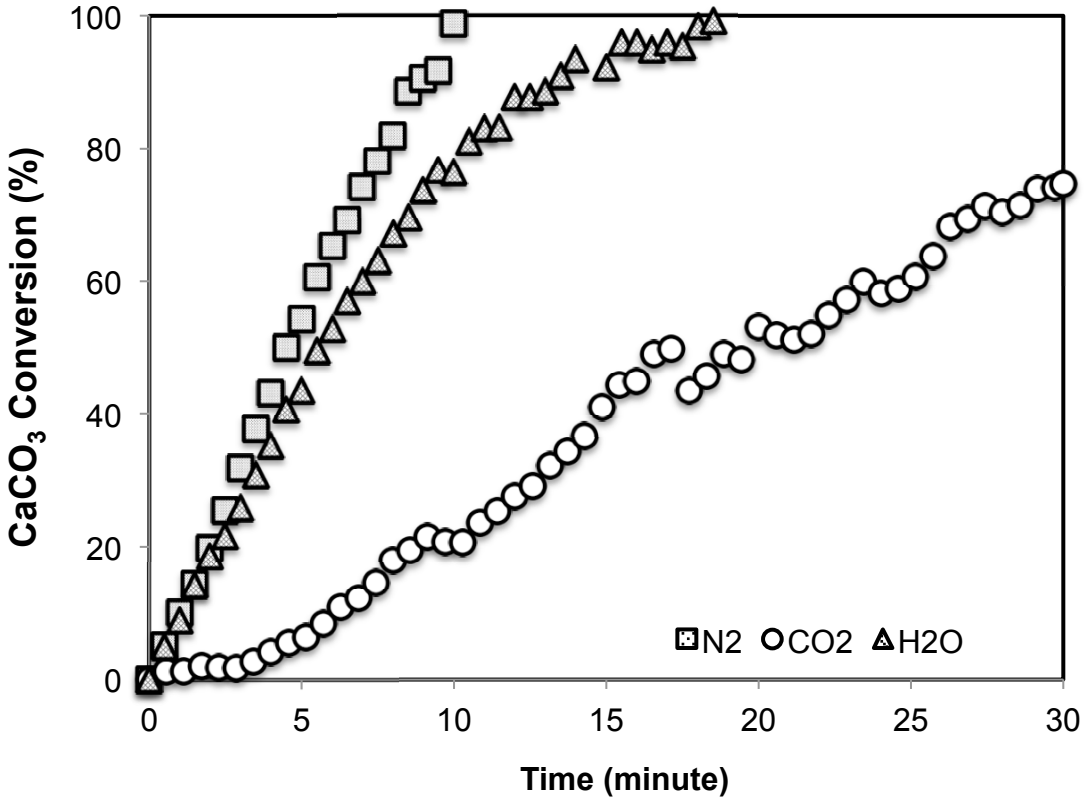

Figure 5.2: $CaCO_3$ conversion at 950°C obtained with time in the presence of three different medium

The fractional conversion of $CaCO_3$, X is expressed empirically as a function of temperature θ and time τ, (These empirical relations are valid for the range of temperature and time studied as shown in Table 5.1)

For H_2O:

$$X = -1627 + 1.68\,\theta + 46.1\,\tau - 0.0416\,\theta\,\tau \qquad [R^2 = 88.8\%] \qquad [5.2]$$

For CO_2:

$$X = -359 + 0.446\,\theta \qquad [R^2 = 79.3\%] \qquad [5.3]$$

For N_2:

$$X = 186 - 0.126\,\theta - 14.6\,\tau + 0.0188\,\theta\,\tau \qquad [R^2 = 99.1\%] \qquad [5.4]$$

Here, θ = Temperature (°C), τ = time (min) and X = conversion of $CaCO_3$ (%).

From Table 5.1 it is apparent that the calcination of $CaCO_3$ in the presence of H_2O reduces with reduction in temperature, but there is a sharp order of magnitude drop in conversion when the temperature drops from 700°C to 600°C. Reasons for this large reduction below 700°C could not be explained at this time. Nevertheless, this finding is significant as it defines the lower limit of operation of the regenerating riser of a CFB-CLG system, which could have direct bearing on the energy efficiency of the system.

5.3.2 Effect of Particle Size on Calcination and Carbonation

The effect of particle size on the calcination (Fig 5.3) and carbonation (Fig 5.4) reactions was studied for particle of size 325, 275, 230 and 135 microns. Fig 5.3 shows that the calcination rate is higher for smaller sized particles. Larger particles need a longer time for complete conversion.

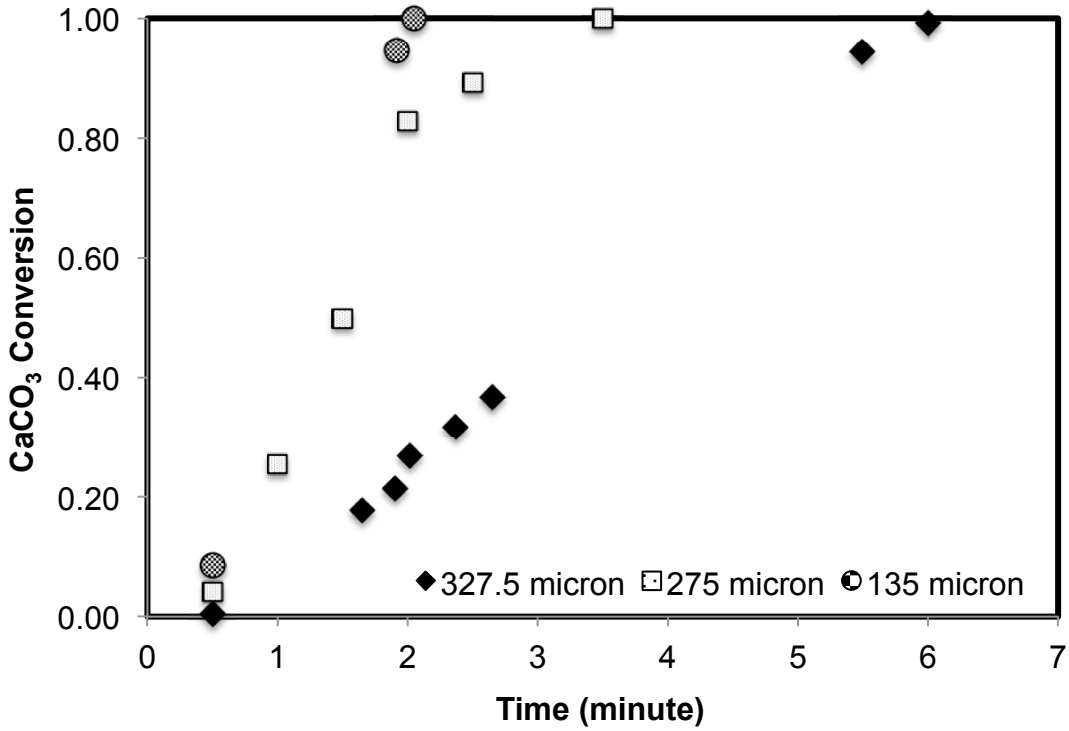

Figure 5.3: Effect of particle size on calcination reaction

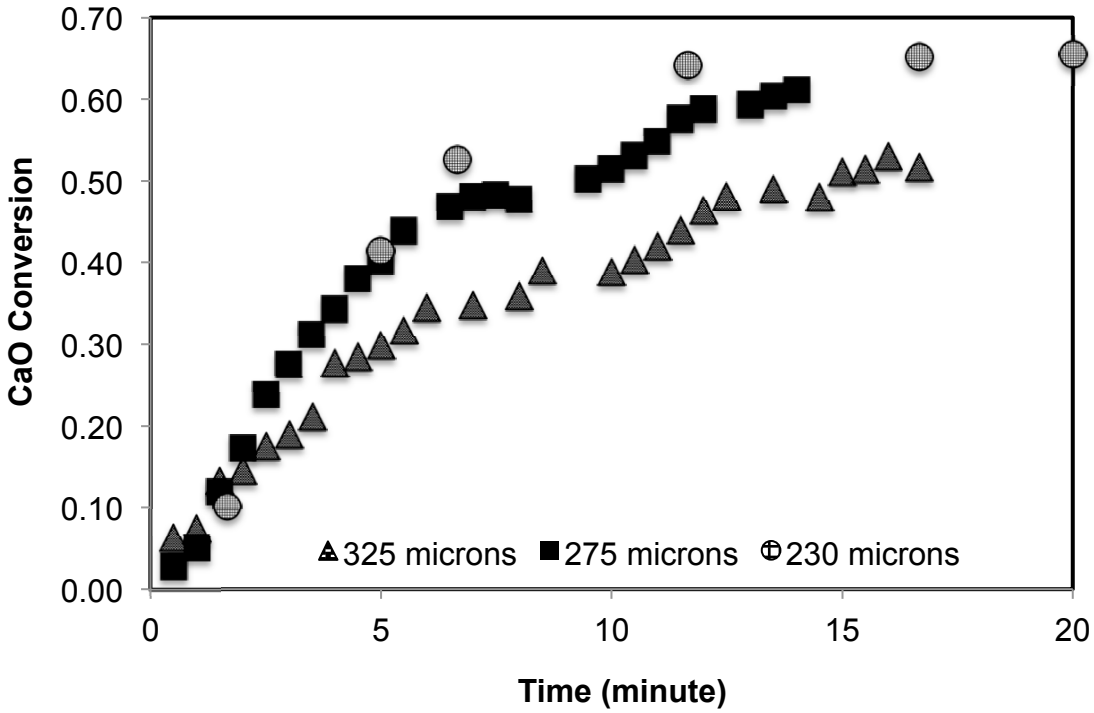

Figure 5.4: Effect of particle size on carbonation reaction

To explain the effect of particle size on carbonation, it is first necessary to examine how the carbonation reaction occurs and what determines its rate of reaction. As shown by others (Grasa and Abanades, 2006; Florin and Harris, 2008), the carbonation reaction consists of two reaction regimes. The first one is a very fast surface reaction that is responsible for most of the conversion during carbonation. The second reaction is controlled by pore diffusion is therefore relatively slow. Finer particles have a larger external surface area that allows a greater part of the carbonation reaction to occur through faster surface reaction in a short amount of time, whereas for the coarser particles, a slow pore reaction takes the major share and hence conversion ia lower at any given time. From Fig 5.4, one notes that during the initial stage of the carbonation reaction, the effect of particle size seems to be negligible as the conversion is mostly dominated by the fast surface reaction. However, once a thick layer of calcium carbonate is formed then further conversion will be controlled by diffusion. In that case, larger sized

particles offer much higher resistance for diffusion to occur resulting in lower conversion. As the particle size decreases, the overall conversion of CaO during the carbonation reaction increases.

So for using CaO as sorbent, the initial reaction rate would be important. Gasifying in presence of CaO as bed material in a CFB based chemical looping gasifier may result in higher carbon dioxide capture. As the initial reaction rate is very fast, it will instantaneously capture the carbon dioxide produced during gasification. Furthermore, by using CaO as the bed material, one maintains a very high ratio of CaO to carbon dioxide in the gasifier. Also fluidized bed helps to maintain the circulation, constantly replacing the used sorbent with fresh ones maintaining the level of CO_2 capture in the gasifier. However, loss in sorbent's reactivity over time may reduce the carbon dioxide capture. So this aspect needs further exploration.

5.3.3 Kinetics of Calcination

The intrinsic rate constant of calcination has been determined at each temperature. By use of the Arrhenius plot; the activation energy is calculated. The values of the activation energy and the reaction rate constant for the calcination reaction occurring in the presence of three media are shown in Table 5.2. The activation energies for the calcination reaction are within an order of magnitude similar to the one obtained by Acke and Panas (1997), that is 201 kJ/mol.

Table 5.2: Kinetics of calcination under three different mediums

	N_2	CO_2	H_2O
E_a (kJ/mol)	257.78	180.56	248.62
k_o (1/s)	4.82×10^{10}	2.12×10^{6}	3.63×10^{10}

Figure 5.5 illustrates the differences of reaction kinetics in the presence of three different media. It is evident from the graph that the kinetic rate in the presence of steam is close to that in the presence of nitrogen whereas the CO_2 kinetics rate is significantly lower. Calcination occurs much faster for a given temperature in the presence of steam and nitrogen then carbon dioxide. This is especially the case in CFB-CLG systems where the residence time for the sorbent to undergo calcination is short and the use of steam helps to get higher conversion, as its kinetic rate is higher than others.

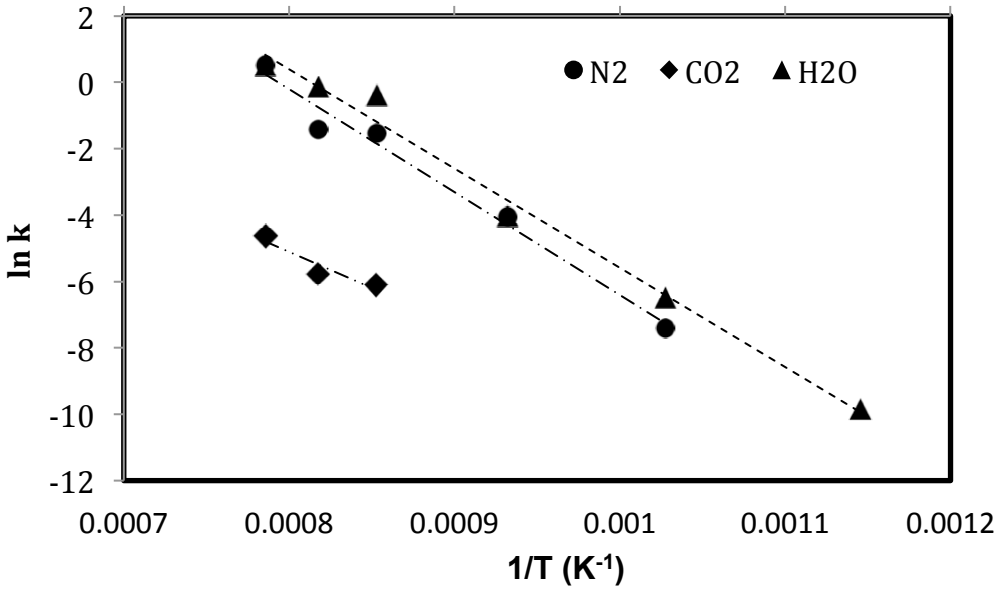

Figure 5.5: Arrehenius plot of the calcination reaction in the presence of different media

5.3.4 The Calcination and Carbonation Reaction Cycle

Figure 5.6 shows the change in the percentage of CaO in the sorbent during its calcination-carbonation cycle, while Fig 5.7 shows the conversion obtained at different cycles.

Calcination in the presence of steam and N_2 shows nearly complete conversion at the beginning of each cycle studied, while the conversion in each cycle in the presence of

CO_2, is only partial. This is mainly because of the increased partial pressure of carbon dioxide, which inhibits the calcination reaction. However, the progressive reduction in conversion after every cycle may be attributed to sintering. It is interesting that the phenomenon of sintering is more pronounced with steam as a medium (Florin and Harris, 2008; Sun et al., 2007; Alvarez et al., 2007), eventhough the conversion obtained is higher in steam. This may be because steam has the ability to weaken the CaO-CO_2 bond, which may result in higher conversion. Also, the lower partial pressure of carbon dioxide may favor higher calcination with steam.

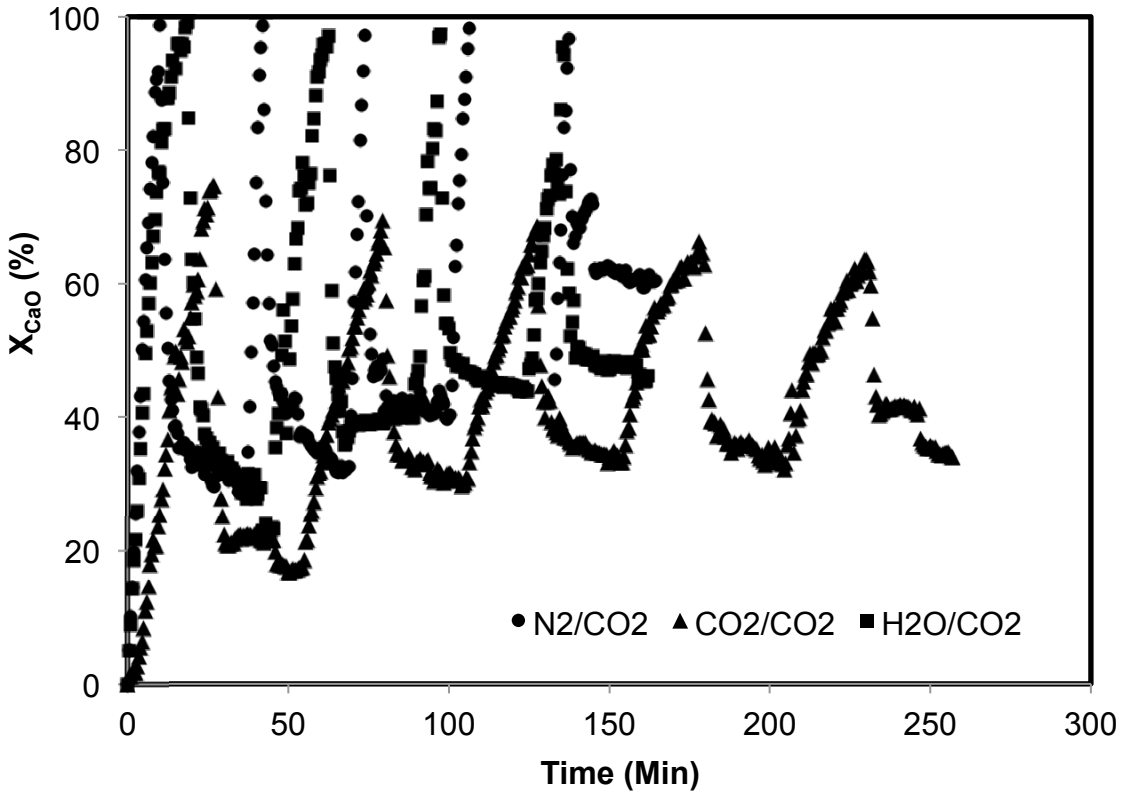

Figure 5.6: Perentage of CaO in the sorbent during alternating calcination and carbonation (Calcination with $N_2/CO_2/H_2O$ at 950^oC and Carbonation with CO_2 at 650^oC)

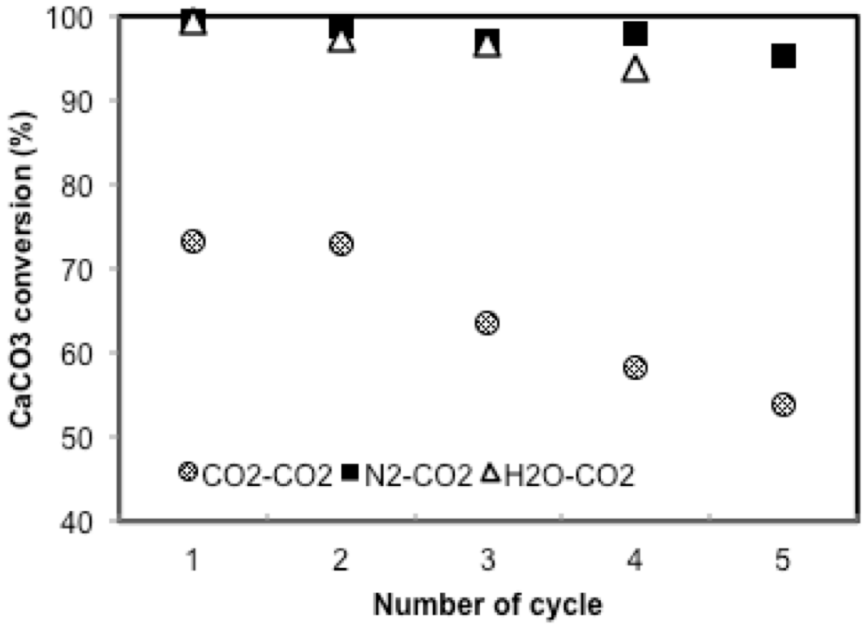

Figure 5.7: Conversion obtained during calcination at the end of each cycle

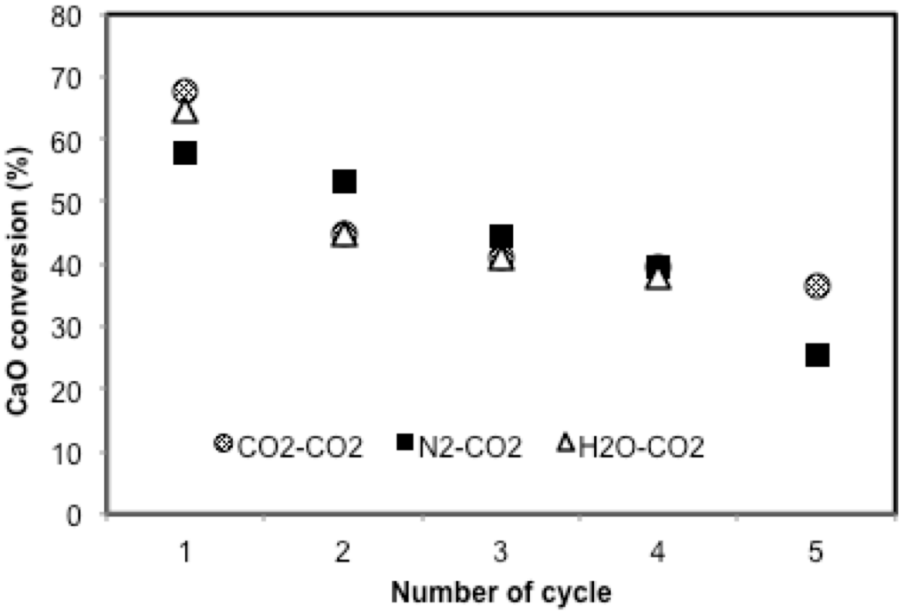

Figure 5.8: Conversion obtained during carbonation at the end of each cycle

Figure 5.8 shows that CaO conversion is not significantly influenced by the type of medium. The ability of the sorbent CaO to capture carbon dioxide decreases with increasing number of cycles irrespective of the medium used for calcination. Stanmore

and Gilot (2005) inferred that in high temperature calcination, the calcium particles sinter leading to decrease in porosity. Furthermore, the high molar volume of $CaCO_3$ tends to block entry to the pores of CaO during carbonation resulting in loss of conversion. To quantify this loss in ability of the sorbent to capture CO_2, sorbent conversion is plotted against the number of cycle in Fig 5.9. An empirical relation between the conversion, X_{CaO} and the number of cycles, N ($1 \leq N \leq 5$)) is developed from it.

$$X_{CaO} = -18.63 \ln(N) + 62.598 \quad [5.5]$$

By using this relation one can estimate the frequency at which fresh sorbent needs to be charged into the CFB-CLG system. This model's limitation is that it only accounts for the effect of high temperature sintering but does not include the other effects that may appear in a commercial chemical looping gasification system. The deposition of tar and carbon on the sorbent are examples of such reducers which can only be studied in the real-life chemical looping gasification system.

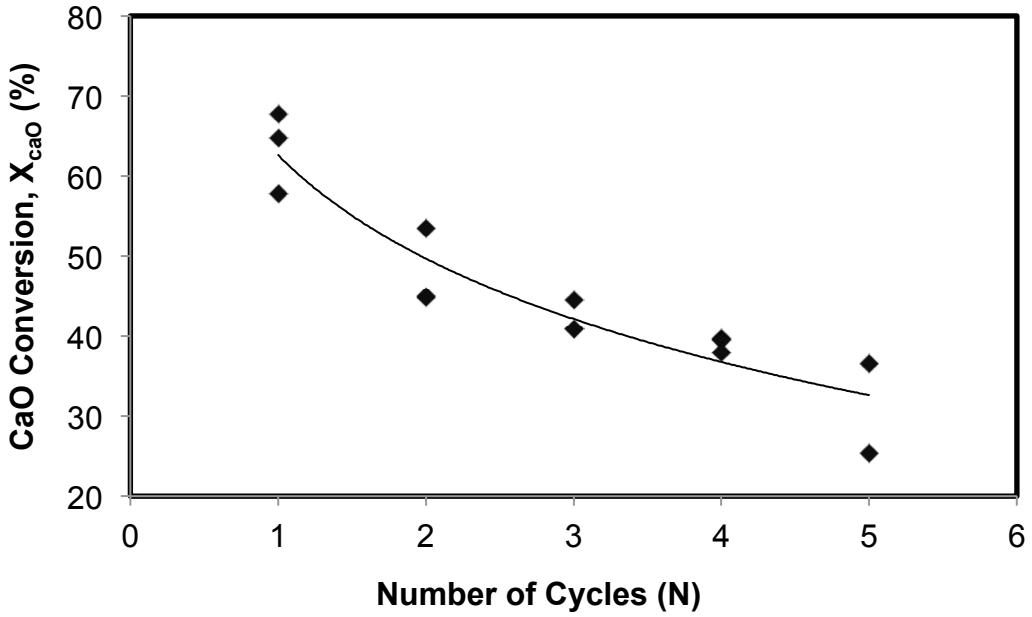

Figure 5.9: Experimental and calculated conversion obtained during carbonation against the number of cycles

5.4 CONCLUDING REMARK

Due to several factor including sintering and pore pluggage, the CO_2 absorbing capacity of CaO reduces progressively as it goes through alternating cycles of carbonation and calcination. The study of calcination of $CaCO_3$ in the presence of different media showed that the degrees of calcination in the presence of H_2O and N_2 are very similar. The kinetic rate of calcination is much higher when measured in H_2O and N_2 than in CO_2. The presence of steam yields a conversion of $CaCO_3$ higher than any other medium at all temperature. Steam offers high conversion at a relatively low temperature. Therefore it can reduce the calcination energy requirement, which may partially offset the energy required to produce additional steam. This low temperature operation also reduces the chances of sintering. Taking this into consideration along with the potential dilution of the product gas with N_2, we arrive at the conclusion that steam is the best possible medium to be used in the regenerator of a CFB-CLG system. However low conversion in a chemical looping system is not to be surprising because of the low residence time for the limestone particles. Further studies need to be conducted on chemical looping gasification system itself to know the variation in conversion obtained. These studies are presented in chapter 6.

However, the results obtained for steam calcination during the alternating calcination-carbonation reaction cycle are somewhat discouraging when it comes to the operation of CFB-CLG systems. In every cycle, there is a continuous drop in conversion during carbonation, which suggests that even with steam, sintering of the sorbent when calcined at higher temperature cannot be avoided. As previously mentioned, in order to maintain

the gasifier temperature, the suitable temperature for steam calcination of 700^{o}C cannot be achieved in the regenerator. The only solution could be to regenerate the reactivity of the sorbent so that it can be used for longer cycles. This possibility has not been explored here but can be considered for future research. Nevertheless, the complete conversion obtained in each cycle during calcination performed in the presence of steam ensures that high regeneration efficiencies can be obtained in the regenerator of a CFB-CLG system. This increases the fraction of CaO in the solid going into the gasifier, which might offset the loss in sorbent reactivity due to sintering and maintain a higher carbon dioxide capture in the gasifier.

CHAPTER 6: BIOMASS GASIFICATION IN A CIRCULATING FLUIDIZED BED BASED CHEMICAL LOOPING GASIFIER

This chapter presents the experimental results of gasification of biomass in a circulating fluidized bed (CFB) based chemical looping gasification (CLG) system. The studies on the calcination-carbonation cycle are presented in the first section, followed by the experiments conducted solely in a bubbling fluidized bed without running the calcium loop. Finally, gasification is performed in a CFB-CLG system operating both the bubbling fluidized bed gasifier and the fast bed regenerator in tandem. At the end of the chapter, a kinetic model for the gasification of biomass in the presence of CaO is developed and its results are compared with the experimental ones.

6.1 STUDY OF CALCINATION/CARBONATION CYCLE IN A CFB-CLG SYSTEM

The experimental results on calcination-carbonation obtained in the QWM (chapter 5) helped to understand the reaction closely but did not predict the conversion that can be obtained in a CFB-CLG reactor. The particles moving in a CFB-CLG loop maintained a residence time much lower than that in the QWM reactor. This may result in lower conversion in the CFB-CLG system. Thus, experiments were conducted in a CFB-CLG system to gain a better understanding of the calcination/carbonation reaction,.

6.1.1 Methodology

Detailed description of the CFB-CLG system was presented in chapter 3**.** Before beginning the experiment, the whole system was heated up to the operating temperature. The regenerator was operated at 900^{o}C while the temperature of gasifier was maintained within

the range of 550-600^{o}C. The regenerator was heated quickly to the desired temperature with ceramic heaters that enclose the whole regenerator section. The heat carried by solid coming from the regenerator and with the fluidizing medium heats the gasifier. Initially it was necessary to maintain a minimum amount of solid limestone in the loop to make sure it carried enough energy to heat up the gasifier to the required temperature and at same time to maintain the proper solid exchange in the loop. For this reason, limestone was fed into the loopseal. Since the loopseal and the regenerator were connected, it not only filled up the loopseal but also the lower section of the regenerator. The regenerator was then fluidized with air. An appropriate velocity was maintained such that the limestone particles got entrained and were separated in a cyclone. Solid falling into the standpipe started to fills up the gasifier. Once filled with limestone the gasifier was fluidized with air to fill up the connecting pipes between the gasifier and the loopseal with the solid. After that the heaters enclosing the regenerator and the one below the gasifier was turned on. Initially, both the regenerator and the gasifier were fluidized with air such that both of them operated in a bubbling mode. Once the temperature in the gasifier reaches 300-350^{o}C, the limestone particle was circulated between the reactors, by fluidizing the loopseal. In this case, the regenerator was operated in a fast fluidization mode whereas the gasifier and loopseal in a bubbling mode. After 4 to 5 hours of operation, the temperature in the gasifier increased to 550-600^{o}C. Once this condition was achieved, the experiment on the calcination-carbonation cycle was started.

The main aim of this experiment was to determine the amount of carbon dioxide capture that could be obtained in the gasifier and how it varies over time. Any additional benefits

that can be obtained by conducting calcination with steam were also to be identified. As calcination in the presence of carbon dioxide results in poor conversion as shown in chapter 5, only steam and air was used as the fluidizing media in the regenerator. To study the carbon dioxide capture that can be obtained, the gasifier was fluidized with a mixture of gases containing carbon dioxide and nitrogen. The carbon dioxide fraction in the total gas supplied to the gasifier was maintained such that it approximated the concentration of carbon dioxide produced during biomass gasification.

For the first study, the regenerator was fluidized with steam, the gasifier with nitrogen and the loopseal with air. Carbon dioxide was supplied to the base of the gasifier bed, which is comprised of 22-25% gaseous medium (N_2 + CO_2). The gas composition and the flow of the outlet gas stream from the gasifier were continuously measured by online gas analyzer, and thus by knowing the change in the composition and the flow, the actual carbon dioxide capture in the bed was calculated. The flow rate at the outlet was calculated by conducting a nitrogen balance between the inlet and the outlet stream, assuming there was no change in the amount of nitrogen. Solid samples were also collected from the bed of the gasifier and were analyzed to identify the fraction of calcium oxide in them. The experiment was then repeated with air as the fluidizing medium in the regenerator.

The analysis of solid samples to determine the fraction of CaO was conducted in the laboratory. Initially, the sample was heated at 105^{o}C for 2 hours to remove moisture, which account for the change in weight. The dried sample was then heated at 500^{o}C for 5 hours. The loss in weight during this heating period comes from the decomposition of magnesium

carbonate. Finally, the sample was heated to and left at 950^{o}C for 2 hours. The weight loss at this stage is the result of the calcination of calcium carbonate. Accounting for the masses of moisture, magnesium carbonate, magnesium oxide, inert materials and the calcium carbonate in the sample, the remaining solid was assumed to be calcium oxide. The properties of the limestone and the validation of this methodology is shown in Appendix D. Table 6.1 shows the operating conditions necessary to maintain the circulation of solid in the loop where the regenerator was operated as a fast bed and the gasifier and loop seal as fluidized beds.

Table 6.1: Flow stream in fluidizing different reactors

Reactor type	With air	With steam
Regenerator	$2.7x10^{-4}$ (Air, Nm^3/s)	1.5 (steam, kg/h)
Gasifier	$3x10^{-4}$ (N_2, Nm^3/s) + $8.3x10^{-5}$ (CO_2, Nm^3/s)	$3x10^{-4}$ (N_2, Nm^3/s) + $8.3x10^{-5}$ (CO_2, Nm^3/s)
Loopseal	$1.96x10^{-4}$ (Air, Nm^3/s)	$1.96x10^{-4}$ (Air, Nm^3/s)

6.1.2 Particle Size Distribution

The particle size distribution of solid collected from the gasifier bed after the experiment shows that although present, the attrition of particles was not significant. Thus, it is not necessary to add fresh sorbent to maintain the minimum amount of solid in the system for proper circulation.

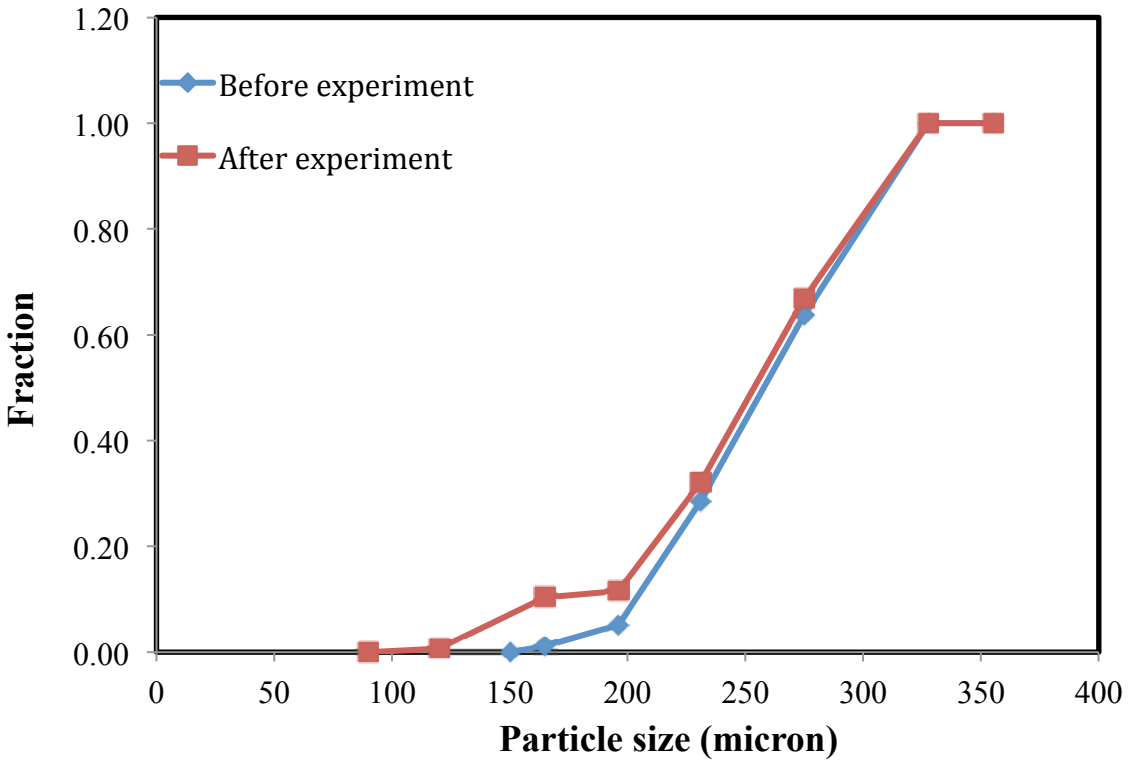

Figure 6.1: The particle size distribution of limestone

6.1.3 Hydrodynamics and the Pressure Distribution

To verify the fluidization regime in the regenerator, the static pressure along the height of the riser was measured. Fig 6.2 shows the suspension density profile in the regenerator calculated from the measured pressure. The nature of this suspension profile as well as the pressure balance around the loop (Fig 6.3) is similar to that observed in CFB boilers (Basu, 2006). The average voidage in the turbulent bed section of the regenerator was 0.78, which then increases to 0.97 around the exit. The average voidage in the bubbling fluidized bed gasifier was found to be 0.58. The pressure balance around the loop shows that the pressure drop at the base of the loop seal is much higher than that in the regenerator and therefore no gas will escape the regenerator through the loop seal. Also, since the pressure at the top of the loop seal is much higher than that at the top of the gasifier, no air going into the

loopseal could flow into the gasifier. This is also observed during the experiment as negligible amounts of air were detected through measurement at the outlet of the gasifier.

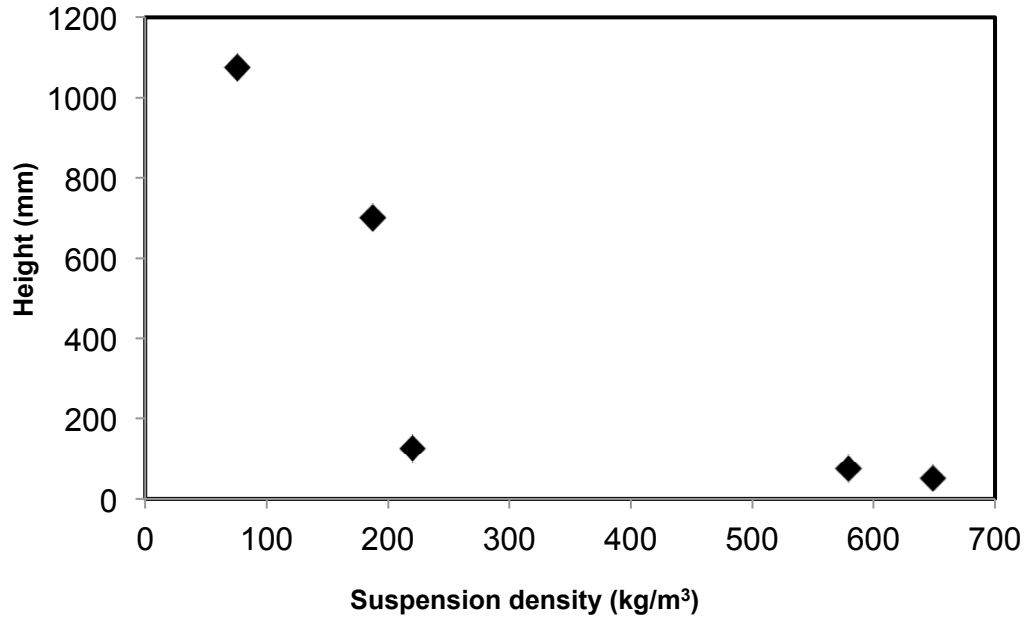

Figure 6.2: Suspension density profile along the height of the regenerator

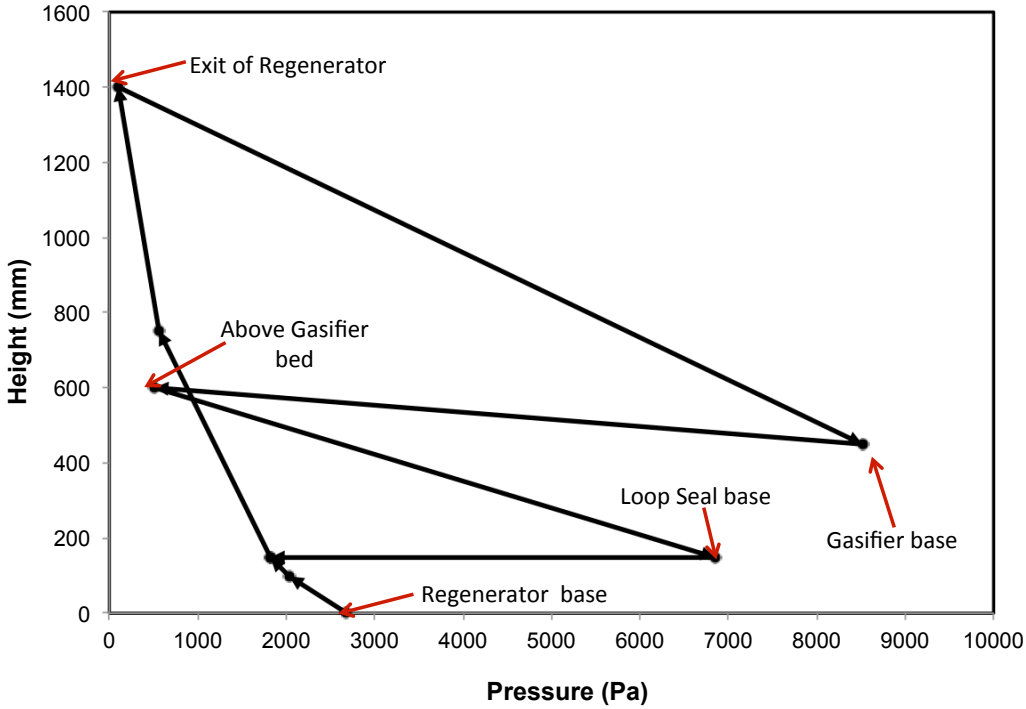

Figure 6.3: Pressure distribution in the chemical looping gasification system (arrow shows the direction of solid flow between the different reactors)

6.1.4 Result and Discussion

Figure 6.4 shows the percentage of carbon dioxide capture obtained in the gasifier versus time.

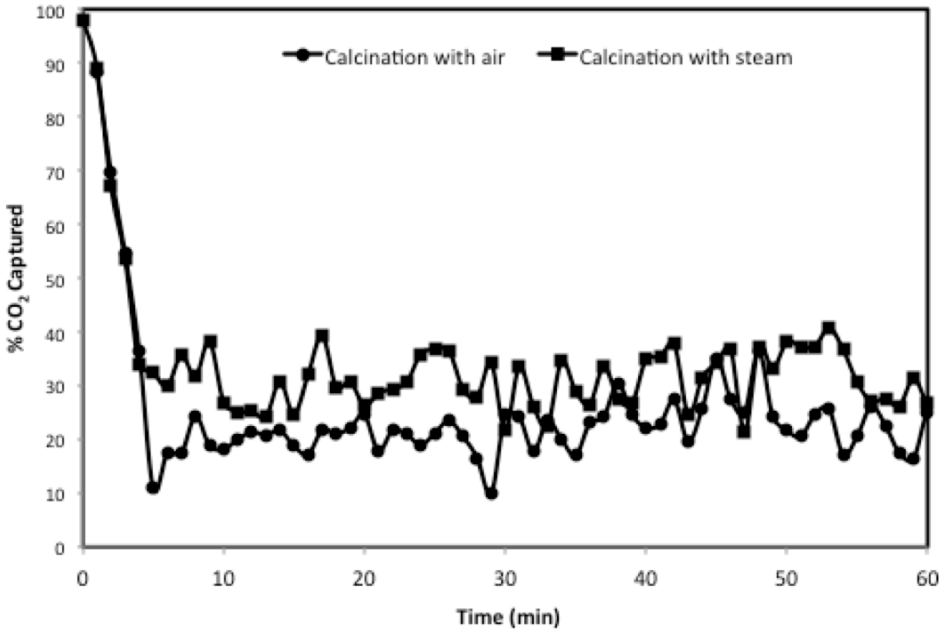

Figure 6.4: Percentage of carbon dioxide capture in the gasifier

When the calcination in the regenerator was done with steam, a carbon dioxide capture of up to 40% was obtained. On the other hand, the capture is lower at about 20% when air was used as the medium. This demonstrates that the fluidizing medium in the regenerator influence carbon dioxide capture in the gasifier. It can be seen that steam calcination in the riser-regenerator results in a higher carbon dioxide capture in the gasifier compared to that obtained with air in the riser. This can be explained from the results obtained from the QWM studies, (Table 5.1) where we noted that when calcined with steam, a CO_2 conversion was 73% even at the lower temperature of 700^{o}C.. Thus, for the same period of operation in the CFB-CLG, calcination with steam begins much earlier than that with air and the fraction of calcium oxide in the solids leaving the regenerator and dropping into the

gasifier will be higher. This is also apparent from the analysis of solid samples collected from the gasifier (Fig 6.5).

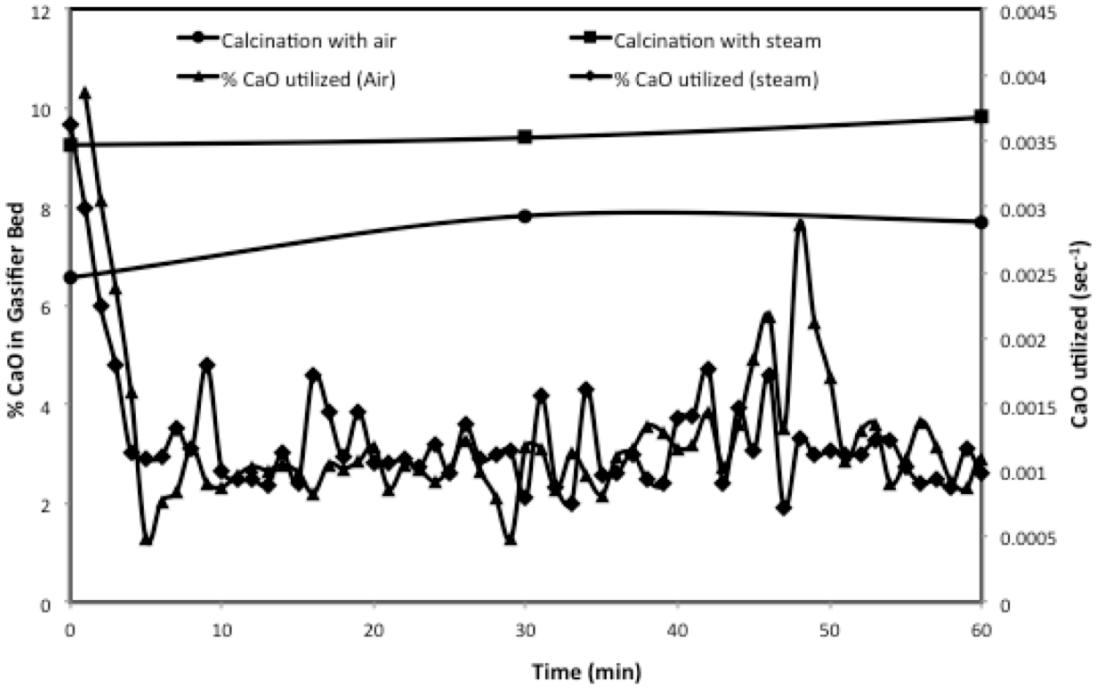

Figure 6.5: Percentage of CaO in the bed material from the gasifier and the rate of conversion obtained

In case of steam calcination, the fraction of CaO in the bed was about 10% but only 8% in air calcination. One may argue that even this smaller fraction of CaO present in the gasifier is more than the theoretical amount required to capture carbon dioxide supplied to the gasifier and as such the reduction in the CaO in bed material should not affect the CO_2 capture in the gasifier. However because the bubbling fluidized bed is made of two phases: bubble and emulsion, most of the gas may escape as bubbles through the bed of the gasifier. There is less than perfect gas-solid contact in the gases. Therefore, one needs to maintain a higher than theoretical concentration of CaO in order to achieve complete capture of carbon dioxide. In a CFB-CLG system, this can be realized by maintaining a higher circulation of solid. It is especially important when the CFB based chemical looping

system is operated for biomass gasification as the ability of CaO to capture carbon dioxide reduces with time due to sintering, char, ash and tar deposition in the gasifier. This is where CFB system becomes advantageous as it can be designed easily to work with higher circulation of solids. Maintaining a higher circulation around the CFB loop works well on an ideal case where there is no decrease in sorbent ability to capture carbon dioxide. However as shown in chapter 5, the sorbent's ability to capture carbon dioxide reduces drastically over a finite number of cycles and therefore the amount and the frequency of fresh sorbent being fed into the system has to be increased. Hydration of sorbent as suggested by the Fan (2011, p. 131) could be an option for improving the performance of calcium-based sorbents. Hydration helps to retain the CO_2 capture capability for an extended period of time, but at the same time it makes the sorbent fine in size resulting in increased elutriation.

The fluctuation in the percentage of carbon dioxide as seen in Fig 6.4 and Fig 6.5 may be due to the fact that the pressure of the bed when it is under the fluidized condition and the flow of the carbon dioxide supplied at the base, fluctuate. Therefore, when the flow is on lower side, the carbon dioxide capture is high and vice versa.

Calcination-carbonation cycle in a dual fluidized bed is being studied as an alternative to solvent based technologies for post capturing of carbon dioxide from flue gas (Gupta and Fan, 2002; Abanades et al., 2004; Sun et al., 2007). However, the calciner of such a system needs to be fluidized with pure oxygen, the generation of which is an energy intensive process. Therefore, there is a reason to believe that by proper arrangement of the reactor into the combustor, one could avoid the need to have combustion inside the calciner. In that

case, the calciner could be easily fluidized with steam to produce pure carbon dioxide. Nevertheless, the above experimental results prove the attractiveness of dual fluidized bed technologies for capturing carbon dioxide from flue gas.

6.2 GASIFICATION OF BIOMASS IN A BUBBLING FLUIDIZED BED

The experiment on gasification of biomass in a bubbling bed gasifier was conducted with calcium oxide as the bed material. The results were compared with the gasification results obtained with inert sand as the bed material. This experiment will confirm the advantages of using CaO as bed material for increasing the hydrogen yield as well as for enhancing carbon dioxide capture.

6.2.1 Methodology

Figure 6.6 shows the schematic of the system set up to study the gasification of biomass in the bubbling bed gasifier of a CFB-CLG system. Sawdust with a mean particle size of 500 micron was the biomass used for experiment. Its proximate and ultimate analysis is shown in Table 6.2. Here the biomass is fed on the bed from the top. When the biomass is fed manually, the two-valve system insures that there is no infiltration of air into the gasifier or leakage of gas out from gasifier,. The pressure and temperature above and below the distributor plate and the freeboard were measured. Saturated steam was generated in a steam generator and was superheated in the reactor located below the gasifier, after which it was supplied to the gasifier as the fluidizing medium. During start up, the heater below the gasifier was turned on and the air was supplied. It took around 4-5 hours to attain the temperature of 500^{o}C in the gasifier bed. Owing to the limitation of the heater the gasifier

could not be operated at a temperature above 575^{o}C. Afterwards, the air was replaced with steam and the biomass feeding was started when the temperature in the bed stabilized at 550^{o}C. Saturated steam was supplied at a rate of 1.5 kg/hr, and was superheated before entering into the gasifier. The gas existing the gasifier was cooled in a two-stage condenser.and was collected in gasbag to be later analyzed in a gas chromatography (GC). Experiments were then conducted with sand as the bed material and the results were compared with those of CaO. Mean particle size of both the bed material was 275 microns. While performing experiment with CaO, the biomass and CaO were mixed together in a 1:2 ratio and was fed from the top. The loopseal and the pipes connecting to gasifier were filled with sand to ensure sufficient resistance against any gas leaks out from the gasifier.

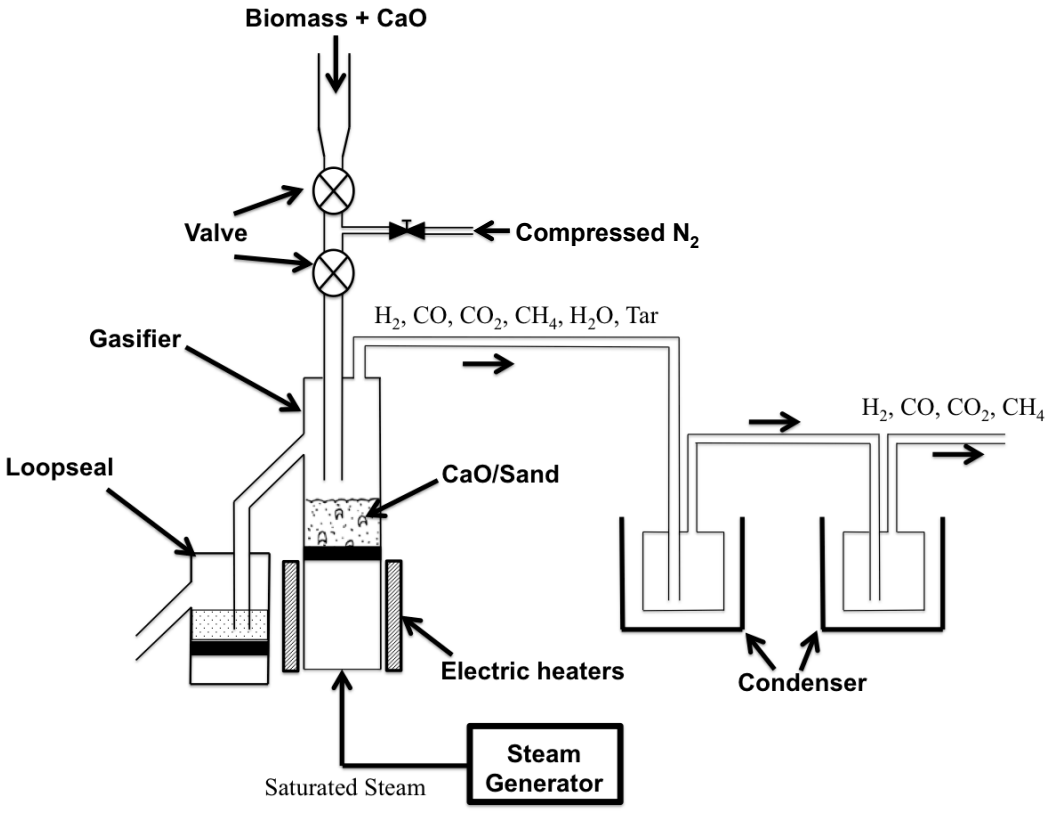

Figure 6.6: Experimental set up for the bubbling fluidized bed gasifier

Table 6.2: Proximate and ultimate analysis of biomass used for gasification

Biomass type	C %	H %	N %	O %	S %	Ash %	MC %	VM %	FC %	HHV MJ/kg
Wood sawdust	48.36	6.91	0.04	33.7	3.5	6.11	3.7	82.05	8.14	19.72

6.2.2 Results and Discussion

Table 6.3 show the measured volumetric gas composition obtained through gasification of biomass with sand and CaO as the bed material.

Table 6.3: Gas composition obtained from biomass gasification in bubbling fluidized bed

Bed material	Sand	CaO
Biomass feed rate (kg/hr)	0.5	0.5
Steam feed rate (kg/hr)	1.5	1.5
CaO feed rate (kg/hr)	-	1
Temperature (^{o}C)	575±25	575±25
Gas composition (%)		
H_2	40.53	70.97
CO	17.48	10.43
CO_2	31.17	1.64
CH_4	10.83	16.97
Gas flow (l/kg of biomass)	23.15	64.62

The major gasification reactions that took place are:

$$\text{Biomass}+H_2O \rightarrow H_2 + CO + CO_2 + CH_4 + H_2O + \text{tar} + \text{char} \quad [6.1]$$

$$CO + H_2O \rightarrow H_2 + CO_2 - 42.2 \text{ kJ/mol} \quad [6.2]$$

In case of biomass gasification in presence of CaO, carbon dioxide produced during biomass gasification reaction and water gas shift reaction reacts with CaO to produce calcium carbonate.

$$CaO+CO_2 \rightarrow CaCO_3 - 178.8 \text{ kJ/mol} \quad [6.3]$$

It is clear from the gas composition shown in Table 6.2, that the presence of CaO not only helps to capture carbon dioxide during the process but also increases the hydrogen content of the product gas. In-situ capture reduces the partial pressure of CO_2 in the gasifier bed, moving water gas shift reaction in the forward direction. This results in higher conversion of CO and higher higher hydrogen yield, which explains why the, hydrogen concentration increased by 75% and CO_2 concentration dropped by 94%. This effect is explained more clearly in Table 6.4. If CaO only removed carbon dioxide without having any effect on the water gas shift reaction, the gas composition would be as shown in column B of the Table 6.4. However, the hydrogen concentration obtained by using CaO as the bed material is higher than the value in column B. The discrepancy is due to the increased water gas shift reaction. As shown in column D, 12.09 % is contributed to the total concentration of hydrogen by the increased water gas shift reaction, whereas the carbon monoxide concentration was decreased by 14.96%. As predicted, the methane concentration did not change significantly because methane does not take part in any of the reactions when the gasifier is operated at 575^{o}C.

Table 6.4: Effect of in-process capture of CO_2 by CaO on product gas composition

	Gas composition (%)			
Gas component	With sand as bed material (A)	% If only CO_2 was captured (B = A/(100-31.17)	With CaO as bed material (C)	Difference D=(C-B)
H_2	40.53	58.88	70.97	+12.09
CO	17.48	25.395	10.43	-14.96
CO_2	31.17	0	1.64	-
CH_4	10.83	15.73	16.97	+1.24

The overall gas yield is also higher when CaO was used as the bed material. This could be due to the fact that CaO also acts as a catalyst to break down tar, resulting in higher gas yield. As discussed in chapter 4 a similar observation was made while studying gasification in a fixed bed reactor. Although the relative gas yield is high, its absolute value is very low because of the low temperature in the gasifier. The only source of heating here is the super-heated steam, and thus very high temperatures cannot be achieved. This limits the biomass gasification reaction and reduces the overall gas production.

6.3 GASIFICATION OF BIOMASS IN A CFB-CLG SYSTEM

An experimental study on the gasification of biomass in a CFB-CLG system was conducted to examine the concentration of hydrogen and carbon dioxide in the product gas and to identify the ability of sorbent to capture carbon dioxide. A number of problems were encountered while running the experiment with the major one being the choking of the end of the pipes close to the condenser due to the deposition of tar. The consequential increase in the pressure inside the reactor resulted in gas flowing the opposite way through the

biomass feeder and the loopseal, and eventually out from the regenerator. This limited the time duration of the experiment to a maximum of 2.5 hours.

6.3.1 Methodology

Figure 6.7 provides the schematic diagram of the CFB-CLG system used for studying the gasification of biomass. The calcium oxide used in the experiment was produced from the calcination of limestone in an oven at 950^{o}C. The startup procedure was similar to that employed for the study of the calcination-carbonation cycle (section 6.1.1). Once the temperature in the gasifier bed reached 550^{o}C, superheated steam was supplied to the gasifier as the regenerator and the loopseal were fluidized with nitrogen. Because of the limitation related to the steam supply and its capacity, both the regenerator and the loopseal were fluidized with nitrogen. As shown in chapter 5, nitrogen closely resembles the calcination reaction's reactivity with steam. The biomass feeder was then turned on to feed the biomass at a constant rate into the gasifier bed and the product gas leaving the gasifier was condensed in a condenser. Finally, the gas was collected in a gasbag and analyzed in a gas chromatograph (GC). The time required to fill the gasbag was noted in order to calculate the flow of the product gas at a particular moment of the experiment. The gas sample coming out from the regenerator was continuously monitored.

Table 6.5: Operating parameters for studying biomass gasification in chemical looping system

	Medium	Flow rate (Nm^3/s)	Minimum fluidization velocity, U_{mf} (m/s)	Superficial velocity, U (m/s)
Regenerator	N_2	$2.9x10^{-4}$	0.03	3.32
Gasifier	Steam	$4.17x10^{-7}$	0.05	0.19
Loopseal	N_2	$2.08x10^{-4}$	0.04	0.07

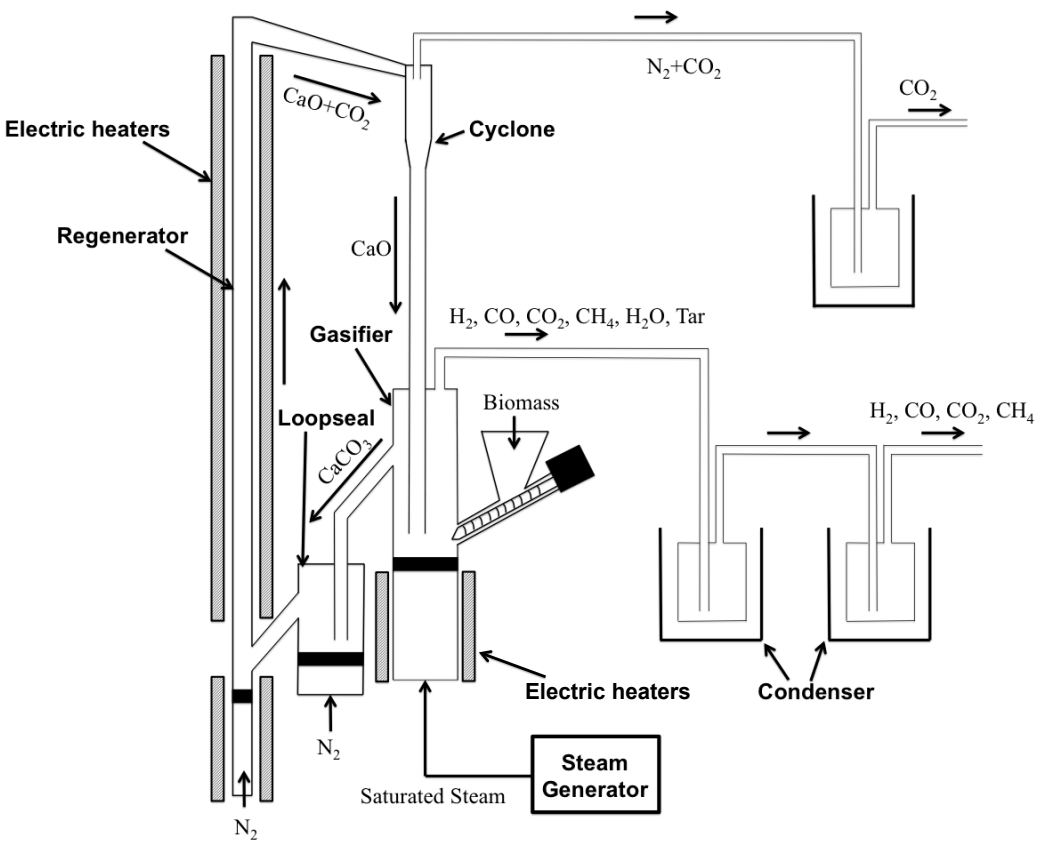

Figure 6.7: Schematic of CFB-CLG system for experimental studies

6.3.2 Result and Discussion

Table 6.6 show the gas composition obtained while gasifying sawdust in a CFB-CLG gasifier. The hydrogen concentration in the product gas reached up to 80.94% while the carbon dioxide concentration was 5.7%. The carbon monoxide and methane concentration in the product gas were 3.04% and 10.30%, respectively.

Table 6.6: Gas composition obtained from biomass gasification in CFB-CLG system

Biomass feed rate (kg/hr)	0.2
Steam feed rate (kg/hr)	1.5
Bed material	CaO
Temperature (^{o}C)	575±25
Gas composition (%)	
H_2	80.94
CO	3.04
CO_2	5.71
CH_4	10.30
Gas flow (l/kg of biomass)	96.94

The gas composition measured during the experiment (Fig 6.8) shows that, the hydrogen initially dropped and then started to increase until it finally became steady at around 80.94%. The opposite trend was noted for methane, which initially increased and latter started to decrease. Change in carbon monoxide composition was minimal. The carbon dioxide concentration remained negligible for the first two hours and only increased to 5.7% at the end. The slight increase in CO_2 may be due to the loss in the ability of calcium oxide to capture carbon dioxide. As it goes through the loop, sintering and deposition of ash and tar might lower its performance to capture CO_2 with time.

The initial drop in the concentration of hydrogen and the corresponding increase in methane suggest that hydrogasification reaction (Eqn. 6.4) took place.

$$C+2H_2 \rightarrow CH_4\text{-}74.8 \text{ kJ/mol} \quad [6.4]$$

The hydrogasification reaction under atmospheric pressure occurs at relatively low temperature (500-550^{o}C). When gasification was started, the temperature was well within this range and the hydrogen formed by biomass gasification reaction (Eqn. 6.1) and the water gas shift reaction, quickly reacted with char to form methane. The reaction ceased as the temperature later rose, increasing the hydrogen concentration in the product gas while correspondingly decreasing that of methane. This increase in temperature could be the result of the exothermic carbonation reaction.

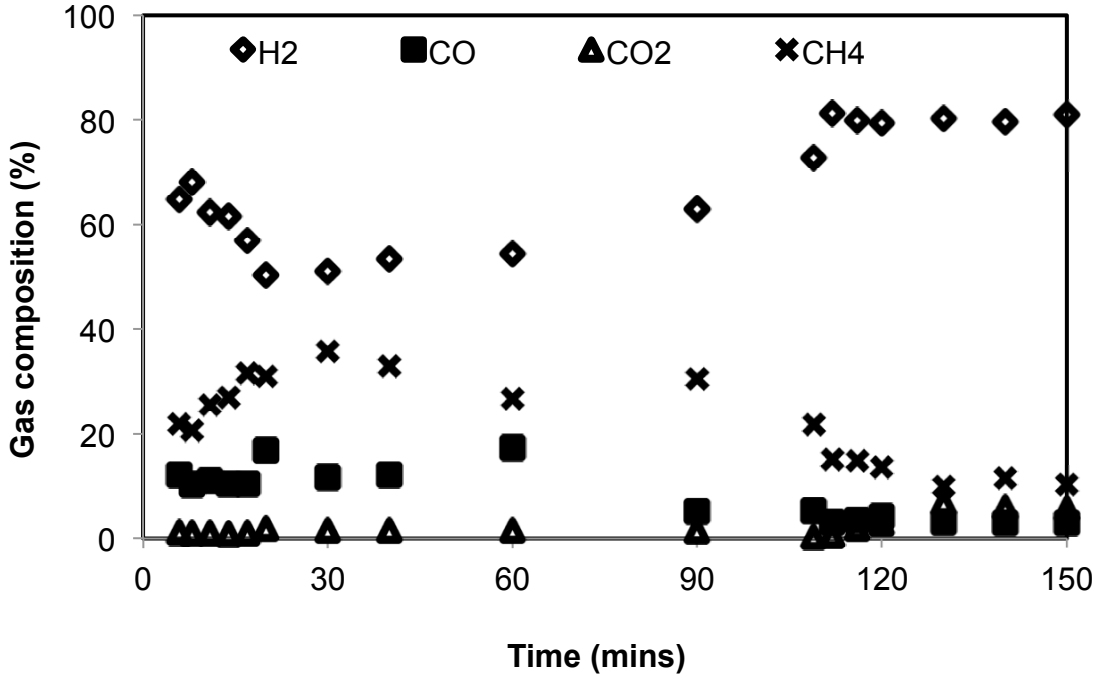

Figure 6.8: Gas composition obtained by gasifying biomass sawdust in a chemical looping gasification system

6.4 KINETIC MODELING OF THE GASIFIER OF A CFB-CLG SYSTEM

Modeling will help to design the gasifier by determining the size of and mass flow in and out of the gasifier, and composition of product gas obtained. Besides assisting the design, modeling could also help to evaluate the performance of the existing system. Commonly

used modeling methods for gasification are equilibrium modeling and the kinetic modeling. As discussed in chapter 4, equilibrium modeling assumes complete conversion. and the results obtained represents the maximum possible values. Kinetic modeling on other hand closely predicts the system performance by taking into account the kinetics of the gasification reaction. However, equilibrium models are easy to develop and give results quickly, whereas kinetic models are comparatively more complex and the results obtained are susceptible to errors in the reaction rates considered for modeling. Inayat et al. (2010) developed a kinetic model to study the biomass gasification in presence of CaO. As predicted by their model, the hydrogen fraction in the product gas was up to 81% at 950 K, the steam to biomass ratio was 3 and sorbent to biomass ratio was 1. Proll and Hofbauer (2008) used a simple process simulation to model the dual fluidized bed gasifier with and without carbon dioxide capture in it with CaO mixed with olivine used as the bed material. Other than these studies, modeling bubbling fluidized bed gasifier with CaO as bed material has not been significantly explored. Thus, a kinetic model is developed here to study the performance of the gasifier of the CFB-CLG system.

6.4.1 System Description

The schematic of the system considered for the kinetic study is shown inside the dotted line in Fig 6.9. The gasifier of the CFB based chemical looping gasification system operates as a bubbling fluidized bed and for modeling purposes, it is divided into two distinct zones: the lower dense zone and the upper freeboard zone. An one-dimensional two-phase model is used for modeling the lower dense zone, and a single-phase model is used for the freeboard zone. According to the two-phase model, the bed is divided into the bubble phase and the emulsion phase and the mass transfer between them is defined by the mass transfer

coefficient (Kunii and Levenspiel, 1991). The single-phase model assumes that the freeboard contains only gases with fine particles entrained from the bed.

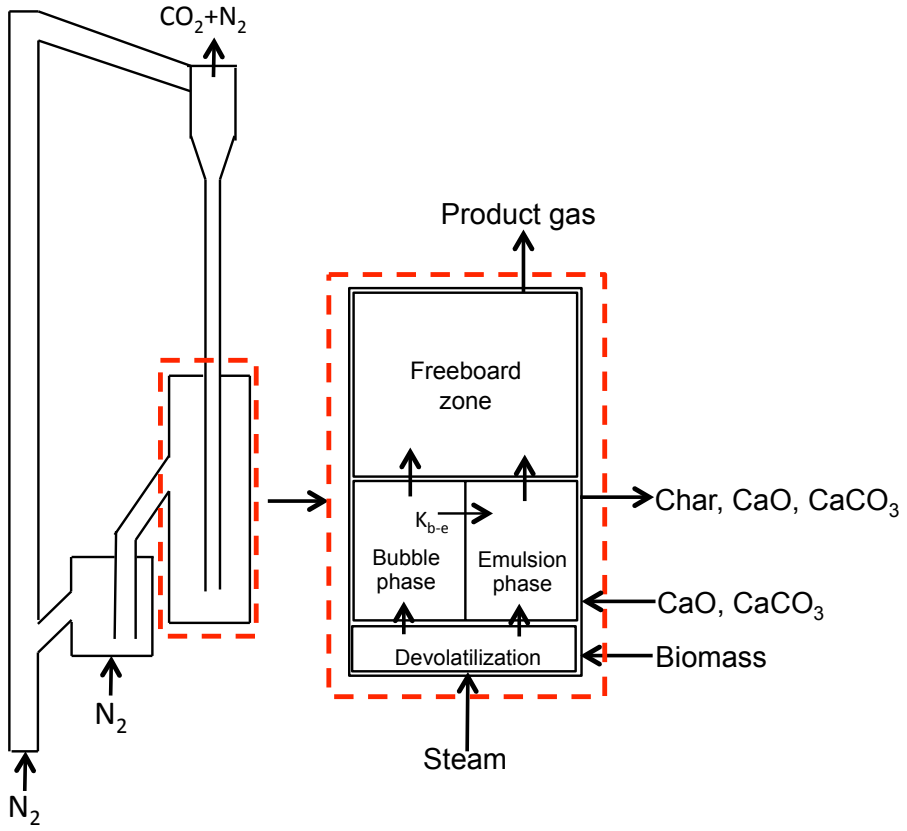

Figure 6.9: Defining the gasifier system for kinetics studies

6.4.2 Model Assumptions

The following assumptions were made in developing the model:

1. The temperature is uniform in the gasifier bed.
2. The tar produced during devolatilization is not considered in the model.
3. The nitrogen and oxygen present in the biomass do not affect gasification.
4. No combustion takes place during the entire gasification process.
5. Solids are uniform in size and perfectly mixed with no attrition.
6. Bubbles are spherical in shape and contain no solid particles.

7. The emulsion phase is under minimum fluidization with the gas velocity equal to the minimum fluidization velocity.
8. No heat is lost during the process

6.4.3 Development of the Model

For developing the kinetic model, two sub models were developed: reaction sub model and the hydrodynamic sub model. Conservation equations are used for the mass balance of the gas species in the bubble and the emulsion phase as well as in the freeboard section.

6.4.3.1 Reaction Sub-Model

The overall gasification reaction consists of: drying, devolatilization (pyrolysis), and gasification. The fluidized bed is maintained at a high temperature and gas-particle heat transfer rate, so the biomass particles dry instantaneously once they enter the bed. This moisture in the biomass adds to the steam supplied as the fluidizing medium to make up the total steam available for the further reactions. Next is the devolatilization step, during which the biomass decomposes to produce a mixture of char, volatiles and condensable tar. In the absence of relation for devolatilization at lower temperature in a fluidized bed, an experimental value given by Scott and Piskorz (1982) for the gas yield and char yield is being used for this model. Also, the composition of gas produced during devolatilization is taken from Gerber et al. (2010). These are shown in Table 6.7.

The devolatilization step is followed by the gasification reactions. The major gasification reactions considered for the model, along with their kinetic rates, are shown in Table 6.8. Kinetic data was taken from different sources as indicated.

Table 6.7: Product yield during devolatilization consider for kinetic modeling

Product	Yield (Mass fraction of wood fed)	Reference
Char	0.127	Scott and Piskorz (1982)
Gas	0.15	
Gas composition (mass fraction of total gas yield)		
H_2	0.032	Gerber et al. (2010)
CO	0.270	
CO_2	0.386	
CH_4	0.056	
H_2O	0.256	

Table 6.8: The reactions considered for the model and their reaction kinetics

Reaction	Kinetic constant (k, sec^{-1})	Reaction rate (RR) ($kmol/m^3/s$)	Reference
$C + CO_2 = 2CO$	$342\ T \exp\left(-\frac{15600}{T}\right)$	$RR = kC_{CO2}$	Gerber et al. (2010) Armstrong et al. (2011)
$C + H_2O = CO + H_2$	$342\ T \exp\left(-\frac{15600}{T}\right)$	$RR = kC_{H2O}$	
$CO + H_2O = CO_2 + H_2$	$2780 \exp\left(-\frac{1510}{T}\right)$	$RR = k (C_{CO}*C_{H2O} - C_{CO2}*C_{H2}/(0.0265 \exp(3958/T)))$	
$CaO + CO_2 = CaCO_3$	$10.45\times10^3 \exp\left(-\frac{44.5}{T}\right)$	$RR = kC_{CO2}$	Inayat et al. (2010)

6.4.3.2 The Hydrodynamics Sub-Model

To develop this sub model, the hydrodynamic parameters are calculated using empirical relations from literature, which are shown in Table 6.9.

Table 6.9: Empirical relation to model the hydrodynamic of fluidized bed

Name of symbol	Unit	Correlation	Reference
Archimedes Number, Ar	-	$Ar = \rho_{gas}(\rho_{solid} - \rho_{gas}) g \, {D_{solid}}^3 / \mu_{gas}^2$	Basu (2006)
Reynolds Number, Re	-	$Re = \sqrt{(C_1^2 + C_2 Ar)} - C_1$ (C1 = 27.2, C2 = 0.0408)	Basu (2006)
Minimum fluidization velocity, U_{mf}	m/s	$U_{mf} = Re \, \mu_{gas} / (D_{solid} \, \rho_{gas})$	Kunii and Levenspiel (1991)
Voidage at minimum fluidization, ε_{mf}	-	$Ar = \frac{1.75}{(\varepsilon_{mf}^3 \varphi)} Re^2 + \frac{150(1-\varepsilon_{mf})}{(\varepsilon_{mf}^2 \varphi^2)} Re$	Barea and Leckner (2010)
Bubble void fraction, ε_b	-	$\varepsilon_b = \left[1 + \left(1.3/f\right)(U_o - U_{mf})^{-0.8}\right]^{-1}$	Barea and Leckner (2010)
Bed expansion factor, f	-	$f = 1 + \frac{\left(14.31(U_o - U_{mf})^{0.738} D_{solid}^{1.006} \rho_{solid}^{0.376}\right)}{(\rho_{gas}^{0.126} U_{mf}^{0.937})}$	Barea and Leckner (2010)
Bubble diameter, d_b	m	$d_b = 0.54(U_o - U_{mf})^{0.4}(h + 4\sqrt{A_{bed}})^{0.8} g^{-0.2}$	Barea and Leckner (2010)
Rise velocity of bubble, U_{br}	m/s	$U_{br} = 0.711(g d_b)^{1/2}$	Barea and Leckner (2010)
Bubble velocity, U_b	m/s	$U_b = (U_o - U_{mf}) + U_{br}$	Kunii and Levenspiel (1991)
Bubble to emulsion mass transfer coefficient, $k_{b\text{-}e}$	1/s	$k_{b-e} = \frac{2U_{mf}}{d_b} + \frac{12(D_g \varepsilon_{mf} U_b)^{1/2}}{\pi d_b^{3/2}}$	Barea and Leckner (2010)

6.4.3.3 Conservation Equations

Gas exchange in any section of the bed takes place between the bubble and the emulsion phase. The conservation equation's for the mass balance of the gas species in the bubble and the emulsion phase of the dense lower bed zone are taken from Barea and Leckner (2010).

For the bubble zone:

$$\frac{1}{A_{bed}} \frac{dF_i}{dz} = \varepsilon_b RR_{gg,i}^b \times MM_i + f_{b-e,i} \qquad [6.5]$$

Where, F_i is flow of the gas species in the bubble zone in kg/s

For the emulsion zone:

$$\frac{1}{A_{bed}}\frac{dF_i}{dz} = \varepsilon_e(1-\varepsilon_b)RR^e_{gg,i}\times MM_i - f_{b-e,i} + \sum_m(1-\varepsilon_e)(1-\varepsilon_b)\alpha_m RR^e_{gs,m,i}\times MM_i \quad [6.6]$$

The mass exchange rate between the bubble and the emulsion phase, $f_{b\text{-}e,\,I}$ (kg/m^3/s) is defined as:

$$f_{b-e,i} = \varepsilon_b a_b k_{b-e,i}\left(\rho_{i,e} - \rho_{i,b}\right) + f_n\frac{\rho_{i,e}}{\rho_{gas,e}} \quad [6.7]$$

Where, f_n (kg/m^3/s) is the total gas generated in the emulsion phase by the devolatilization of biomass, and the char and homogeneous reactions occurring in the emulsion phase.

$$f_n = \varepsilon_e(1-\varepsilon_b)\sum_i RR^e_{gg,i}\times MM_i + (1-\varepsilon_e)(1-\varepsilon_b)\sum_i\sum_m \alpha_m RR^e_{gs,m,i}\times MM_i \quad [6.8]$$

The mass balance for the solid in the dense lower zone can be written as:

$$F_{m,in} - F_{m,out} = \int_0^Z\left(A_{bed}(1-\varepsilon_e)(1-\varepsilon_b)\alpha_m\sum_i RR^e_{gs,m,i}\times MM_i\right)\,dz \quad [6.9]$$

The mass conservation equation for the freeboard above the gasifier bed can be written as:

$$\frac{1}{A_{FB}}\frac{dF_{i,FB}}{dz_{FB}} = \varepsilon_{FB}RR^{FB}_{gg,i} + \sum_m(1-\varepsilon_{FB})\alpha_m RR^{FB}_{gs,m,i}\times MM_i \quad [6.10]$$

6.4.4 Methodology

The algorithm used for the formulating and solving the model is shown in Fig 6.10. MATLAB was used to solve the equations by developing different sub programs, which were called by the main programs. The major sub programs DEVOL, HYDRODY, KINETIC, CONSERVATION was called by the MAIN program. DEVOL calculates the char and gas yield and the composition of gas obtained during devolatilization. HYDRODY calculates the hydrodynamic parameters, while KINETIC calculates the reaction rates and CONSERVATION conducts the mass balance and determines the flow of different gas components in the bed and the freeboard. The ODE45 operator was used to solve the differential equation while the QUAD operator was used to solve the integral

equation. This model is being used to develop commercial software for gasifier design, so program code is not included in this thesis.

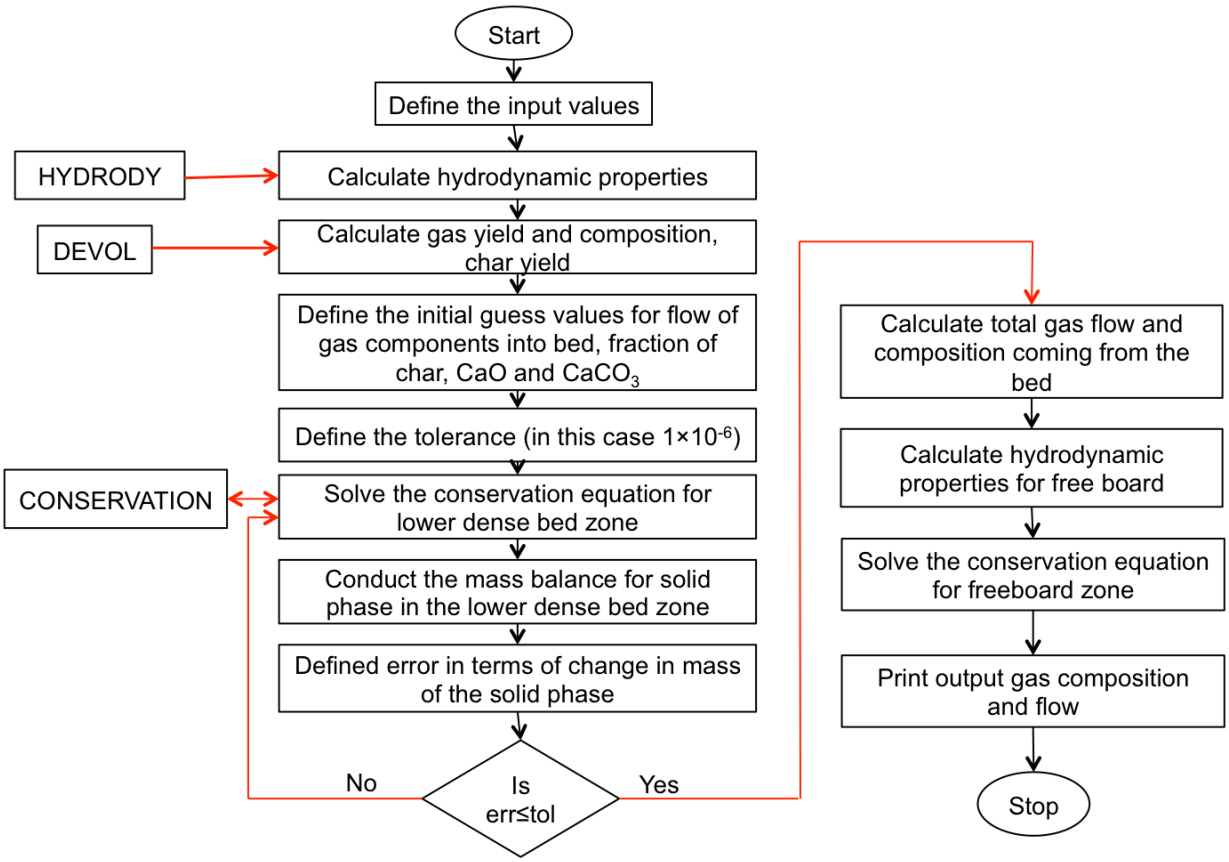

Figure 6.10: Algorithm for solving the MAIN program

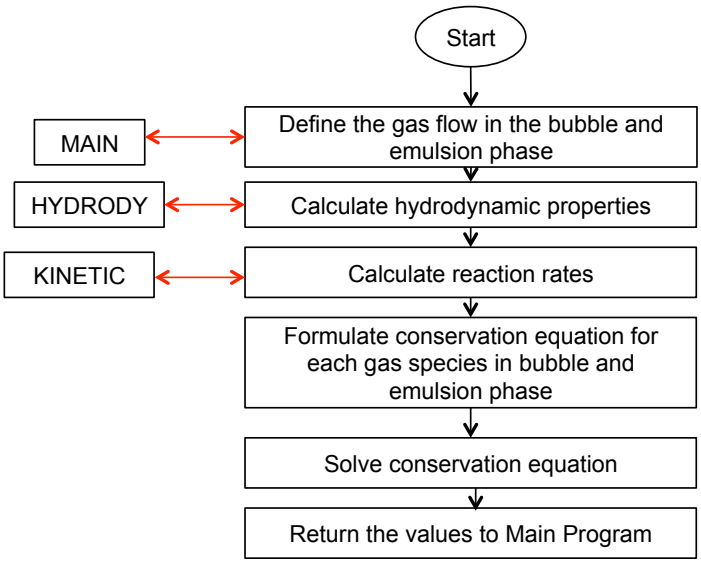

Figure 6.11: Algorithm for solving CONSERVATION sub program

6.4.5 Result and Discussion

Table 6.10 summarize the results obtained from the kinetic modeling of the gasifier of the CFB-CLG system. The modeling was carried out to examine the already built CFB-CLG system and to verify the experimental results.

Table 6.10: Results of kinetics modeling of the gasifier of CFB-CLG system

Input data	
Biomass feed rate (kg/hr)	0.2
Char input through biomass (kg/hr)	0.0240
Steam feed rate (kg/hr)	1.5
Bed material	CaO
Temperature (^{o}C)	575
Predicted by the model	
Final gas composition (%)	
H_2	75.56
CO	8.89
CO_2	0.76
CH_4	15.54
Product gas flow (Nm^3 /kg of biomass)	0.04239
Char out after gasification (kg/hr)	0.0220
Char Conversion (%)	8.36

Under the conditions at which the CFB-CLG system was operated, the kinetic modeling predicted the maximum hydrogen concentration in the product gas to be around 75%, while the CO, CO_2 and CH_4 concentrations were 8.89%, 0.76% and 15.54% respectively. The predicted char conversion during gasification was only 8.36% and the reason behind it can be explained as follows:

a. The lower operating temperature (575^{o}C compared to 700^{o}C in typical gasification) gives a lower reaction rate. For a finite residence time one could expect poor char conversion.

b. Second reason could be the inherent limitation of the simple two-phase model. The two-phase model underestimates the char conversion due to the total neglect of gas-solid reaction in the bubble phase (Kaushal, 2006) and the overestimation of the gas bypassing the bed by assuming that any gas in excess of that required for minimum fluidization passes through the bubble phase. The model assumes that all the solid particles remain in the emulsion phase and that the bubble does not carry any solid. These aspects of the simple two-phase model could contribute to a low prediction of conversion during gasification.

The lower char conversion results in lower gas yield as well, reducing the overall gasification efficiency.

The low char conversion has great implications in designing a CFB-CLG system. Because of the low char conversion in the gasifier, more char moves into the regenerator and gets converted into gases, thereby diluting the carbon dioxide. Thus, a pure stream of carbon dioxide cannot be obtained as for what the CFB-CLG system is designed for. The modification that must be made is to have a classifier between the gasifier and the regenerator to screen the char particles and send them back to the gasifier, while allowing calcium oxide to move into the regenerator.

Figure 6.12 shows a graph of the predicted gas composition along the height of the gasifier. Initially, a sharp rise in the concentration of CO, H_2 and CH_4 and a similar decline in the concentration of CO_2 are observed. As CO_2 is captured instantaneously by CaO, the

concentrations of other gases are increased. The carbon dioxide concentration remains almost zero and no change in methane concentration is observed. No reaction for methane conversion is considered in the model because such reactions are relatively insignificant at the operating temperature considered. A continuous increasing trend for H_2 and decreasing trend for CO is observed as the gas rises up inside the gasifier. This is because of the water gas shift reaction ($CO + H_2O = CO_2 + H_2$), which consumes carbon monoxide to produce H_2 and CO_2. The sorbent CaO instantaneously captures the carbon dioxide produced and therefore its concentration remains almost zero. The entrainment of solid particles into the free board is taken into account in the model by assuming a constant voidage of 0.998 in the freeboard. Therefore, the CaO particles entrained in the freeboard further capture the CO_2 produced in this zone, thereby keeping the concentration of CO_2 very low.

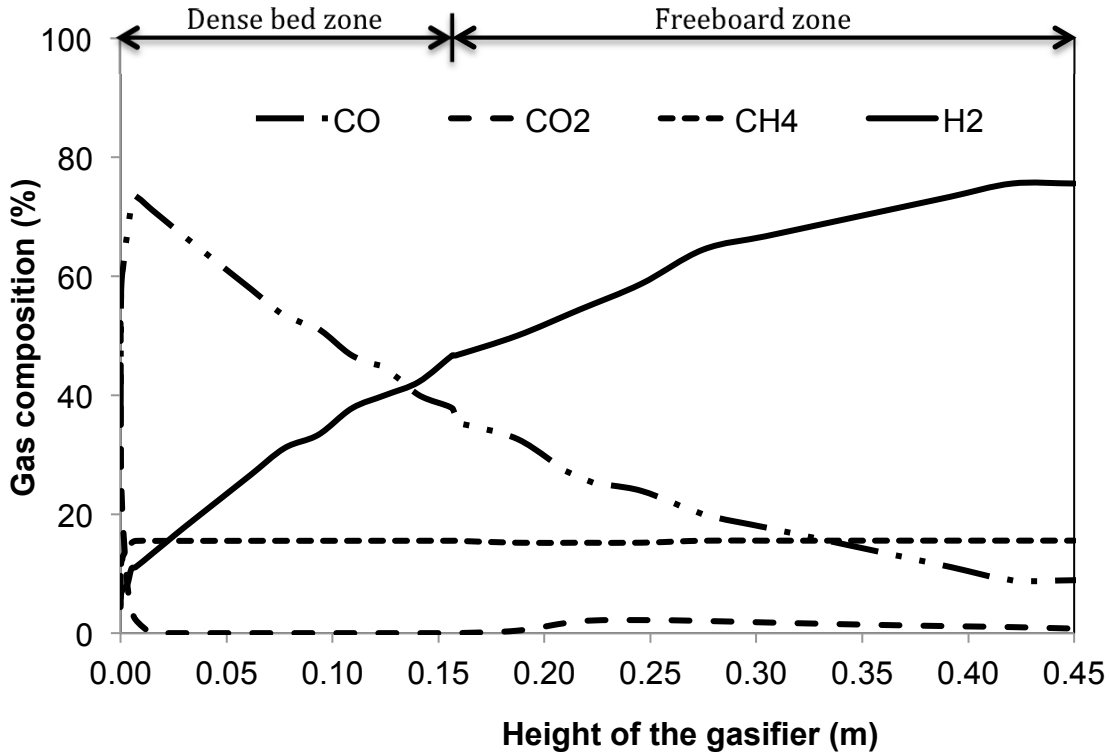

Figure 6.12: Variation of predicted gas composition against the height in the gasifier of CFB-CLG system

6.4.6 Experimental Validation of the Model

A graph of the product gas composition obtained by experiment and predicted by the kinetic and the non-stoichiometric equilibrium model of the CFB-CLG system is shown in Fig 6.13. There is a close agreement between the H_2 and CO concentrations obtained from experiment with those predicted by the models. The CO_2 concentration predicted by the kinetic model is much lower than that obtained experimentally. However this concentration is almost identical to the concentration of CO_2 that was obtained initially during the experiment (Fig 6.8). The rise in CO_2 concentration during the experiment may be due to the decay in sorbent reactivity, which was not considered in the model.

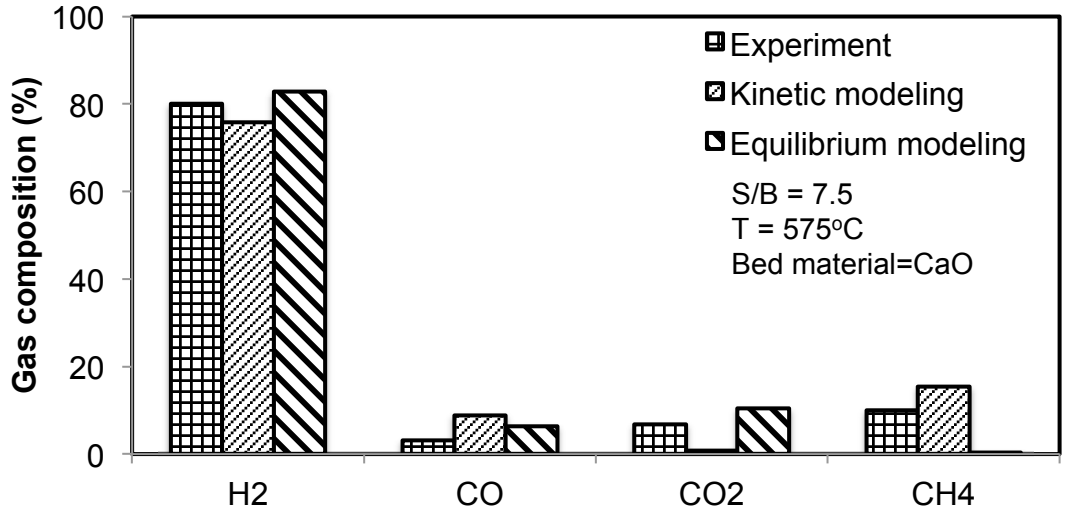

Figure 6.13: Comparison of results obtained for gas composition from biomass gasification from a) experiment in a CFB-CLG system b) kinetic modeling and c) non-stoichiometric equilibrium modeling

The methane concentrations obtained from the experiment and the kinetic modeling is similar but higher than the value from the equilibrium model. As mentioned earlier and also explained in chapter 4, methane comes from the devolatilization of the biomass. Since the kinetic model considers the devolatilization step, its prediction of the concentration of

methane is close to that obtained experimentally. Equilibrium model does not consider the devolatilization step, and therefore predicts a low methane concentration in the product gas.

The lower char conversion and gas yield obtained from the experiment (0.097 Nm^3/kg of biomass) and predicted by the kinetic model (0.04239 Nm^3/kg of biomass) resulted in poor gasification efficiency. A gasification efficiency of only 7.27% was obtained during the experiment and 1.82% was predicted by the kinetic model (the calculations are shown in Appendix D). Also, the gas yield predicted by the model is lower than that obtained experimentally. This may be due to the fact that the model only considers the gas and char yields but does not take into account the tar formed. During the experiment, the tar may get reformed in the presence of steam, resulting in higher gas yield. Furthermore, the presence of CaO acting as a catalyst in breaking the tar and char into gases could be another reason for the higher gas yield obtained from the experiment.

6.5 CONCLUDING REMARKS

The study on the calcination-carbonation cycle in a CFB-CLG system shows that high temperature steam calcination has a positive effect on the overall carbon dioxide capture in the carbonator (the gasifier of CFB-CLG system). Steam calcination offers high regeneration and increases the fraction of CaO in the carbonator resulting in higher carbon dioxide capture. Carbon dioxide capture of 40% is obtained when calcination is carried out with steam as opposed to 20% capture obtained with air calcination.

Experimental studies done in the bubbling fluidized bed gasifier with sand and CaO as the bed materials show that the use of CaO increases the hydrogen concentration by 75% and at same time reduces the carbon dioxide concentration by 94%. The results also shows that 12% of total hydrogen concentration comes from the increased water gas shift reaction caused by in-situ removal of carbon dioxide by CaO.

The gasification study conducted in the CFB-CLG system shows 80.94% concentration of hydrogen in the product gas with 5.71% carbon dioxide after operating for 2.5 hrs. However, very low product gas yield and therefore low gasification efficiency were noted., A kinetic model was developed to better understand this phenomenon. The model predicted a poor char conversion, which was the main reason for the low gas yield, and gasification efficiency. A comparison drawn between the experiment and the kinetic and non-stoichiometric models showed that the results predicted by the models agree well with the experimental findings. Any differences noted are a result of the limitations of the models and they are addressed and explained properly with scientific reasoning.

CHAPTER 7: CONCLUSIONS AND RECOMMENDATIONS

This chapter includes the overall conclusions of the studies conducted and presents recommendations for future work.

7.1 OVERALL CONCLUSIONS

This work concluded that chemical looping gasification of biomass in a circulating fluidized bed system with CaO sorbent can produce hydrogen enriched and CO_2 lean gas without downstream gas separation. However, deactivation of the sorbent through successive calcination and carbonation remains a problem. More detailed and specific conclusions are given below:

- The energy and exergy efficiency of circulating fluidized bed (CFB) based chemical looping system (CFB) is calculated be 87.49% and 83.14% respectively.
- Sensitivity analysis showed that the overall efficiency increases from 53% to 75% when the regeneration efficiency is increased from 50% to 100% maintaining a 60% carbon dioxide capture in the gasifier.
- Experiments on steam gasification of biomass in presence of CaO in a fixed bed showed that with increase in S/B ratio, hydrogen concentration increases in the product gas.
- The presence of CaO not only captured the carbon dioxide but also acted as a catalyst to break down the tar and char resulting in higher gas yield. By increasing the CaO/B ratio from 1.5 to 2, a 63% increase in gas yield is obtained.
- The hydrogen concentration in the product gas increases with temperature but decreases at still higher temperature showing an optimum temperature of 670^{o}C.

- Measured values of hydrogen concentration found to be lower than that predicted by non-stoichiometric equilibrium model.
- The extent of calcination of $CaCO_3$ depends on both temperature and on the gaseous ambience around it. The calcination is faster and higher at higher temperature.
- Experiments conducted in the quartz wool matrix reactor show that calcination in presence of steam has higher conversion than that in presence of nitrogen or carbon dioxide. For example at 800^oC, calcination obtained is 97% in steam, 96% in nitrogen, but only 7.5% in CO_2.
- Kinetic rate equation, developed for calcination, shows that the rates are much higher for the steam and nitrogen as compared to carbon dioxide.
- The ability of the sorbent to calcine reduces possibly due to sintering as it goes through alternative cycles of calcination and carbonation. Experiments conducted for 5 cycles showed that irrespective of the medium used for calcination, there is a loss in ability of sorbent to capture carbon dioxide in each successive cycle. This loss is given by the empirical relation developed, $X_{CaO} = - 18.63 \ln (N) + 62.598$
- Experimental studies on effect of particle size shows that larger particle size needs longer time to attain the full conversion as compared to smaller particles. For carbonation, initially the particle size does not have much effect as the reaction is governed by the surface absorption, which is very fast.
- Experiments on calcination and carbonation reaction in the CFB-CLG pilot plant showed that carbon dioxide capture is higher when the regenerator of CFB-CLG system is fluidized with steam than compared to air. About 40% of carbon dioxide

capture is obtained compared to about 20% obtained with air as fluidizing medium. Analysis of solid samples from the gasifier bed of CFB-CLG system shows higher percentage of CaO for steam calcination, which could be the reason for higher carbon dioxide capture obtained.

- A comparison of gasification of biomass in the bubbling bed with CaO as bed material shows an increase in hydrogen concentration by 75% and a drop in carbon dioxide by 94% compared with the results obtained using sand as bed material.
- Experiment conducted on gasification of biomass in the CFB-CLG pilot plant shows the product gas to contain as high as 80.94% hydrogen and a carbon dioxide as low as 5.71% when run continuously for 2.5 hrs at temperature of 575^{o}C and steam to biomass ratio of 7.5. The gas yield was, however, low because of a rather low gasification temperature that resulted in poor char conversion.
- Predictions from the kinetic model (75.5% hydrogen and 0.76% carbon dioxide) for same operating condition, at which the gasifier of the CFB-CLG system is operated for experimental studies, show good agreement with that measured. Predicted char conversion is only 8.36% at 575^{o}C. This explains the lower gas production obtained during experiment.
- Experimental results agree well with that predicted by the equilibrium model and the kinetic model.

7.2 RECOMMENDATION FOR FUTURE WORK

This thesis presents one of the early works of this relatively unexplored area of biomass gasification. As such it was not possible to explore this subject fully. Following is a list a suggest work that might help better understand this process.

1. The progressive loss in sorbent reactivity during its use in a CFB-CLG could be a major deterrent in commercial use of this otherwise attractive system. So, it is necessary to research how to improve the reactivity of the sorbent. One such option could be water hydration through injection of water into the standpipe of the CFB. The sorbent gets hydrated and thereby it may result in an improved carbon dioxide capture for extended number of cycles of operation. However one needs to control the flow of water to avoid temperature drop in the gasifier.
2. The present kinetic model for the bubbling fluidized bed gasifier could be extended to include the calcination in the riser giving a model of the complete circulating fluidized bed based chemical looping system. As discussed in chapters 6 a classifier between the gasifier and the regenerator could improve the quality of CO_2 leaving the regenerator. This component should also be included in the model.
3. Study on the tar produced from the CFB-CLG system can be studied further.
4. Experiments in the CFB-CLG system were carried out using steam in gasifier, nitrogen in the regenerator and loopseal. Further experiments may be conducted using steam in all three reactors as it might give better calcination in the regenerator.

5. An integrated research program may be undertaken where the CFB-CLG system is connected with a fuel cell system to examine the power output from the overall plant.

REFERENCES

Abanades, J.C., and Alvarez, D.,."Conversion Limits in the Reaction of CO_2 with Lime", Energy and Fuel: 17, 308-315 (2003)

Acharya, B., Dutta, A. and Basu, P.,."Chemical Looping Gasification of Biomass for Hydrogen Enriched Gas Production with In-Process Carbon Dioxide Capture", Energy and Fuels, 23, 5077–5083 (2009)

Acke, F., and Panas, I.,"Activation Energy for Calcination of Lime Stone by Means of a Temperature Programmed Reaction Technique", Thermochimica Acta: 303, 151-154 (1997).

Adhikari, S., Fernando, S., and Haryanto, A., "A Comparative Thermodynamic and Experimental Analysis on Hydrogen Production by Steam Reforming of Glycerin", Energy & Fuels: 21, 2306-2310 (2007)

Alvarez, D., Pena, M., and Borrego, A.G., "Behavior of Different Calcium-Based Sorbents in a Calcination/Carbonation Cycle for CO_2 Capture", Energy & Fuels: 21, 1534-1542 (2007)

Armstrong, L. M., Gu, S., and Luo, K.H., "Parametric Study of Gasification Processes in a BFB Coal Gasifier", Industrial and Engineering Chemistry Research: 50, 5959–5974 (2011)

Asadullah, M., Kaoru, F., and Keiichi, T.,."Catalytic Performance by Rh/CeO2 in the Gasification of Cellulose to Synthetic Gas at Low Temperature", Industrial Engineering Chemistry Research: 40, 5894–5900 (2001)

Basu, P., "Biomass Gasification and Pyrolysis: Practical Design and Theory", Academic Press: ISBN 978-0-12-374988-8 (2010)

Basu, P., "Combustion and gasification in fluidized beds", CRC/Taylor & Francis (2006)

Basu, P., Acharya, B., and Dutta, A., ,"Gasification In Fluidized Beds – Present Status & Design", 20th International Conference on Fluidized Bed Combustion, China (2009)

Balat, M., "Potential Importance of Hydrogen as Future Solution to Environmental and Transportation Problems", International Journal of Hydrogen Energy: 33, 4013-4029 (2008)

Barea, G.A., and Leckner, B.,"Modeling of Biomass Gasification in Fluidized Bed," Progress in Energy and Combustion Science: 36,444–509 (2010)

Bhattacharya, S.C., San, S.H., and Pham, H.L., ,"A Study on a Multi-Stage Hybrid Gasifier-Engine System", Biomass and Bioenergy: 21, 445-460 (2001)

British Petroleum, "BP Statistical review of world energy June 2006", (2006)

Cho, P., Mattisson T., and Lyngfelt, A.,."Comparison of Iron, Nickel, Copper and Manganese-Based Oxygen Carriers for Chemical-Looping Combustion," Fuel: 83, 1215–1225 (2004)

Cormos, C., Starr, F., Tzimas, E., and Peteves, S.,."Innovative Concepts for Hydrogen Production Processes Based on Coal Gasification with CO_2 Capture", International Journal of Hydrogen Energy: 33, 1286–1294 (2008)

Corella, J., Toledo, J. M., and Molina, G., "Steam Gasification of Coal at Low−Medium (600−800 °C) Temperature with Simultaneous CO_2 Capture in Fluidized Bed at Atmospheric Pressure: The Effect of Inorganic Species. 1. Literature Review and Comments", Industrial & Engineering Chemistry Research: 45, 6137-6146 (2006)

Dalai, A.K., Sasaoka, E., Hikita, H., Ferdous, D.,"Catalytic Gasification of Saw Dust Derived from Various Biomass", Energy and Fuels: 17, 1456–1463 (2003)

Das, D., and Veziroglu, T.N., "Hydrogen Production by Biological Processes: A Survey of Literature", International Journal of Hydrogen Energy 26, 13–28 (2001)

De Diego, L. F., Garcia-Labiano, F., Adanez J.,"Development of Cu-Based Oxygen Carriers for Chemical-Looping Combustion," Fuel: 8313, 1749–1757 (2004)

Demirbas, A., "Hydrogen—rich gas from fruit shale via supercritical water extraction," International Journal of Hydrogen Energy: 29,1237–43 (2004)

Drift, A.V, Boerrigter, H., Coda, B., Cieplik, M.K., and Hemmes, K., ,"Entrained Flow Gasification of Biomass; Ash Behavior, Feeding Issues, and System Analyses," ECN-C--04-039 (2004)

Dutta, A., and Acharya, B., "Handbook of Biofuel Production-Processes and Technologies: Production of Bio-syngas and Biohydrogen via Gasification", Woodhead Publishing (2011)

Dutton, G.,"Hydrogen Energy Technology", Tyndall Working Paper No. 17 (2002)

Evans, R., Boyd, L., Elam, C., Czernik, S., French, R., Feik,"Hydrogen from Biomass-Catalytic Reforming of Pyrolysis Vapors," Progress Report, National Renewable Energy Laboratory (2003)

Fang, H., Haibin, L., and Zengli, Z.,"Advancements in Development of Chemical-Looping Combustion: A Review", International Journal of Chemical Engineering; doi: 10.1155/2009/710515 (2009)

Fan, L.S.,"Chemical Looping Systems for Fossil Energy Conversions", WILEY publication, ISBN: 978-0-470-87252-9 (2011)

Florin, N.H., and Harris, A.T., "Hydrogen Productions from Biomass Coupled with Carbon Dioxide Capture: The Implications of Thermodynamic Equilibrium," International Journal of Hydrogen Energy: 32: 4119 – 4134 (2007)

Florin, N.H., and Harris, A.T., "Enhanced Hydrogen Productions from Biomass with In-Situ Carbon Dioxide Capture using Calcium Oxide Sorbents," Chemical Engineering Science; 63: 287–316 (2008)

Gerber, S., Behrendt, F., and Oevermann, M.,"An Eulerian Modeling Approach of Wood Gasification in a Bubbling Fluidized Bed Reactor using Char as Bed Material", Fuel: 89, 2903–2917 (2010)

Grasa, G.S., and Abanades, J.C.,"Capture Capacity of CaO in Long Series of Carbonation/Calcination Cycles", Industrial and Engineering Chemistry Research: 45, 8846-8851 (2006)

Guan, J., Wang, Q., Li, X., Luo, Z., and Cen, K., "Thermodynamic Analysis of a Biomass Anaerobic Gasification Process for Hydrogen Production with Sufficient CaO," Renewable Energy: 32, 2502-2515 (2007)

Gupta, H., and Fan, L.S., "Carbonation-Calcination Cycle using High Reactivity Calcium Oxide for Carbon Dioxide Separation from Flue Gas," Industrial and Engineering Chemistry Research: 41, 4035-4042 (2002)

Guoxin, H., and Hao, H., "Hydrogen Rich Fuel Gas Production by Gasification of Wet Biomass using a CO_2 Sorbent," Biomass and Bioenergy; 33, 899-906 (2009)

Hamelinck, C. N., Faaij, A. P. C., Denuil H., and Boerrigter H., "Production of FT Transportation Fuels from Biomass; Technical Options, Process Analysis and Optimisation, and Development Potential," Energy: 29, 1743-1771 (2004),

Hanaoka, T., Yoshida, T., Fujimoto, S., Kamei, K., Harada, M., Suzuki, Y., Hatano, H., Yokoyama, S., and Minowa, T., "Hydrogen Production from Woody Biomass by Steam Gasification using a CO_2 Sorbent," Biomass and Bioenergy: 28, 63-68 (2005)

Harrison D.P., "The role of solids in CO2 captures: a mini review", Proceedings of the 7th International Conference on Greenhouse Gas Control Technologies Vancouver, Canada, 1101–1106 (2004)

Higman, C., and Burgt, M. V. D., "Gasification", USA, Gulf Professional Publication (2003)

Higman, C., and Burgt, M. V. D., ,"Gasification", Elsevier Science: second edition (2008)

Huang, H.J., & Ramaswamy, S., "Modeling Biomass Gasification Using Thermodynamic Equilibrium Approach," Applied Biochem Biotechnol;154, 193–204 (2009)

Hulteberg, P.C., and Karlsson, H.T., "A Study of Combined Biomass Gasification and Electrolysis for Hydrogen Production," International Journal of Hydrogen Energy: 34, 772–782 (2009)

Inayat, A., Ahmad, M. M., Yusup, S., and Mutalib, M. I. A., "Biomass Steam Gasification with In-Situ CO_2 Capture for Enriched Hydrogen Gas Production: A Reaction Kinetics Modelling Approach", Energies: 3, 1472-1484 (2010)

Ivar S. E., "Sensitivity of the Chemical Exergy for Atmospheric Gases and Gaseous Fuels to Variations in Ambient Conditions", Energy Conversion and Management: 48, 1983-1995 (2007)

Iyer, M., Gupta, H., Wong, D., and Fan, L.S., "Enhanced Hydrogen Production Integrated with CO_2 Separation in a Single-Stage Reactor", Annual Technical Progress Report, DOE Contract No: DE-FC26-03NT41853 (2005)

Jarungthammachote, S., and Dutta, A., "Thermodynamic Equilibrium Model and Second Law Analysis of a Downdraft Waste Gasifier," Energy: 32, 1660–1669 (2007)

Jarungthammachote, S., and Dutta, A., "Equilibrium Modeling of Gasification: Gibbs Free Energy Minimization Approach and its Application to Spouted Bed and Spout-Fluid Bed Gasifiers," Energy Conversion and Management: 49, 1345-1356 (2008)

Javier, G., Caballero, M.A., Martin, J.A., Aznar, M.P., & Corella, J., "Biomass Gasification with Air in Fluidized Bed: Effect of the in Bed use of Dolomite under Different Operational Conditions", Industrial and Engineering Chemistry Research: 38, 4226–4235 (1999)

Johansson, M., "Screening of Oxygen-Carrier Particles Based on Iron-, Manganese-, Copper and Nickel Oxides for Use in Chemical Looping Technologies", Ph.D. Thesis, Department of Chemical and Biological Engineering, Environmental Inorganic Chemistry, Chalmers University of Technology (2007)

Kaushal, P., "Modeling of the Fast Bed Fluidized Combustion Reactor of a Dual Fluidized Bed Biomass Gasification System", Ph.D dissertation, Institute of Chemical Engineering, Vienna University of Technology (2006)

Kaushal, P., Pröll, T., and Hofbauer, H., "Model for Biomass Char Combustion in the Riser of a Dual Fluidized Bed Gasification Unit: Part 1-Model Development and Sensitivity Analysis", Fuel Processing Technology: 89, 651-659 (2009)

Kunii, D., and Levenspiel, O., "Fluidization Engineering", Butterworth-Heinemann E.U.A., (1991)

Laursen, K., Duo, W., Grace, J.R., and Lim, C.J., "Cyclic Steam Reactivation of Spent Limestone", Industrial and Engineering Chemistry Research 43, 5715-5720 (2004)

Lee, J.Y., Yu, M.S., Cha, K. H, Lim, T.W and Hur, T., "A Study on the Environmental Aspects of Hydrogen Pathways in Korea", International Journal of Hydrogen Energy: 34, 8455–8467 (2009)

Leion, H., Mattisson, T. and Lyngfelt, A., "Solid Fuels in Chemical-Looping Combustion", International Journal of Greenhouse Gas Control: 2, 180–193 (2008)

Levin, D.B., Pitt, L., and Love, M., "Biohydrogen Production: Prospects and Limitations to Practical Application", International Journal of Hydrogen Energy: 29, 173 – 185 (2004)

Lin, S., Harada, M., Suzuki, Y., and Hatano, H., "Continuous Experiment Regarding Hydrogen Production by Coal/Cao Reaction with Steam (II) Solid Formation," Fuel: 85, 1143–1150 (2006)

Lin, S., Kiga, T., Katsuhiro, N., and Suzuki, Y., "Coal Power Generation with In-Situ CO_2 Capture HyPr-RING method-Effect of Ash Separation on Plant Efficiency" Energy Procedia: 4, 378–384 (2011)

Luo, S., Xiao, B., Hu, Z., Liu, S., Guo. X., and He, M., "Hydrogen-Rich Gas from Catalytic Steam Gasification of Biomass in a Fixed-Bed Reactor: Influence of Temperature and Steam on Gasification Performance", International Journal of Hydrogen Energy: 34, 2191-2194 (2009)

Lyngfelt, A., "Oxygen-Carriers for Chemical-Looping Combustion-Operational Experience", 1st International Conference on Chemical Looping, Lyon, 17-19 March (2010)

Mahishia, M. R., and Goswami, D.Y., "An Experimental Study of Hydrogen Production by Gasification of Biomass in the Presence of a CO_2 Sorbent", International Journal of Hydrogen Energy 32, 2803-2808 (2007)

Manovic, V. & Anthony, E. J., "Lime-Based Sorbents for High-Temperature CO_2 Capture-A Review of Sorbent Modification Methods", International Journal of Environment Research and Public Health: 7, 3129-3140 (2010)

Mattisson, T., Lyngfelt, A., and Leion, H., "Chemical-Looping with Oxygen Uncoupling for Combustion of Solid Fuels," International Journal of Greenhouse Gas Control: 3, 11–19 (2009)

Moghtaderi, B., "Effects of Controlling Parameters on Production of Hydrogen by Catalytic Steam Gasification of Biomass at Low Temperatures", Journal of Fuel: 86, 2422–2430 (2007)

Ni, M., Leung, D.Y.C., Leung, M.K.H., and Sumathy, K., "An Overview of Hydrogen Production from Biomass", Fuel Processing Technology: 87, 461 – 472 (2006)

Pröll, T., and Hofbauer, H., "H_2 rich syngas by selective CO_2 removal from biomass gasification in a dual fluidized bed system—Process modelling approach", Fuel Process. Technol: 89, 1207–1217 (2008)

Ptasinski, K.J., Prins, M. J., and Pierik, A., "Exergetic Evaluation of Biomass Gasification", Energy: 32, 568–574 (2007)

Rapanga, S., Jand, N., Kiennemann, A., and Foscolo, P.U., "Steam-gasification of biomass in a fluidized-bed of olivine particles", *Biomass and Bioenergy* **19**, 87–197 (2000)

Rizeq, G., West, J., Subia, R., Frydman, A., Zamansky, V., and Das, K., "Advanced-Gasification Combustion: Bench-Scale System Design and Experimental Results", 27th International Technical Conference on Coal Utilization & Fuel Systems, Clearwater, Florida, USA March 4-7 (2002)

Saxena, R.C., Seal, D., Kumar, S., and Goyal, H. B., "Thermo-Chemical Routes for Hydrogen Rich Gas from Biomass: A Review". Renewable and Sustainable Energy Reviews (2007)

Scott, S. A., Dennis, J. S., Hayhurst, A. N., and Brown, T., "In Situ Gasification of a Solid Fuel and CO_2 Separation Using Chemical Looping", AIChE Journal: 52, 3325–3328 (2006)

Scott D.S., and Piskorz, J., "The Flash Pyrolysis of Aspen-Poplar Wood", The Canadian Journal of Chemical Engineering: 60, 666-674 (1982)

Shen, L., Gao, Y., and Xiao, J., "Simulation of Hydrogen Production from Biomass Gasification in Interconnected Fluidized Beds", Biomass and Bioenergy: 32: 120-127 (2008)

Siyi, L., Xiao, B. Guo. X., Hu Z., Liu S., and He M.,. "Hydrogen-Rich Gas from Catalytic Steam Gasification of Biomass in a Fixed Bed Reactor: Influence of Particle Size on Gasification Performance", International Journal of Hydrogen Energy: 34, 1260 – 1264 (2009)

Sigfusson T. I., "Pathways to hydrogen as an energy carrier". Philosophical Transactions of the Royal Society A: Mathematical, Physical and Engineering Sciences: 365, 1025-1042 (2007)

Stassen, H., and Knoef, H., "Small Scale Gasification Systems", Technical report, Biomass Technology Group BV (2001)

Stanmore, B.R., and Gilot, P., "Review-Calcination and Carbonation of Limestone During Thermal Cycling for CO_2 Sequestration", Fuel Processing Technology: 86, 1707–1743 (2005)

Steiner, C., Kameda, O., Oshita, T., and Sato, T., "EBARA's Fluidized Bed Gasification: Atmospheric 2 x 225 t/d for Shredding Residues Recycling and Two-stage Pressurized 30 t/d for Ammonia Synthesis from Waste Plastics", The 2nd International Symposium on Feedstock Recycling of Plastics (2002)

Sun, P., Grace, J.R., Lim, C.J., and Anthony, E.J., "The Effect of CaO Sintering on Cyclic CO_2 Capture in Energy System", AICHE Journal: 53, 2432-2442 (2007)

Tijmensen, M. J. A., Faaij, A. P. C., Hamelinck, C. N., and Hardeveld, M. R. M. "Exploration of the Possibilities for Production of Fischer Tropsch Liquids and Power via Biomass Gasification", Biomass and Bioenergy: 23, 129-152 (2002)

Wang Y and Thomson W.J., 1995. "The effects of steam and carbon dioxide on calcite decomposition using dynamic X-ray diffraction", Chem. Eng. Sci. 50, 1373–1382

Wang, L., Weller, C. L., Jones, D. D., and Hanna, M. A., "Contemporary Issues in Thermal Gasification of Biomass and its Application to Electricity and Fuel Production", Biomass and Bioenergy: 32, 573-581 (2008)

Wu, S. and Basu, P, "Surface Reaction Rates of Coarse Bituminous Char Particles in the Temperature Range 600 to 1340K", Fuel: 72, 1429-1433 (1993)

Yildiz, K., Arif, H., and Ibrahim, D., "Biomass-based hydrogen production: A review and analysis", International Journal of Hydrogen Energy: 34, 8799-8817 (2009)

Zhang, W., "Automotive Fuels from Biomass via Gasification", Fuel Processing Technology: 91, 866-876 (2010)

APPENDIX A: CONSTRUCTION OF CFB-CLG UNIT

This section of the appendix includes detailed description of the different components of the CFB-CLG system and the calculations performed to design them. Tables of the energy and exergy efficiency calculations are also included at the end of this Appendix.

A1 Introduction

A laboratory scale circulating fluidized bed chemical looping gasification was built and installed in the circulating fluidized research laboratory of Dalhousie University. The work on fabrication was started in late December 2009 and was completed by July 2010. The experimental work on the set up was started early September 2010 and was completed by March 2011. Before describing the various components, the limitations and problems that occurred during the experiments should be mentioned.

1. The lack of space in the laboratory limited the height of the system to be used. Another limitation was imposed by the supply of electricity available. CFB-CLG system need around 120 amperes supply to run the heaters, steam generators and other electrical equipment. This limited the quantity of the heaters and at the same time the size of the reactor used.
2. Frequent melt down of the heater cables,required the system to be stopped, cooled down, and repaired. Blockage of the pipelines with tar was also a problem. The sensor lines that measured pressure and temperature would also become blocked and gives faulty readings.

A2 Design of the CFB-CLG system

Assumption for the design

- CaO/Biomass ratio = 2
- Steam to biomass ratio = 2
- Maximum char conversion, X = 80%
- Velocity of fluidizing medium in gasifier is equal to its bubbling velocity
- Superficial velocity in regenerator is 4 m/s
- 100% utilization of CaO in gasifier
- External solid circulation rate for fast bed, R = 3 kg/(m^2 s)

Regenerator dimensions

Based on the external solid circulation rate, the dimensions of the regenerator were estimated and are shown in in Table A1.

Table A1: Diameter choice for different circulation rate

R	3	kg/(m^2.sec)					
Required CaO circulation	2	kg/h					
Solid Circulation rate (kg/h)	2	3	4	5	6	7	8
Regeneration efficiency (%)	100.00	66.67	50.00	40.00	33.33	28.57	25.00
Diameter of regenerator (mm)	15.36	18.81	21.72	24.29	26.60	28.73	30.72

Regeneration efficiency (%) = flow rate of CaO/total solid flow rate

Total solid flow rate = flow rate of CaO + flow rate of $CaCO_3$

One can expect very low regeneration efficiencies and may choose a higher diameter for the reactor. However, a larger size reactor will need a higher capacity electric heater, which increases the cost. A compromise between cost and performance must therefore be made and was taken into consideration in this study. Since the amount of electricity supplied in

the laboratory where the reactors were located was limited, a 25.4 mm diameter was chosen for the regenerator. The height of the regenerator was solely determined by the space availability and was taken to be 1500 mm.

Gasifier dimensions

The gasifier had to be operated in the bubbling fluidized bed mode, and the fluidizing medium had to be able to maintain the bed in this mode.

Maximum steam flow rate, M_{steam} = 2 kg/h

Volumetric steam flow rate, $Q_{steam} = M_{steam}/\rho_{steam@650oC}$ = 2 x 4.028 = 8.056 m^3/h

Taking superficial velocity, V = 0.3 m/s

Cross-sectional area of the gasifier, $A_{gasifier} = Q_{steam}/V$ = 8.056/(0.3 x 3600) = 7.459E-03 m^2

Diameter of the gasifier, $D_{gasifier} = \sqrt{(4A_{gasifier}/\pi)}$ = 0.0974 m = 3.89 inch

Thus a 4-inch (101.1 mm) diameter reactor was chosen for the gasifier.

Bed height = 1.5 x diameter of gasifier = 6 inch = 152.4 mm

Cyclone dimensions

Taking the gas inlet velocity, V_e = 25 m/s

So, the volumetric gas flow to the cyclone, $Q = K*L*V_e$

Total gas flow rate, Q = flow rate of gas into (regenerator + loopseal)

= 17.5 (SLPM) + 12.5 (SLPM)

= 30 (SLPM)

= 1.8 (m^3/h)

Since the gas exits the regenerator at 900^{o}C,

Total gas flow rate, $Q_{@900^oC}$ = 7.08 m^3/hr

For the design of an efficient cyclone;

- K/D_c = 0.44
- L/D_c = 0.21
- H/D_c = 3.9
- E/D_c = 0.4
- m/D_c = 0.4

Substituting the value of V_e, K and L into the equation for volumetric flow rate,

(0.44 D_c)*(0.21D_c)*25 = (7.08/3600)

So, D_c = 0.0291 m (1.14")

The diameter of the cyclone was chosen to be 1.5 inch. With this diameter, the inlet velocity drops to 15 m/s.

To verify the design, the cut off size and the collection efficiency need to be calculated.

Cut off size

The cut off size gives the performance of the cyclone and shows up to what particle size it can capture with 50% efficiency. It is defined as:

$$d_{50} = \sqrt{\frac{18 \times \mu \times L}{2\pi N_c V_e (\rho_p - \rho_g)}}$$

Where, viscosity of gas, μ = 0.00004767 kg/m-s

L = 0.21*0.0492 = 0.0103 m

Number of turns, N_c = 4.5

Density of particles, ρ_p = 3200 kg/m^3

Substituting these values and calculating, we obtain d_{50} = 1.96 microns

Loopseal dimensions

The term "loopseal" refers to a bubbling bed reactor. Based on the availability of reactor sizes, the following dimensions are chosen for the loopseal:

Diameter of loopseal reactor = 101 mm

Height of loopseal reactor = 135 mm

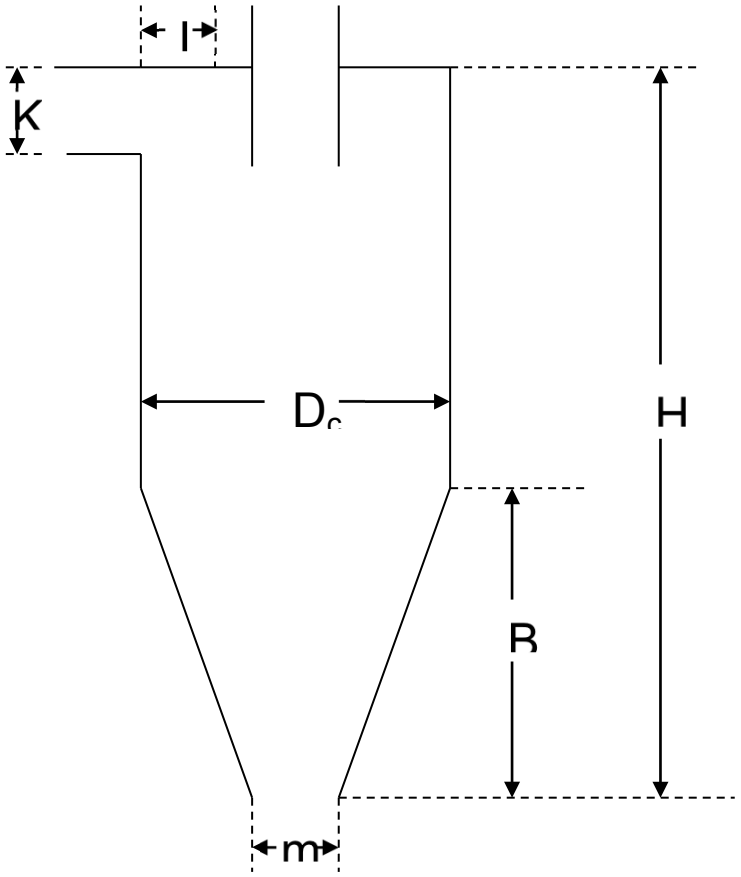

Figure A.1: Design of cyclone

Table A2 summarizes the sizes and shows the material information of the different components

Table A2: Material list of the different components of the CFB-CLG system

Component	**Description**
Gasifier	4 inch SCH 40 316 stainless steel pipe
Loopseal	4 inch SCH 40 316 stainless steel pipe
Regenerator	1 inch SCH 40 316 stainless steel pipe
Cyclone	1.5 inch stainless steel
Expansion Joints	1 inch nominal ID, 4 inch length 310 stainless steel
Flanges	1 inch 150#RFSW STD 316 4 inch 150#RFSW STD 316
Distributor plate	1.88 inch OD, ¼ inch thick porous ceramic disk 3.98" inch OD, ½ inch thick porous ceramic disk
Electrical heater	2 inch ID, 12 inch long, 120 V 550W semi-cylindrical ceramic fiber heater 2 inch ID, 18 inch long, 120 V 750W semi-cylindrical ceramic fiber heater 5 inch ID, 18 inch long, 120 V 1250 W semi cylindrical ceramic fiber heaters
Steam generator	9.0 lb/hr capacity electric steam generator, with 120 VAC control circuit,
Fittings	Stainless steel Swagelok fittings
Gasket	Spiral wound gasket
Insulation	High temperature glass wool

During the experiment, temperature and pressure were continuously measured and recorded in a computer. The table below summarizes the instruments used for the data monitoring and acquisition.

Table A3: Equipment list of the different measurement instruments

Parameters measured	**Description**
Temperature	1/16 inch thickness K type thermocouple
Pressure	0-30 psi transducer with 4 to 20 mA output
Data acquisition system	OMB-DAQ-56 omega
Flow meters	FMA-1608A 20 SLPM mass flow meter FMA-A2317 50 SLPM mass flow meter

A2 Energy efficiency calculation

The energy efficiency based on the first law of thermodynamic is calculated for the CFB-CLG system. The table below shows the calculation for the special case where carbon dioxide capture obtained in the gasifier is 80% and the regeneration efficiency is 50%. The regeneration efficiency refers the percentage of calcium carbonate being calcined in the regenerator.

Table A4: Energy balance of chemical looping gasification

Regeneration efficiency	0.5
Carbon dioxide capture efficiency	0.8
Drain from regenerator	0

Table A5: The mass flow rates of the different substances

Biomass	m_f	1	kg/s
Steam	m_{st}	1.07	kg/s
Calcium oxide leaving regenerator	m_{CaO}	2.41	kg/s
Calcium Carbonate leaving gasifier	m_{CaCO3}	3.44	kg/s
Calcium oxide leaving gasifier	m'_{CaO}	0.48	kg/s
Calcium oxide drained from regenerator	$m'_{CaOdrain}$	0.000	kg/s
Calcium carbonate drained from regenerator	$m_{CaCO3drain}$	0.000	kg/s
Mass of calcium oxide internally re-circulated in regenerator	$m_{solidCaO}$	1.203	kg/s
Amount of fresh calcium carbonate required	$m_{CaCO3fresh}$	7.732	kg/s
Carbon dioxide leaving the regenerator	m'_{CO2}	2.84	kg/s
Carbon dioxide entering the regenerator	m_{CO2}	0.95	kg/s
Mass of calcium carbonate internally re-circulated in regenerator	m_{solid}	5.58	kg/s
Product gas hydrogen	m_{prH2}	0.18	kg/s
Product gas carbon dioxide	m_{prCO2}	0.38	kg/s

Table A6: The operating temperature of the reactors and substances flowing in and out of the system

Gasifier	T_g	800	^oC
Regenerator	Tre	950	^oC
Fuel	T_f	30	^oC
Steam	T_{st}	300	^oC
Calcium oxide leaving regenerator	T_{CaO}	950	^oC
Calcium Carbonate leaving gasifier	T_{CaCO3}	800	^oC
Carbon dioxide leaving the regenerator	T'_{CO2}	950	^oC
Carbon dioxide entering the regenerator	T_{CO2}	30.0	^oC
Product gas	T_{pr}	800	^oC

Table A7: The specific heat capacities of the different substances considered for the energy balance

Fuel	C_{pf}	0.420	kJ/kg K
Steam	C_{pst}	2.007	kJ/kg K
Calcium Carbonate	C_{pCaCO3}	0.900	kJ/kg K
Calcium Oxide	C_{pCaO}	0.700	kJ/kg K
Carbon dioxide	C_{pCO2}	0.849	kJ/kg K
Carbon dioxide	C'_{pCO2}	1.289	kJ/kg K

Table A8: Data for the energy balance of the gasifier ((-) sign is for the energy associated with flow going into the system & (+) is for the energy associated with flow coming out of system)

Power with the incoming biomass	Q_f	-12.6	kW
Power with the steam	Q_{st}	-644.62	kW
Power with Calcium Oxide coming into gasifier	Q_{CaO}	-1599.69	kW
Power with Calcium Carbonate leaving gasifier	Q_{CaCO3}	2474.28	kW
Power with Calcium oxide leaving gasifier	Q''_{CaO}	269.42	kW
Power with product gas leaving gasifier	Q_{pr}	2597.48	kW
Power from overall gasification reaction	$Q_{gasification}$	-3075.66	kW
Power loss from the gasifier	Q_{loss}	926.35	kW
Power Energy for gasifier	$Q_{balance}$	934.95	kW

Table A9: Data for the energy balance of the regenerator ((-) sign is for the energy associated with flow going into the system & (+) is for the energy associated with flow coming out of system)

Power with carbon dioxide leaving regenerator	Q'_{CO2}	3471.067	kW
Power with carbon dioxide entering regenerator	Q_{CO2}	-24.082	kW
Power with Calcium Oxide leaving regenerator	Q_{CaO}	1599.69	kW
Power with Calcium Carbonate entering regenerator	Q_{CaCO3}	-2474.28	kW
Power with Calcium oxide entering regenerator	Q'_{CaO}	-269.42	kW
Power lost in drain of solid	Q_{drain}	0	kW
Power with the solid internally circulated	Q_{solid}	5574.43	kW
Power required for regeneration	$Q_{regeneration}$	7646.21	kW
Power with the fresh calcium carbonate	$Q_{CaCO3fresh}$	-208.76	kW
Power loss	Q_{loss}	926.35	kW
Balance Power for regenerator	$Q_{balance}$	16241.21	kW

Table A10: Efficiency calculation for the CFB-CLG system

Power with the product gas (a)	E_{pr}	25623.18	kW
Total Power needed for gasification (b)	E_{extgas}	934.95	kW
Total Power needed for regeneration (c)	E_{extreg}	16241.21	kW
Useful Power (d=a-b-c)	E_{useful}	8447.011	kW
Available sensible power (e)	$E_{sensible}$	4103.08	kW
Heating value of the biomass	**HHV**	**19.95**	**MJ/kg**
Thermal efficiency of the system (d+e)/$HHV_{biomass}$	**η_{system}**	**57.98**	**%**

A3 Exergy Efficiency Calculation

The exergy efficiency of the same system considered for the energy efficiency is carried out and the calculations are shown in the tables below.

Table A11: Standard chemical exergy and heat of formation for the different gases and solids

Gases	Chemical Exergy (P= 1 atm & T = 298 K)	Heat of formation
	kJ/mol	kJ/mol
Carbon dioxide	20.14	-393.5
Carbon monoxide	275.43	-110.6
Methane	836.51	-74.8
Hydrogen	238.49	0
Water vapor	11.71	241.5
Nitrogen	0.72	0
Oxygen	3.97	0
Carbon	410.82	0
Calcium oxide	110.00	604.46

Table A12: Properties of gases (JANAF thermodynamic table)

Gases	Temperature K	C_p (J/mol K)	h-h_{298} (kJ/mol)	S-S_{298} (J/mole)
CO_2	800	51.6306	22.9026	43.89
	900	53.2014	28.1484	50.064
	1000	54.516	33.5328	55.7424
	1100	55.6206	39.0432	60.8034
	1200	56.5572	44.6544	65.8728
	1300	57.3552	50.3496	70.4298
CO	800	32.0208	15.2334	29.7318
	900	32.7012	18.4674	33.5412

	1000	33.3102	21.7686	37.0188
	1100	33.8394	25.1286	40.2192
CH_4	800	63.1722	24.7674	46.4436
	900	67.8594	31.437	54.159
	1000	72.072	38.325	61.5342
	1100	75.8184	45.7254	65.9358
H_2	800	29.7654	14.7588	28.9758
	900	30.0216	17.7492	32.4996
	1000	30.3198	20.7648	35.6748
	1100	30.66	23.814	38.5812
H_2O	500	35.343	10.5378	17.7576
	600	36.4392	14.238	24.297
	900	40.0974	22.008	39.7488
	1000	41.3742	26.0778	44.0412

Table A13: Data for the ultimate analysis of biomass including the flow and inlet temperatures

Carbon	51.13	%
Hydrogen	6.1	%
Oxygen	41.96	%
Sulphur	0.01	%
Nitrogen	0.01	%
Ash	0.25	%
HHV	19.95	MJ/kg
Feed rate of biomass	1	kg/h
Temperature of inlet biomass	25	^oC

Table A14: Data of exergy balance for the gasifier

β (=Chemical Exergy/LHV)	1.12	
Chemical Exergy of biomass	22177.29	kJ/h
Physical Exergy of biomass	0.00	kJ/h
Chemical exergy of inlet steam	539.96	kJ/h
Physical exergy of inlet steam	322.66	kJ/h
Chemical exergy of product gas	21464.10	kJ/h
Difference in Enthalpy (=Δh)	1868.83	kJ/h
Difference in entropy (=To*(ΔS))	956.80	kJ/h
Physical Exergy of product gas	912.03	kJ/h

Table A15: Data of exergy balance for the regenerator

Physical Exergy of CaO	1560.475	kJ/h
Chemical Exergy of CaO	4733.93	kJ/h
Physical Exergy of $CaCO_3$	2999.25	kJ/h
Chemical Exergy of $CaCO_3$	0	kJ/h
Chemical exergy of inlet CO_2	434.84	kJ/h
Physical exergy of inlet CO_2	0.00	kJ/h
Chemical exergy of outlet CO_2	1299.95	kJ/h
Physical exergy of outlet CO_2	1615.21	kJ/h
Total exergy requirement of regenerator	5775.46	kJ/h

Table A16: Data of exegetic efficiency calculation

Net Exergy of the product gas	14995.23	kJ/h
Exergy of the flue Gas from combustor	1605.44	kJ/h
Exergy of Steam generation	862.62	kJ/h
Exergy of CO_2 coming out from regenerator	2915.15	kJ/h
Exegetic efficiency of CLG system	**83.14**	**%**

APPENDIX B: EXPERIMENTAL RESULTS OF STUDIES CONDUCTED IN A BATCH REACTOR

This part of appendix provides the data of the experiment done to study the effects of steam/biomass (S/B) ratio, calcium oxide/biomass (CaO/B) ratio and temperature (T) on the composition of the gas obtained from the gasification of biomass in the presence of steam and CaO. These results are discussed in chapter 4.

B1. Experimental results

This section includes the results of the experiment conducted in a fixed reactor to study the effects of S/B ratio, CaO/B ratio, and temperature on the hydrogen and carbon dioxide concentrations in product gas and on the gas yield.

Table B1: Effect of CaO/biomass ratio (T = 670^{o}C, S/B = 0.83)

Date	CaO/B ratio	Total Gas yield	Gas Composition (%)				H_2 yield (ml/g)
		ml/g	H_2	CO_2	CO	CH_4	
Aug-04	0.0	435	23.29	22.50	38.99	15.21	101.33
Jul-30	1.0	411	52.63	2.11	23.34	21.92	216.50
Jul-23	1.5	419	54.96	1.42	21.98	21.42	230.28
Aug-07	2.0	690	54.43	1.56	21.92	21.58	375.567

Table B2: Effect of steam/biomass ratio (T = 670^{o}C, CaO/B = 1.5)

Date	S/B ratio	Total Gas yield	Gas Composition (%)				H_2 yield (ml/g)
		ml/g	H_2	CO_2	CO	CH_4	
Jul-22	0.58	446	51.27	1.76	24.53	21.22	228.83
Jul-23	0.83	419	54.96	1.42	21.98	21.42	230.28
Jul-16	1.08	415	55.32	0.92	21.39	22.37	229.59
Jul-18	1.58	350	55.55	1.90	21.52	21.02	194.42

Table B3: Effect of temperature (S/B = 0.83, CaO/B = 1.5)

Date	Temperature (^{o}C)	Total Gas yield	Gas Composition (%)				H_2 Yield (ml/g)
		ml/g	H_2	CO_2	CO	CH_4	
Aug-12	600	315	53.13	1.40	25.86	20.67	167.36
Jul-23	670	419	54.96	1.42	21.98	21.42	230.28
Jul-07	710	610	51.65	2.18	21.68	24.49	315.08

B2 Non-stoichiometric modeling results

This section provides the data obtained from the non-stoichiometric equilibrium modeling of biomass gasification in the presence of CaO and steam.

Table B4: Effect of steam to biomass ratio (T = 700°C, CaO/B = 0)

S/B ratio	Composition of product gas (%)			
	CO_2	CO	CH_4	H_2
0.53	15.00	35.24	9.78	39.98
0.60	15.86	33.30	8.70	42.13
0.68	16.62	31.62	7.77	43.99
0.75	17.28	30.14	6.96	45.62
0.90	18.41	27.64	5.62	48.33
1.06	19.37	25.58	4.56	50.49
1.21	20.20	23.83	3.73	52.24
1.36	20.94	22.33	3.07	53.66
1.51	21.61	21.00	2.54	54.85
1.89	23.04	18.29	1.62	57.05
2.26	24.22	16.17	1.07	58.54
3.02	26.03	13.09	0.50	60.38

Table B5: Effect of steam to biomass ratio (T=700°C, CaO/B = 1.5)

S/B ratio	Composition of product gas (%)			
	CO_2	CO	CH_4	H_2
0.53	0.21	6.31	28.70	64.78
0.60	0.75	9.07	20.83	69.36
0.68	1.32	10.32	16.23	72.13
0.75	1.98	10.93	13.12	73.97
0.90	3.12	11.30	9.13	76.45
1.06	4.12	11.18	6.65	78.05
1.21	5.00	10.86	4.98	79.17
1.36	5.77	10.45	3.80	79.98
1.51	6.45	10.00	2.94	80.61
1.89	7.85	8.91	1.63	81.61
2.26	8.91	7.93	0.96	82.19
3.02	10.41	6.40	0.39	82.80

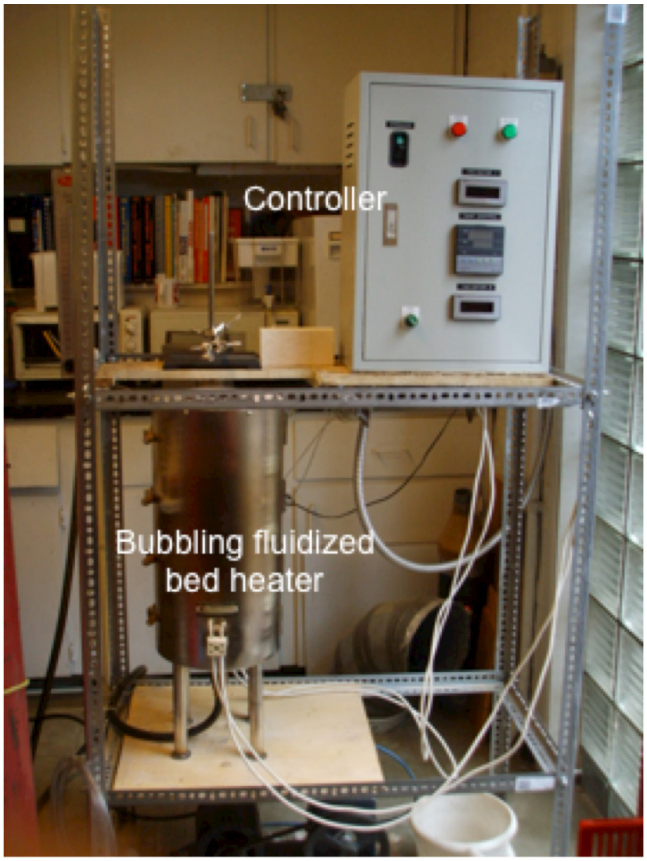

Figure B1: Bubbling Fluidized bed heater used for batch scale study

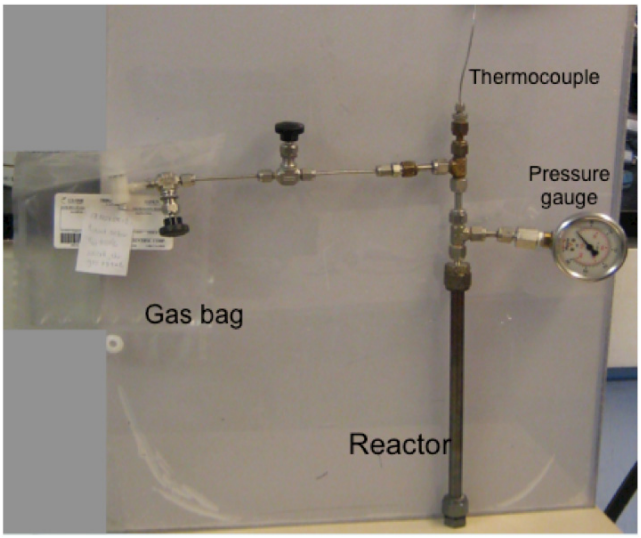

Figure B2: Experimental arrangement

APPENDIX C: EXPERIMENTAL RESULTS DATA FOR STUDIES CONDUCTED TO EXAMINE CHARACTERISTICS OF THE SORBENTS CAO

This part of appendix provides the data collected from the experiment conducted to study the calcination and carbonation reaction discussed in chapter 5.

C1 Particle loading for the different experiments

Table C1 shows the masses of the samples being considered for the different studies done in the QWM reactor. To study the calcination-carbonation cycle, a higher mass is taken to ensure that measurable changes can be obtained during carbonation.

Table C1: Particle loading for different experiments

Experiments	Particle loading (gm of $CaCO_3$)
Effect of temperature and residence time	1
Effect of particle size	1
Effect of media on calcination/carbonation	3

C2 Effect of particle size

The effects of particle size on the calcination and carbonation are shown in Table C2 and Table C3 respectively.

Table C2: Effect of particle size on calcination

Mean particle size (microns)					
327.5		275		135	
Time (sec)	Conversion	Time (sec)	Conversion	Time (sec)	Conversion
30	0.00	30	0.04	30	0.09
99	0.18	60	0.26	115	0.95
114	0.21	90	0.50	123	1.00
121	0.27	120	0.83		
142	0.32	150	0.89		
159	0.37	210	1.00		
330	0.94				
360	0.99				

Table C3: Effect of particle size on carbonation

Mean particle size (microns)					
325		275		230	
Time (sec)	Conversion	Time (sec)	Conversion	Time (sec)	Conversion
30	0.06	30	0.03	100	0.10
60	0.07	60	0.05	300	0.41
90	0.13	90	0.12	400	0.53
120	0.14	120	0.17	700	0.64
150	0.17	150	0.24	1000	0.65
180	0.19	180	0.28	1200	0.65
210	0.21	210	0.31		
240	0.28	240	0.34		
270	0.28	270	0.38		
300	0.30	300	0.40		
330	0.32	330	0.44		
360	0.34	390	0.47		
420	0.35	420	0.48		
480	0.36	450	0.48		
510	0.39	480	0.48		
600	0.39	570	0.50		
630	0.40	600	0.51		
660	0.42	630	0.53		
690	0.44	660	0.55		
720	0.46	690	0.58		
750	0.48	720	0.59		
810	0.49	780	0.59		
870	0.48	810	0.60		
900	0.51	840	0.61		
930	0.51				
960	0.53				
1000	0.52				

C3 Effect of media on calcination

To observe the effect of the medium used for calcination on the calcination rate, an experiment was conducted by calcining in the presence of CO_2, H_2O and N_2. The results are shown in Table C4. A kinetics rate equation for calcination was also developed for each medium and the results are shown in Table C5.

Table C4: Conversion of $CaCO_3$ with time during calcination in the presence of three media (T = 950^oC)

Medium used for calcination reaction					
N_2		CO_2		H_2O	
Time (sec)	$CaCO_3$conversion	Time (sec)	$CaCO_3$conversion	Time (sec)	$CaCO_3$conversion
0	0.00	0	0.00	0	0.00
30	5.11	30	4.99	30	1.28
60	10.10	60	8.87	60	1.26
90	14.40	90	14.23	90	2.02
120	19.78	120	18.55	120	1.84
150	25.46	150	21.61	150	1.74
180	31.83	180	25.84	180	2.72
210	37.74	210	30.75	210	4.16
240	43.13	240	35.19	240	5.50
270	50.10	270	40.60	270	6.35
300	54.34	300	43.51	300	8.40
330	60.56	330	49.56	330	10.91
360	65.32	360	52.84	360	12.29
390	69.14	390	57.02	390	14.59
420	74.20	420	60.03	420	18.00
450	78.15	450	63.11	450	19.51
480	82.02	480	67.11	480	21.56
510	88.68	510	69.58	510	20.79
540	90.54	540	73.66	540	20.70
570	91.73	570	76.80	570	23.63
600	98.78	600	76.52	600	25.38
		630	81.16	630	27.64
		660	83.11	660	29.12
		690	83.23	690	32.23
		720	87.80	720	34.36
		750	87.82	750	36.70
		780	88.60	780	40.97
		810	90.96	810	44.42
		840	93.43	840	45.01
		900	92.18	870	49.14
		930	95.97	900	49.86
		960	95.99	930	43.50
		990	94.92	960	45.71
		1020	95.96	990	49.07
		1050	95.43	1020	48.28
		1080	98.39	1050	53.17
		1110	99.12	1080	51.89
				1110	51.27

				1140	52.14
				1170	54.87
				1200	57.18
				1230	59.92
				1260	58.19
				1290	58.84
				1320	60.70
				1350	63.74
				1380	68.19
				1410	69.35
				1440	71.27
				1470	70.31
				1500	71.40
				1530	73.88
				1560	74.05
				1590	74.65
				1620	74.70

Table C5: Kinetics of calcination in the presence of three media

	H_2O					
k	0.000053	0.001519	0.017600	0.666667	0.869868	1.666667
ln k	-9.84	-6.49	-4.04	-0.41	-0.14	0.51
T	0.00115	0.00103	0.00093	0.00085	0.00082	0.00079
E_a *(kJ/mol)*	248.62					
K_o *(1/s)*	36333281358.27					
	N_2					
k	0.000609	0.017107	0.217246	0.239879	1.666667	
ln k	-7.40	-4.07	-1.53	-1.43	0.51	
T	0.00103	0.00093	0.00085	0.00082	0.00079	
E_a *(kJ/mol)*	257.78					
K_o *(1/s)*	48169891252.08					
	CO_2					
k	0.002213	0.003104	0.009584			
ln k	-6.11	-5.78	-4.65			
T	0.00085	0.00082	0.00079			
E_a *(kJ/mol)*	180.56					
K_o *(1/s)*	212139.64					

C4 Studies on the calcination-carbonation cycle

To examine the change in reactivity of the sorbent with the number of calcination-carbonation cycles, experiments were conducted in a QWM reactor where the sorbent underwent 5 cycles of calcination-carbonation. Calcination was performed with CO_2, H_2O, and N_2 and carbonation with pure CO_2. The results are shown in Table C6.

Table C6: Total conversion obtained in each calcination and carbonation cycle

	Carbonation (CaO conversion, %)			Calcination ($CaCO_3$ conversion, %)		
Cycle	CO_2-CO_2	N_2-CO_2	H_2O-CO_2	CO_2-CO_2	N_2-CO_2	H_2O-CO_2
1	67.68	57.78	64.74	73.38	99.31	99.50
2	44.99	53.40	44.80	72.89	98.72	97.46
3	40.89	44.47	40.91	63.53	97.07	96.72
4	39.70	39.45	37.91	58.12	97.83	93.77
5	36.56	25.40		53.78	95.32	

APPENDIX D: EXPERIMENTAL RESULTS DATA FOR GASIFICATION OF BIOMASS IN CFB-CLG SYSTEM

This section of the appendix includes the data for the biomass gasification done in CFB-CLG system. It also shows the calculation for the analysis of limestone.

D1 Gasification studies in a bubbling bed

Gasification was initially only studied in a bubbling bed using CaO and sand as the bed material. Experimental results for sand as bed material is shown in Table D1 and with CaO is shown in Table D2.

Table D1: Results of gasification of biomass in a bubbling bed with sand as the bed material

Gas component	Time (min)					
	2	5	15	20	25	30
H_2 (%)	13.48	11.18	28.49	40.61	40.53	39.74
CO (%)	43.73	44.81	26.31	15.17	17.48	14.91
CO_2 (%)	29.41	31.42	34.97	34.82	31.17	35.74
CH_4 (%)	13.38	12.59	10.23	9.40	10.83	9.61

Table D2: Results of gasification of biomass in a bubbling bed with CaO as the bed material

Gas component	Time (min)							
	2	5	10	15	25	27	32	35
H_2 (%)	25.06	36.25	54.58	53.64	56.21	65.41	70.97	70.23
CO (%)	31.62	25.47	21.26	17.57	19.45	12.44	10.43	10.67
CO_2 (%)	10.13	8.42	3.95	4.36	5.78	2.36	1.64	1.65
CH_4 (%)	33.19	29.86	24.84	24.43	18.56	19.79	16.97	17.45

D2 Gasification studies in a CFB-CLG system

Table D3 shows the results for the gas composition obtained while gasifying biomass in a CFB-CLG system.

Table D3: Results of biomass gasification in a CFB-CLG system

Time	Gas composition (%)			
	H_2	CO	CO_2	CH_4
6	64.77	12.22	1.20	21.81
8	68.05	10.38	1.01	20.56
11	62.27	11.12	1.08	25.53
14	61.62	10.44	0.94	27.01
17	56.95	10.45	1.00	31.60
20	50.28	16.87	1.87	30.99
30	51.12	11.69	1.46	35.73
40	53.40	12.10	1.55	32.94
60	54.37	17.29	1.57	26.77
90	62.89	5.18	1.44	30.48
109	72.67	5.28	0.35	21.70
112	81.16	3.15	0.57	15.13
116	79.76	3.43	1.91	14.90
120	79.28	4.26	2.82	13.64
130	80.13	3.13	6.72	10.02
140	79.51	3.05	5.87	11.57
150	80.94	3.04	5.71	10.30

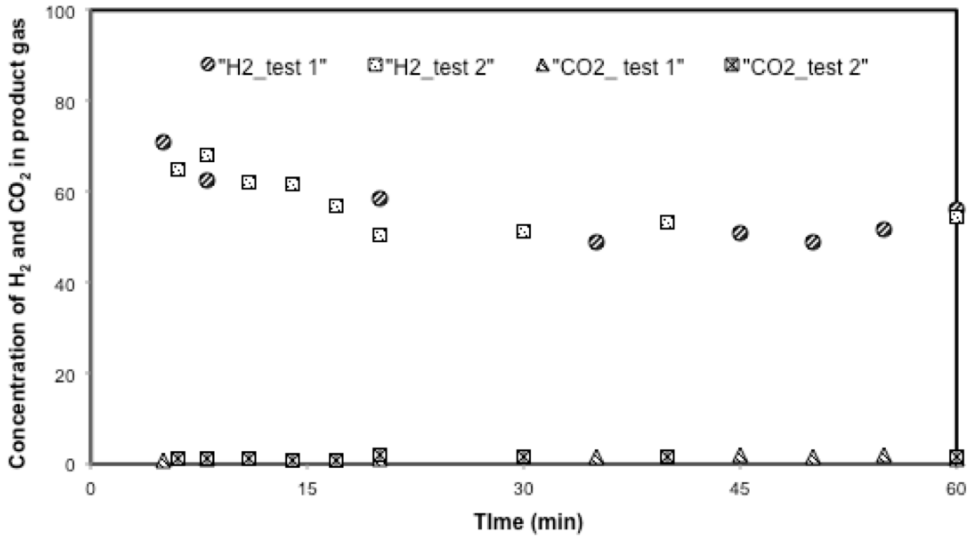

Figure D1: Comparison of results obtained during 2 tests run of CFB-CLG system

Figure D1 shows the results for two tests runs done for the gasification of biomass in the CFB-CLG system. Test 1 was stopped after one hour of operation because of the problem with the heaters. However, if we compare the results of the concentration of hydrogen and carbon dioxide for the first one-hour operation of the two tests, the similarities observed verify the repeatability of the results.

D3 Gasification efficiency calculation

The measured flow rate of product gas = 96.94 liter/kg of biomass

Table D4: Calculation of energy with the product gas

Product gas composition (%)		Liter/kg of biomass	Liter/s	Gas flow rate Nm^3/s	Power with product gas MJ/s
H_2	80.94	78.47	0.0044	$4.35945*10^{-06}$	$5.55612*10^{-05}$
CO	3.04	2.95	0.00016	$1.63952*10^{-07}$	$2.0712*10^{-06}$
CO_2	5.71	5.53	0.000307	$3.07417*10^{-07}$	0
CH_4	10.30	9.99	0.000555	$5.54895*10^{-07}$	$2.20954*10^{-05}$
			Total	$5.38571*10^{-06}$	$7.97277*10^{-05}$

(Heating value of H_2 = 12.745 MJ/Nm^3, CO = 12.633 MJ/Nm^3 and CH_4 = 39.819 MJ/Nm^3)

Heating value of biomass = 19.72 MJ/kg

Biomass flow rate = 0.2 kg/hr

Cold gas efficiency = (energy with product gas/energy with biomass)*100%
= 7.27%

The low gasification temperature gives poor char conversion, leading to lower gas yield. Therefore, very low gasification efficiency is obtained during the experiment. These results are also validated with the kinetic model.

D4 Kinetic modeling of biomass gasification

A kinetics model was developed to predict the performance of the gasifier of the CFB-CLG system. Table D5 shows the input values considered in the model.

Table D5: Input parameters for the kinetic model

Input parameters	Values
Feed rate of biomass (kg/hr)	0.2
Feed rate of steam (kg/hr)	1.5
Bed material	CaO
S/B ratio	7.5
Temperature of gasifier bed (^oC)	575
Temperature of freeboard (^oC)	400
Pressure (atm)	1
Crossectional area of bed (m^2)	0.00807
Crossectional area of freeboard (m^2)	0.00807
Mean particle size of limestone (microns)	275
Voidage in the freeboard (-)	0.998

Figure D2 shows the yield for char and gas during devolatilization against temperature developed experimentally by Scott et al (1982). The value for char and gas yield during devolatilization in the model is taken from this graph.

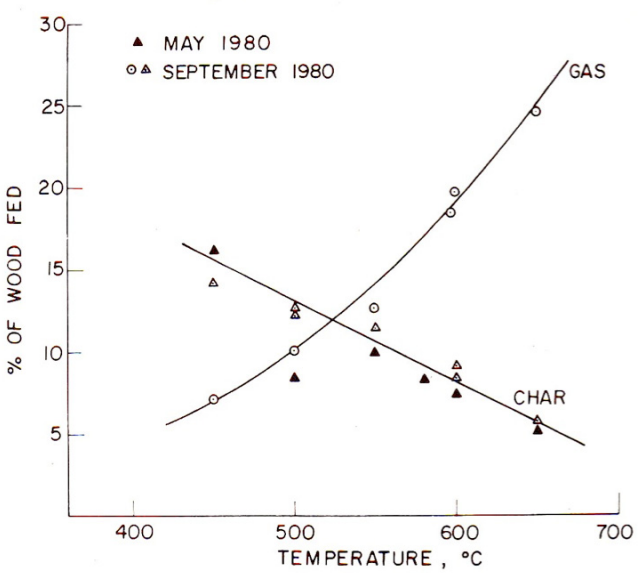

Figure D2: Experimental results for char and gas yield during devolatilization of biomass (Scott et al. (1982))

D5 Analysis of limestone

Point Aconi Power Plant, Sydney Nova Scotia of Nova Scotia Power, provided limestone used for the experiment. The samples were collected before the crushing mill of the power

plant. The stones of larger size were crushed in a Mineral Engineering Centre to the desired size. Table D6 shows the analysis of the sample according to the methodology described in chapter 6 in section 6.1.1. Table D7 compares the results with the analysis done in the Mineral Engineering Centre and the analysis of limestone provided by Point Aconi Power. The results shows that the method used in this thesis gives the values that agrees well with analysis done in the laboratory. Therefore, through out the thesis the same approach is used for analyzing the limestone.

Table D6: Analysis of Limestone

Wt. of crucible (gram)	24.7159
Wt. of sample (gram)	1.0150
Wt. after drying (gram)	25.7289
Wt. after heating at 500^{o}C (gram)	25.7220
Wt. after heating at 900^{o}C (gram)	25.3013
Wt. of moisture (gram)	0.002
% of moisture	0.20
Wt. of dry sample (gram)	1.013
Wt. loss after heating at 500^{o}C (gram)	0.007
Wt. of magnesium carbonate (gram)	0.013
% of Magnesium carbonate	1.31
Wt. of sample after heating at 500^{o}C (gram)	1.006
Wt. loss after heating at 900oC (gram)	0.421
Wt. of Calcium carbonate (gram)	0.956
Wt. of inert material (gram)	0.050
% of moisture	0.20
% of Magnesium carbonate	1.31
% of Calcium carbonate	94.39
% of Inert material	4.93

Table D7: Validation of limestone analysis

Components	Analysis of limestone		
	In this thesis	Provided by Nova Scotia Power	Mineral Energy Center, Dalhousie University
	%	%	%
Calcium carbonate	94.39	93.93	94.3
Magnesium carbonate	1.31	0.81	-
Inert material	4.93	5.26	-

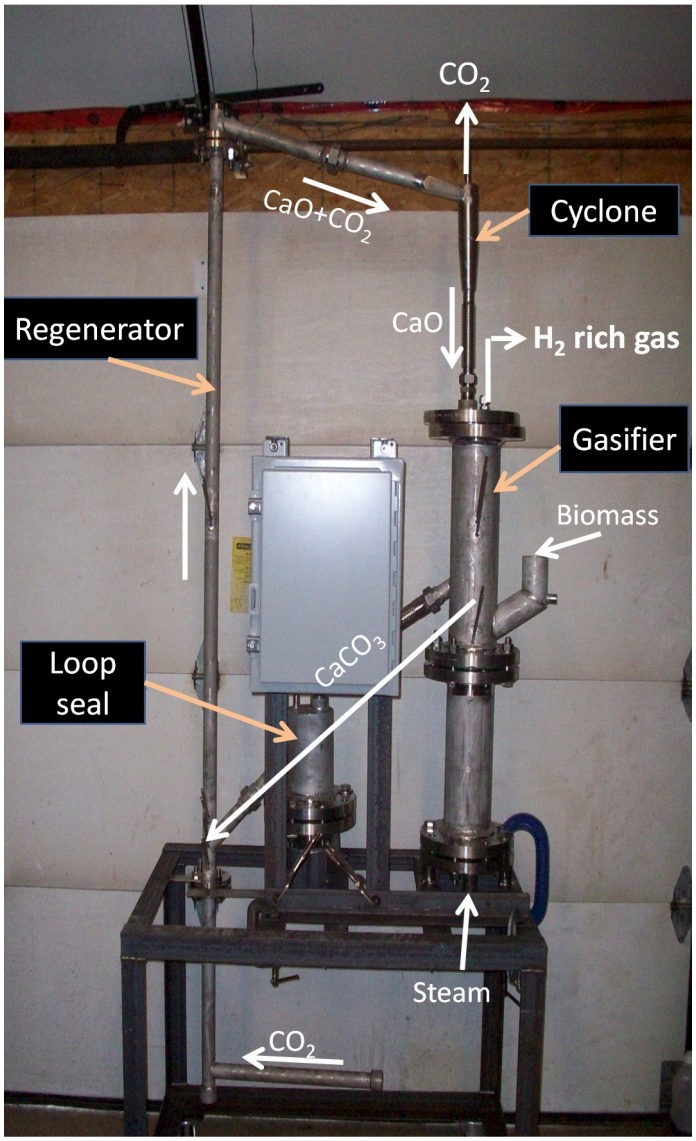

Figure D3: CFB-CLG unit during fabrication

APPENDIX E: COPYRIGHT FROM THE PUBLISHER

E1 Copyright acceptance for the paper:

Acharya, B., Dutta, A., and Basu, P., "An Investigation into Steam Gasification of Biomass for Hydrogen Enriched Gas production in Presence of CaO", *International. Journal of Hydrogen Energy*, 2010; 35; 1582-1589

This is a License Agreement between Bishnu Acharya ("You") and Elsevier ("Elsevier") provided by Copyright Clearance Center ("CCC"). The license consists of your order details, the terms and conditions provided by Elsevier, and the payment terms and conditions.

Terms and conditions

INTRODUCTION

1. The publisher for this copyrighted material is Elsevier. By clicking "accept" in connection with completing this licensing transaction, you agree that the following terms and conditions apply to this transaction (along with the Billing and Payment terms and conditions established by Copyright Clearance Center, Inc. ("CCC"), at the time that you opened your Rightslink account and that are available at any time at http://myaccount.copyright.com).

GENERAL TERMS

2. Elsevier hereby grants you permission to reproduce the aforementioned material subject to the terms and conditions indicated.

3. Acknowledgement: If any part of the material to be used (for example, figures) has appeared in our publication with credit or acknowledgement to another source, permission must also be sought from that source. If such permission is not obtained then that material may not be included in your publication/copies. Suitable acknowledgement to the source must be made, either as a footnote or in a reference list at the end of your publication, as follows:
"Reprinted from Publication title, Vol /edition number, Author(s), Title of article / title of chapter, Pages No., Copyright (Year), with permission from Elsevier [OR APPLICABLE SOCIETY COPYRIGHT OWNER]." Also Lancet special credit - "Reprinted from The Lancet, Vol. number, Author(s), Title of article, Pages No., Copyright (Year), with permission from Elsevier."
4. Reproduction of this material is confined to the purpose and/or media for which permission is hereby given.

5. Altering/Modifying Material: Not Permitted. However figures and illustrations may be altered/adapted minimally to serve your work. Any other abbreviations, additions, deletions and/or any other alterations shall be made only with prior written authorization of Elsevier Ltd. (Please contact Elsevier at permissions@elsevier.com)

6. If the permission fee for the requested use of our material is waived in this instance, please be advised that your future requests for Elsevier materials may attract a fee.

7. Reservation of Rights: Publisher reserves all rights not specifically granted in the combination of (i) the license details provided by you and accepted in the course of this licensing transaction, (ii) these terms and conditions and (iii) CCC's Billing and Payment terms and conditions.

8. License Contingent Upon Payment: While you may exercise the rights licensed immediately upon issuance of the license at the end of the licensing process for the transaction, provided that you have disclosed complete and accurate details of your proposed use, no license is finally effective unless and until full payment is received from you (either by publisher or by CCC) as provided in CCC's Billing and Payment terms and conditions. If full payment is not received on a timely basis, then any license preliminarily granted shall be deemed automatically revoked and shall be void as if never granted. Further, in the event that you breach any of these terms and conditions or any of CCC's Billing and Payment terms and conditions, the license is automatically revoked and shall be void as if never granted. Use of materials as described in a revoked license, as well as any use of the materials beyond the scope of an unrevoked license, may constitute copyright infringement and publisher reserves the right to take any and all action to protect its copyright in the materials.

9. Warranties: Publisher makes no representations or warranties with respect to the licensed material.

10. Indemnity: You hereby indemnify and agree to hold harmless publisher and CCC, and their respective officers, directors, employees and agents, from and against any and all claims arising out of your use of the licensed material other than as specifically authorized pursuant to this license.

11. No Transfer of License: This license is personal to you and may not be sublicensed, assigned, or transferred by you to any other person without publisher's written permission.

12. No Amendment Except in Writing: This license may not be amended except in a writing signed by both parties (or, in the case of publisher, by CCC on publisher's behalf).

13. Objection to Contrary Terms: Publisher hereby objects to any terms contained in any purchase order, acknowledgment, check endorsement or other writing prepared by you, which terms are inconsistent with these terms and conditions or CCC's Billing and Payment terms and conditions. These terms and conditions, together with CCC's Billing and

Payment terms and conditions (which are incorporated herein), comprise the entire agreement between you and publisher (and CCC) concerning this licensing transaction. In the event of any conflict between your obligations established by these terms and conditions and those established by CCC's Billing and Payment terms and conditions, these terms and conditions shall control.

14. Revocation: Elsevier or Copyright Clearance Center may deny the permissions described in this License at their sole discretion, for any reason or no reason, with a full refund payable to you. Notice of such denial will be made using the contact information provided by you. Failure to receive such notice will not alter or invalidate the denial. In no event will Elsevier or Copyright Clearance Center be responsible or liable for any costs, expenses or damage incurred by you as a result of a denial of your permission request, other than a refund of the amount(s) paid by you to Elsevier and/or Copyright Clearance Center for denied permissions.

LIMITED LICENSE

The following terms and conditions apply only to specific license types:

15. Translation: This permission is granted for non-exclusive world English rights only unless your license was granted for translation rights. If you licensed translation rights you may only translate this content into the languages you requested. A professional translator must perform all translations and reproduce the content word for word preserving the integrity of the article. If this license is to re-use 1 or 2 figures then permission is granted for non-exclusive world rights in all languages.

16. Website: The following terms and conditions apply to electronic reserve and author websites:
Electronic reserve: If licensed material is to be posted to website, the web site is to be password-protected and made available only to bona fide students registered on a relevant course if:
This license was made in connection with a course,
This permission is granted for 1 year only. You may obtain a license for future website posting. All content posted to the web site must maintain the copyright information line on the bottom of each image,
A hyper-text must be included to the Homepage of the journal from which you are licensing at http://www.sciencedirect.com/science/journal/xxxxx or the Elsevier homepage for books at http://www.elsevier.com , and
Central Storage: This license does not include permission for a scanned version of the material to be stored in a central repository such as that provided by Heron/XanEdu.

17. Author website for journals with the following additional clauses:
All content posted to the web site must maintain the copyright information line on the bottom of each image, and the permission granted is limited to the personal version of your paper. You are not allowed to download and post the published electronic version of your article (whether PDF or HTML, proof or final version), nor may you scan the printed

edition to create an electronic version, A hyper-text must be included to the Homepage of the journal from which you are licensing at http://www.sciencedirect.com/science/journal/xxxxx , As part of our normal production process, you will receive an e-mail notice when your article appears on Elsevier's online service ScienceDirect (www.sciencedirect.com). That e-mail will include the article's Digital Object Identifier (DOI). This number provides the electronic link to the published article and should be included in the posting of your personal version. We ask that you wait until you receive this e-mail and have the DOI to do any posting.
Central Storage: This license does not include permission for a scanned version of the material to be stored in a central repository such as that provided by Heron/XanEdu.

18. Author website for books with the following additional clauses:
Authors are permitted to place a brief summary of their work online only.
A hyper-text must be included to the Elsevier homepage at http://www.elsevier.com
All content posted to the web site must maintain the copyright information line on the bottom of each image

You are not allowed to download and post the published electronic version of your chapter, nor may you scan the printed edition to create an electronic version.
Central Storage: This license does not include permission for a scanned version of the material to be stored in a central repository such as that provided by Heron/XanEdu.

19. Website (regular and for author): A hyper-text must be included to the Homepage of the journal from which you are licensing at http://www.sciencedirect.com/science/journal/xxxxx or for books to the Elsevier homepage at http://www.elsevier.com

20. Thesis/Dissertation: If your license is for use in a thesis/dissertation your thesis may be submitted to your institution in either print or electronic form. Should your thesis be published commercially, please reapply for permission. These requirements include permission for the Library and Archives of Canada to supply single copies, on demand, of the complete thesis and include permission for UMI to supply single copies, on demand, of the complete thesis. Should your thesis be published commercially, please reapply for permission.

E2 Copyright acceptance for the paper:

Acharya, B., Dutta, A., and Basu, P., "Chemical looping gasification of biomass for hydrogen enriched gas production with in-process carbon-dioxide capture", *Energy and Fuel*, 2009; 23, 5077–5083

This is a License Agreement between Bishnu Acharya ("You") and American Chemical Society ("American Chemical Society") provided by Copyright Clearance Center ("CCC"). The license consists of your order details, the terms and conditions provided by American Chemical Society, and the payment terms and conditions.

Terms and Conditions
Thesis/Dissertation
ACS / RIGHTSLINK TERMS & CONDITIONS
THESIS/DISSERTATION

INTRODUCTION
The publisher for this copyrighted material is the American Chemical Society. By clicking "accept" in connection with completing this licensing transaction, you agree that the following terms and conditions apply to this transaction (along with the Billing and Payment terms and conditions established by Copyright Clearance Center, Inc. ("CCC"), at the time that you opened your Rightslink account and that are available at any time at <http://myaccount.copyright.com>).

LIMITED LICENSE
Publisher hereby grants to you a non-exclusive license to use this material. Licenses are for one-time use only with a maximum distribution equal to the number that you identified in the licensing process.

GEOGRAPHIC RIGHTS: SCOPE
Licenses may be exercised anywhere in the world.

RESERVATION OF RIGHTS
Publisher reserves all rights not specifically granted in the combination of (i) the license details provided by you and accepted in the course of this licensing transaction, (ii) these terms and conditions and (iii) CCC's Billing and Payment terms and conditions.

PORTION RIGHTS STATEMENT: DISCLAIMER
If you seek to reuse a portion from an ACS publication, it is your responsibility to examine each portion as published to determine whether a credit to, or copyright notice of, a third party owner was published adjacent to the item. You may only obtain permission via Rightslink to use material owned by ACS. Permission to use any material published in an

ACS publication, journal, or article which is reprinted with permission of a third party must be obtained from the third party owner. ACS disclaims any responsibility for any use you make of items owned by third parties without their permission.

REVOCATION

The American Chemical Society reserves the right to revoke a license for any reason, including but not limited to advertising and promotional uses of ACS content, third party usage, and incorrect figure source attribution.

LICENSE CONTINGENT ON PAYMENT

While you may exercise the rights licensed immediately upon issuance of the license at the end of the licensing process for the transaction, provided that you have disclosed complete and accurate details of your proposed use, no license is finally effective unless and until full payment is received from you (by CCC) as provided in CCC's Billing and Payment terms and conditions. If full payment is not received on a timely basis, then any license preliminarily granted shall be deemed automatically revoked and shall be void as if never granted. Further, in the event that you breach any of these terms and conditions or any of CCC's Billing and Payment terms and conditions, the license is automatically revoked and shall be void as if never granted. Use of materials as described in a revoked license, as well as any use of the materials beyond the scope of an unrevoked license, may constitute copyright infringement and publisher reserves the right to take any and all action to protect its copyright in the materials.

COPYRIGHT NOTICE: DISCLAIMER

You must include the following copyright and permission notice in connection with any reproduction of the licensed material: "Reprinted (“Adapted” or “in part”) with permission from REFERENCE CITATION. Copyright YEAR American Chemical Society."

WARRANTIES: NONE

Publisher makes no representations or warranties with respect to the licensed material.

INDEMNITY

You hereby indemnify and agree to hold harmless publisher and CCC, and their respective officers, directors, employees and agents, from and against any and all claims arising out of your use of the licensed material other than as specifically authorized pursuant to this license.

NO TRANSFER OF LICENSE

This license is personal to you or your publisher and may not be sublicensed, assigned, or transferred by you to any other person without publisher's written permission.

NO AMENDMENT EXCEPT IN WRITING

This license may not be amended except in a writing signed by both parties (or, in the case of publisher, by CCC on publisher's behalf).

OBJECTION TO CONTRARY TERMS
Publisher hereby objects to any terms contained in any purchase order, acknowledgment, check endorsement or other writing prepared by you, which terms are inconsistent with these terms and conditions or CCC's Billing and Payment terms and conditions. These terms and conditions, together with CCC's Billing and Payment terms and conditions (which are incorporated herein), comprise the entire agreement between you and publisher (and CCC) concerning this licensing transaction. In the event of any conflict between your obligations established by these terms and conditions and those established by CCC's Billing and Payment terms and conditions, these terms and conditions shall control.

JURISDICTION
This license transaction shall be governed by and construed in accordance with the laws of the District of Columbia. You hereby agree to submit to the jurisdiction of the courts located in the District of Columbia for purposes of resolving any disputes that may arise in connection with this licensing transaction.

THESES/DISSERTATION TERMS
Regarding your request for permission to include your paper(s) or portions of text from your paper(s) in your thesis/dissertation, permission is now automatically granted; please pay special attention to the implications paragraph below. The Copyright Subcommittee of the Joint Board/Council Committees on Publications approved the following:

Copyright permission for published and submitted material from theses and dissertations
ACS extends blanket permission to students to include in their theses and dissertations their own articles, or portions thereof, that have been published in ACS journals or submitted to ACS journals for publication, provided that the ACS copyright credit line is noted on the appropriate page(s).

Publishing implications of electronic publication of theses and dissertation material
Students and their mentors should be aware that posting of theses and dissertation material on the Web prior to submission of material from that thesis or dissertation to an ACS journal may affect publication in that journal. Whether Web posting is considered prior publication may be evaluated on a case-by-case basis by the journal's editor. If an ACS journal editor considers Web posting to be "prior publication", the paper will not be accepted for publication in that journal. If you intend to submit your unpublished paper to ACS for publication, check with the appropriate editor prior to posting your manuscript electronically.

Reuse/Republication of the Entire Work in Theses or Collections: Authors may reuse all or part of the Submitted, Accepted or Published Work in a thesis or dissertation that the author writes and is required to submit to satisfy the criteria of degree-granting institutions. Such reuse is permitted subject to the ACS' "Ethical Guidelines to Publication of Chemical Research" (http://pubs.acs.org/page/policy/ethics/index.html); the author should secure written confirmation (via letter or email) from the respective ACS journal editor(s) to avoid potential conflicts with journal prior publication*/embargo policies. Appropriate citation of the Published Work must be made. If the thesis or dissertation to be published is in

electronic format, a direct link to the Published Work must also be included using the ACS Articles on Request author-directed link - see http://pubs.acs.org/page/policy/articlesonrequest/index.html
* Prior publication policies of ACS journals are posted on the ACS website at http://pubs.acs.org/page/policy/prior/index.html

If your paper has not yet been published by ACS, please print the following credit line on the first page of your article: "Reproduced (or 'Reproduced in part') with permission from [JOURNAL NAME], in press (or 'submitted for publication'). Unpublished work copyright [CURRENT YEAR] American Chemical Society." Include appropriate information.

If your paper has already been published by ACS and you want to include the text or portions of the text in your thesis/dissertation in print or microfilm formats, please print the ACS copyright credit line on the first page of your article: "Reproduced (or 'Reproduced in part') with permission from [FULL REFERENCE CITATION.] Copyright [YEAR] American Chemical Society." Include appropriate information.

Submission to a Dissertation Distributor: If you plan to submit your thesis to UMI or to another dissertation distributor, you should not include the unpublished ACS paper in your thesis if the thesis will be disseminated electronically, until ACS has published your paper. After publication of the paper by ACS, you may release the entire thesis (not the individual ACS article by itself) for electronic dissemination through the distributor; ACS's copyright credit line should be printed on the first page of the ACS paper.